ฤทธิ์ต้านแบคทีเรียและการควบคุมยีนของแอนติลิโพพอลิแซ็กคาไรด์แฟกเตอร์จาก
กุ้งกุลาดำ *Penaeus monodon*

นางสาวพิชญานันท์ คำแสง

วิทยานิพนธ์นี้เป็นส่วนหนึ่งของการศึกษาตามหลักสูตรปริญญาวิทยาศาสตรมหาบัณฑิต
สาขาวิชาชีวเคมีและชีววิทยาโมเลกุล ภาควิชาชีวเคมี
คณะวิทยาศาสตร์ จุฬาลงกรณ์มหาวิทยาลัย
ปีการศึกษา 2557

ANTIBACTERIAL ACTIVITY AND GENE REGULATION OF ANTILIPOPOLYSACCHARIDE FACTOR FROM BLACK TIGER SHRIMP *Penaeus monodon*

Miss Pitchayanan Kamsaeng

A Thesis Submitted in Partial Fulfillment of the Requirements
for the Degree of Master of Science Program in Biochemistry and Molecular Biology
Department of Biochemistry
Faculty of Science
Chulalongkorn University
Academic Year 2014

Thesis Title	ANTIBACTERIAL ACTIVITY AND GENE REGULATION OF ANTILIPOPOLYSACCHARIDEFACTOR FROM BLACK TIGER SHRIMP *Penaeus monodon*
By	Miss Pitchayanan Kamsaeng
Field of Study	Biochemistry and Molecular Biology
Thesis Advisor	Assistant Professor Kunlaya Somboonwiwat, Ph.D.

Accepted by the Faculty of Science, Chulalongkorn University in Partial Fulfillment of the Requirements for the Master's Degree

.....Dean of the Faculty of Science
(Professor Supot Hannongbua, Dr.rer.nat.)

THESIS COMMITTEE

.....Chairman
(Professor Anchalee Tassanakajon, Ph.D.)

.....Thesis Advisor
(Assistant Professor Kunlaya Somboonwiwat, Ph.D.)

.....Examiner
(Associate Professor Teerapong Buaboocha, Ph.D.)

.....External Examiner
(Pikul Jiravanichpaisal, Ph.D.)

พิชญานันท์ คำแสง : ฤทธิ์ต้านแบคทีเรียและการควบคุมยีนของแอนติลิโพพอลิแซ็กคาไรด์แฟกเตอร์จากกุ้งกุลาดำ *Penaeus monodon* (ANTIBACTERIAL ACTIVITY AND GENE REGULATION OF ANTILIPOPOLYSACCHARIDEFACTOR FROM BLACK TIGER SHRIMP *Penaeus monodon*) อ.ที่ปรึกษาวิทยานิพนธ์หลัก: ผศ. ดร. กุลยา สมบูรณ์วิวัฒน์, 104 หน้า.

แอนติลิโพพอลิแซคคาไรด์แฟกเตอร์ (Antilipopolysaccharide factor, ALF) เป็นเปปไทด์ต้านจุลชีพที่พบในสัตว์ไม่มีกระดูกสันหลัง ในกุ้งกุลาดำ *Penaeus monodon* พบ ALF*Pm*s ทั้งหมด 6 ไอโซฟอร์ม โดยพบว่า ALF*Pm*6 มีบทบาทสำคัญในระบบภูมิคุ้มกันของกุ้งในการต้านเชื้อโรคที่รุกราน ในงานวิจัยนี้ได้ศึกษาคุณสมบัติของโปรตีน ALF*Pm*6 โดยทำการโคลนยีนที่ถอดรหัสให้โปรตีน ALF*Pm*6 เข้าสู่จีโนมของยีสต์ *Pichia pastoris* สายพันธุ์ KM71 และทำการผลิตโปรตีนรีคอมบิแนนท์ ALF*Pm*6 (rALF*Pm*6) โดยโปรตีน rALF*Pm*6 มีขนาดประมาณ 12 กิโลดาลตัน และมีค่า pI 9.69 จากนั้นนำโปรตีนรีคอมบิแนนท์หยาบที่ได้ไปทดสอบฤทธิ์ในการต้านเชื้อแบคทีเรีย พบว่าสามารถต้านเชื้อแบคทีเรียแกรมบวก *Bacillus megaterium* และแบคทีเรียแกรมลบ *Escherichia coli* 363 ได้ เนื่องจากไม่สามารถทำบริสุทธิ์โปรตีน rALF*Pm*6 ได้ ดังนั้นจึงทำการสังเคราะห์เปปไทด์ซึ่งมีลำดับกรดอะมิโนของวงแหวน LPS-binding site ของโปรตีน ALF*Pm*6 (cALF*Pm*6#29-52) และนำมาทดสอบฤทธิ์ในการต้านเชื้อแบคทีเรีย พบว่าเปปไทด์ cALF*Pm*6#29-52 สามารถต้านเชื้อแบคทีเรียแกรมลบ *E. coli* 363 และแบคทีเรียแกรมบวก *B. megaterium Aerococcus viridans* และ *Micrococcus luteus* และมีค่า MBC เท่ากับ 25-50 ไมโครโมลาร์ จากการทดสอบปฏิกิริยาการเกาะกลุ่มของแบคทีเรีย (Bacterial agglutination) พบว่าเปปไทด์สังเคราะห์ cALF*Pm*6#29-52 ทำให้เกิดการเกาะกลุ่มของแบคทีเรียและส่งผลให้เกิดการยับยั้งเชื้อแบคทีเรีย นอกจากนี้ได้ศึกษาการควบคุมการแสดงออกของยีน ALF*Pm*3 และ ALF*Pm*6 เริ่มจากการหาลำดับนิวคลีโอไทด์บริเวณปลาย 5′ ของยีน ALF*Pm*3 และ ALF*Pm*6 โดยใช้เทคนิค Genome walking ได้ลำดับนิวคลีโอไทด์ทางปลาย 5′ ของยีน ALF*Pm*3 และ ALF*Pm*6 ความยาว 1780 และ 504 bp ตามลำดับ เมื่อวิเคราะห์ลำดับนิวคลีโอไทด์ดังกล่าวพบ Transcription factor (TF)-binding site หลายตำแหน่ง จากการทดสอบโปรโมเตอร์โดยเทคนิค narrow down พบว่าบริเวณสำคัญที่เกี่ยวข้องกับการควบคุมการแสดงออกของยีน ALF*Pm*3 และ ALF*Pm*6 คือตำแหน่งนิวคลีโอไทด์ที่ -814 ถึง +302 และ -282 ถึง +85 ตามลำดับ โปรโมเตอร์ของยีน ALF*Pm*3 ที่ตำแหน่งนิวคลีโอไทด์ที่ -814 ถึง -266 ประกอบด้วย TF-binding site ได้แก่ SP-1 ICSBP NF-**K**B และ ลำดับเบสซ้ำ tandem repeat GAAAGAGAGTAAGAG[T/C] 21 หน่วย และโปรโมเตอร์ของยีน ALF*Pm*6 ที่ตำแหน่งนิวคลีโอไทด์ที่ -282 ถึง -81 ประกอบด้วย TF-binding site ได้แก่ SP-1 ICSBP Oct-1 และ C/EBPβ จากนั้นใช้เทคนิค Site-directed mutagenesis ในการตรวจสอบตำแหน่งที่มีผลต่อการแสดงออกของยีน พบว่าที่ตำแหน่ง -280 ถึง -270 ของยีน ALF*Pm*3 ซึ่งคาดว่าเป็นบริเวณจับของ NF-**K**B และ ที่ตำแหน่ง -88 ถึง -78 ของยีน ALF*Pm*6 ซึ่งคาดว่าเป็นบริเวณจับของ C/EBPβ น่าจะเป็น ตำแหน่งที่มี activator มาจับและควบคุมการแสดงออกของยีน นอกจากนี้ ในการทดลองลดการแสดงออกของยีน MyD88 และ Relish ในกุ้งที่ติดเชื้อ *Vibrio harveyi* พบว่า การแสดงออกของยีน ALF*Pm*3 น่าจะถูกควบคุมผ่านทั้ง Toll และ IMD pathway ในขณะที่ ALF*Pm*6 น่าจะถูกควบคุมผ่าน Toll pathway

ภาควิชา ชีวเคมี ลายมือชื่อนิสิต .....

สาขาวิชา ชีวเคมีและชีววิทยาโมเลกุล ลายมือชื่อ อ.ที่ปรึกษาหลัก .....

ปีการศึกษา 2557

5572063223 : MAJOR BIOCHEMISTRY AND MOLECULAR BIOLOGY
KEYWORDS: ANTILIPOPOLYSACCHARIDE FACTOR, ANTIMICROBIAL PEPTIDE, GENE REGULATION, TRANSCRIPTION FACTOR BINDING SITE, SIGNALING PATHWAY

PITCHAYANAN KAMSAENG: ANTIBACTERIAL ACTIVITY AND GENE REGULATION OF ANTILIPOPOLYSACCHARIDEFACTOR FROM BLACK TIGER SHRIMP *Penaeus monodon*. ADVISOR: ASST. PROF. KUNLAYA SOMBOONWIWAT, Ph.D., 104 pp.

Antilipopolysaccharide factor (ALF) is one of the antimicrobial peptide families identified in invertebrates. Six different isoforms of the ALF homologues have been identified from *Penaeus monodon*. Previously, ALF*Pm*6 has been shown to possibly play an important role in shrimp immunity against pathogen invasions. To further characterize ALF*Pm*6, the nucleotide sequences coding for mature peptide of ALF*Pm*6 were cloned and expressed in *Pichia pastoris* strain KM71. The recombinant ALF*Pm*6 protein (rALF*Pm*6) with the expected size and pI of 12 kDa and 9.69, respectively, was successfully produced. The crude rALF*Pm*6 protein showed antibacterial activities against both Gram-positive and Gram-negative bacteria, such as *Bacillus megaterium* and *Escherichia coli* 363*,* respectively. Because of the unsuccessful rALF*Pm*6 purification, the synthetic cyclic ALF*Pm*6#29-52 peptide (cALF*Pm*6#29-52) corresponding to ALF*Pm*6 LPS-binding site was synthesized and analyzed for antibacterial activity. It exhibited the growth inhibition activity against some tested bacteria such as a Gram-negative bacterium, *E. coli* 363 as well as Gram-negative bacteria, *B. megaterium*, *Aerococcus viridans,* and *Micrococcus luteus,* with MBC value of 25-50 μM. Bacterial agglutination assay indicated that cALF*Pm*6#29-52 induced bacterial agglutination mediated bacterial killing. Herein, the regulation of ALF*Pm*3 and ALF*Pm*6 gene expression was also studied. The 5′-upstream sequences of ALF*Pm*3 (1780 bp) and ALF*Pm*6 (504 bp) genes were identified by genome walking technique. Sequence analysis of ALF*Pm*3 and ALF*Pm*6 promoters identified several putative transcription factor (TF)-binding sites. Using narrow down assay, ALF*Pm*3 and ALF*Pm*6-promoter active regions located at nucleotide position (-814/+302) and (-282/+85), respectively, were identified. ALF*Pm*3 promoter active region contained TF-binding sites of SP-1, ICSBP, and NF-**K**B plus 21 units of GAAAGAGAGTAAGAG[T/C] tandem repeat. ALF*Pm*6 promoter active region contained TF-binding sites of SP-1, ICSBP, Oct-1, and C/EBPβ. Afterthat, the activator-binding sites from -814 to -266 of ALF*Pm*3 promoter and -282 to -81 of ALF*Pm*6 promoter were identified. Site-directed mutagenesis at the conserved nucleotide of selected TF-binding sites revealed that Rel/NF-**K**B binding site (-280/-270) and C/EBPβ (-88/-78) binding site were the activator-binding site of ALF*Pm*3 and ALF*Pm*6 promoters, respectively. RNAi knockdown of MyD88 and Relish genes in *Vibrio harveyi*-infected shrimp suggested that ALF*Pm*3 gene expression might be regulated by both Toll and IMD pathways, while ALF*Pm*6 gene expression might be regulated by Toll pathway.

Department: Biochemistry Student's Signature .....
Field of Study: Biochemistry and Molecular Biology Advisor's Signature .....
Academic Year: 2014

ACKNOWLEDGEMENTS

I would like to thank for an intensive support from Assistant Professor Dr. Kunlaya Somboonwiwat, my advisor. Thank you for a very good advice, guidance, enthusiasm and best caring of my livelihood from the beginning to the end of my thesis.

It is a pleasure to thank Professor Dr. Anchalee Tassanakajon, Associate Professor Dr. Teerapong Buaboocha, and Dr. Pikul Jiravanichpaisal for giving me your precious time on being my thesis defense committee and for their valuable comments and also useful suggestions.

My appreciation is also to Associate Professor Dr. Vichien Rimpanitchayakit, Assistant Professor, Dr. Kuakarun Krusong, Dr. Premruethai Supungul, and Miss Sureerat Tang for instruction, warm support, interesting discussion and helping. Thanks are also expressed to all members at CEMs laboratory for their helps and for friendships that help me enjoy throughout my study. Thanks to every friends of mine in the department of Biochemistry and Biotechnology.

I thank a financial support from Thailand Research Fund to A.T. (TRF Senior Scholar No. RTA5580008) and fellowship from the 90th Anniversary of Chulalongkorn University Fund grant for a very generous research support.

Finally, indispensable persons and my gratefulness are my parents and all members in my family for their guidance, understanding, encouragement, endless love, and support along my education.

CONTENTS

Page

THAI ABSTRACT iv

ENGLISH ABSTRACT v

ACKNOWLEDGEMENTS vi

CONTENTS vii

LIST OF TABLES 1

LIST OF FIGURES 1

CHAPTER I INTRODUCTION 1

1.1 General introduction 1

1.2 Disease emergence in shrimp 4

1.2.1 Acute hepatopancreatic necrosis disease (EMS/AHPND) 4

1.2.2 White spot syndrome virus (WSSV) 5

1.3 Shrimp immunity 6

1.4 Antimicrobial peptides 8

1.5 Antilipopolysaccharide factor 9

1.6 Signaling pathways regulating AMP gene 12

1.7 Objective of this thesis 16

CHAPTER II MATERIALS AND METHODS 17

2.1 Materials 17

2.1.1 Equipments 17

2.1.2 Chemicals and Reagents 18

2.1.3 Kits 21

2.1.4 Enzymes 21

Page

2.1.5 Antibiotics 22

2.1.6 Bacterial, yeast and virus strains 22

2.1.7 Softwares 22

2.1.8 Vectors 23

2.2 Expression and characterization of antilipopolysaccharide factor isoform 6 (ALF*Pm*6) 23

2.2.1 Transformation of pALF*Pm*6 into *Pichia pastoris* KM71 23

2.2.2 Screening for the transformants with multiple copy inserts 24

2.2.3 Determination of the integrated ALF*Pm*6 gene in *P. pastoris* genome by PCR technique 25

2.2.4 Expression of recombinant clone 25

2.2.5 Optimization of the condition for the rALF*Pm*6 production 26

2.2.5.1 Effect of cell density on the rALFPm6 protein production 26

2.2.5.2 Effect of induction time on the rALFPm6 protein production 26

2.2.5.3 Effect of temperature on the rALFPm6 protein production 27

2.2.6 Purification of the rALF*Pm*6 protein 27

2.2.7 Antibacterial activity assay 29

2.2.8 Bacterial agglutination assay 30

2.3 Characterization of the ALF*Pm* gene regulation 30

2.3.1 Identification of the promoter of ALF*Pm* gene 30

2.3.2 Prediction of transcription factor binding site on ALF*Pm*3 and ALF*Pm*6 promoter fragments by bioinformatic analysis 32

2.3.3 Construction of the luciferase reporter plasmid containing the ALF*Pm* promoter 32

Page

2.3.4 Promoter activity assay 34

2.3.5 Determination of the regulatory element involved in ALF*Pm*3 and ALF*Pm*6 gene regulation 35

2.3.5.1 Deletion assay 35

2.3.5.2 Site-directed mutagenesis technique 36

2.4 Effect of MyD88 and Relish gene knockdown on the ALF*Pm*3 and ALF*Pm*6 gene expression 38

2.4.1 Preparation of double strand RNA (dsRNA) 38

2.4.2 Total RNA extraction 40

2.4.3 Determination of the quantity and quality of RNA samples 40

2.4.4 DNase treatment of total RNA samples 41

2.4.5 First-strand cDNA synthesis 41

2.4.6 Silencing efficiency of MyD88 dsRNA and Relish dsRNA 41

2.4.7 Preparation of *Vibrio harveyi* infected shrimp 42

2.4.8 MyD88 dsRNA and Relish dsRNA mediated gene knockdown in *V. harveyi* infected shrimp 43

CHAPTER III RESULTS 45

3.1 Expression and characterization of ALF*Pm*6 45

3.1.1 Transformation of pALF*Pm*6 into *P. pastoris* 45

3.1.2 Screening of the recombinant clones expressing rALF*Pm*6 48

3.1.3 Optimization of the rALF*Pm*6 protein production 51

3.1.3.1 Effect of cell density and induction time on the rALFPm6 protein production 51

3.1.3.2 Effect of temperature on the rALFPm6 protein production 53

Page

3.1.4 Purification of the rALF*Pm*6 protein 54

3.1.5 Antimicrobial activity of ALF*Pm*6-derived synthetic peptide 59

3.1.6 Bacterial agglutination property 61

3.2 Characterization of the ALF*Pm*3 and ALF*Pm*6 gene regulation 63

3.2.1 Promoter sequence identification of ALF*Pm*3 and ALF*Pm*6 gene 63

3.2.2 Determination of regulatory elements of ALF*Pm*3 and ALF*Pm*6 gene by bioinformatic analysis 65

3.2.3 Narrow down assay of ALF*Pm*3 and ALF*Pm*6 promoter activity in *Drosophila* S2 cell 67

3.2.4 Determination of the regulatory element involved in ALF*Pm*3 gene regulation 72

3.2.5 Determination of the regulatory element involved in ALF*Pm*6 gene regulation 75

3.3 Effect of knocking-down MyD88 and Relish gene on the transcript level of ALF*Pm*3 and ALF*Pm*6 in the *V. harveyi*-infected *P. monodon* 78

3.3.1 Silencing efficiency of MyD88 dsRNA and Relish dsRNA 78

3.3.2 Effect of MyD88 and Relish gene knockdown on the ALF*Pm*3 and ALF*Pm*6 gene expression 80

CHAPTER IV DISCUSSIONS 83

CHAPTER V CONCLUSIONS 90

REFERENCES 92

VITA 104

LIST OF TABLES

Table1. 1 Types, number of sequences, diversity and antimicrobial activities of the *Penaeus monodon* AMPs from the EST database 9

Table2. 1 The purification condition for rALFPm6 protein 28

Table2. 2 List of primers used for genome walking experiment 32

Table2. 3 List of primers used to amplify ALFPm3 and 6 promoter fragments 34

Table2. 4 List of primers used for site-directed mutagenesis of transcription factor binding sites on ALFPm promoter region 37

Table2. 5 List of primers used for RNA interference 39

Table2. 6 Primer pairs used for quantitative realtime RT-PCR amplification 42

Table2. 7 Primer pairs used for PCR amplification 44

Table3. 1 The deduced amino acid sequence, predicted molecular weight and pI of rALF*Pm*6 46

LIST OF FIGURES

Figure1. 1 The global production of shrimp aquaculture in period from 1995 to 2016. 3

Figure1. 2 The global production of shrimp aquaculture in period from 2009 to 2016. 3

Figure1. 3 Juvenile *Penaeus vannamei* from VietNam showing gross signs of EMS/AHPND 5

Figure1. 4 White spot syndrome virus (WSSV)-infected shrimp 6

Figure1. 5 A schematic model of the shrimp immune system 7

Figure1. 6 The primary and NMR structure of an ALF*Pm*3 from *Penaeus monodon.* 10

Figure1. 7 Comparison of Toll pathways in shrimp and Drosophila (Li and Xiang 2013a). 14

Figure1. 8 Comparison of IMD pathways in shrimp and Drosophila (Li and Xiang 2013a). 15

Figure3. 1 Preparation of SacI-linearized pALF*Pm*6 plasmid for Pichia pastoris KM71 transformation. 46

Figure3. 2 Screening for recombinant yeast containing multi-copy of ALF*Pm*6-expression cassette. 47

Figure3. 3 Analysis of rALF*Pm*6 expression from *P. pastoris* transformants by 15% silver-stained SDS-PAGE 49

Figure3. 4 Antibacterial activity assay of the crude rALF*Pm*6 protein. 50

Figure3. 5 Effect of cell density and induction time on the rALF*Pm*6 protein expression level. 52

Figure3. 6 Effect of temperature on the rALF*Pm*6 protein expression. 53

Figure3. 7 The crude rALF*Pm*6 protein was purified by using 5 ml HiTrap SP HP column (Condition 1)..... 56

Figure3. 8 The crude rALF*Pm*6 protein was purified by using 5 ml HiTrap SP HP column (Condition 2)..... 57

Figure3. 9 The crude rALF*Pm*6 protein was purified by using 5 ml HiTrap SP HP column (Condition 3)..... 57

Figure3. 10 The crude rALF*Pm*6 protein was purified by using 5 ml HiTrap SP HP column (Condition 4)..... 58

Figure3. 11 The crude rALF*Pm*6 protein was purified by using 5 ml HiTrap SP HP column (Condition 5)..... 58

Figure3. 12 Bacterial agglutination mediated by the synthetic cyclic peptide ALFPm6#29-52 (cALFPm6#29-52)..... 62

Figure3. 13 Identification of 5′-upstream sequences of ALF*Pm*3 and ALF*Pm*6 genes by Genome walking technique. 64

Figure3. 14 Genomic sequence of the 5′-upstream region of ALF*Pm*3 (A) and ALF*Pm*6 (B) genes.. 66

Figure3. 15 Functional mapping of the deletion ALF*Pm*3 promoter. 70

Figure3. 16 Functional mapping of the deletion ALF*Pm*6 promoter sequence from position -418 to -80. 71

Figure3. 17 Effect of deleting the 21 units of [GAAAGAGAGTAAGAG(T/C)] tandem repeat on the position -693 to -358 from the ALF*Pm*3 promoter region. 73

Figure3. 18 The consensus and mutated sequences of transcription factor binding sites on the activator-binding region of ALF*Pm*3 and ALF*Pm*6 promoter..... 74

Figure3. 19 Site-directed mutagenesis of transcription factor binding site NF-ĸB on the ALF*Pm*3 promoter active region (-814/-265). 76

Figure3. 20 Site-directed mutagenesis of transcription factor binding sites on the ALF*Pm*6 promoter active region (-282/+85). 77

Figure3. 21 Efficiency of MyD88 and Relish gene silencing mediated by dsRNA in shrimp. 79

Figure3. 22 The MyD88 and Relish gene silencing in *Vibrio harveyi*-infected shrimps. 81

Figure3. 23 Expression of ALF*Pm*3 82

CHAPTER I
INTRODUCTION

1.1 General introduction

The cultured shrimp, mainly the black tiger shrimp (*Penaeus monodon*) and the white shrimp (*Penaeus vannamei*), make an important contribution to Thailand's aquaculture industry. Since 1990, Thailand had been the biggest black tiger shrimp exporter. Shrimp farming contributes a multi-billion dollar and major income to Thailand (Source: Office of Agricultural Economics in cooperation with the Customs Department). The rapid growth of shrimp farming lead to an economic boom. Unfortunately, the increase of shrimp farming came together with several problems of shrimp culturing such as the waste water from the shrimp farm or outbreak diseases. Especially, the outbreaks of viral and bacterial diseases have seriously affected to shrimp industry. These result in the decline of production of the black tiger shrimp production. Therefore, shrimp-farming pattern has changed over and the alternative species such as non-native white shrimp *P. vannamei* had taken over the place of native black tiger shrimp because of the high survival rate and pathogen resistance. Moreover, it has rapid growth, high stocking density tolerance, and low salinities and temperatures tolerance.

According to FAO data, global shrimp production increased approximately at the rate of 4.4 percent per year on average from 2006 to 2012, reaching about 4 million MT in 2012. Between 2012 and 2013, there was a substantial decline in the global production about 19 percent. But based on the survey, it is expected that from 2014 to 2016, the production will recover and reach a growth rate of approximate 8 percent per year (Fig. 1.1).

In 2011, the white shrimp production reached 78 percent of the total global farmed shrimp production while black tiger shrimp production was only 22 percent of the total production. FAO data showed that China is the first world producer of white shrimp with a production of 1.32 million tons in 2011. Thailand and Ecuador ranked in the second and third positions. The shrimp production reached 511,000 tons in Thailand and 260,000 tons in Ecuador. Vietnam is the leading producer of black tiger shrimp in the world with a production of 300,000 tons in 2011, followed by India and Indonesia with a production of 187,900 tons and 126,200 tons respectively.

Since late 2012, farmers in East Asia-from China to Malaysia lost millions of dollars of crops because of the EMS (Early Mortality Syndrome) disease outbreak. The EMS disease first surfaced in China in 2009 and spread into Thailand, Malaysia and Vietnam in the subsequent years. These results in farmed shrimp production declined drastically in 2013. Supply short falls were large and sharp in China, Thailand and Vietnam while shrimp prices increased in the world market. Farming areas extended and intensified in Indonesia and India who did not suffer by EMS. However, their extra supplies were not enough to offset over all large short falls in Asia (Fig. 1.2).

Although this new emerging disease got the attention from the researcher, the knowledge on disease remains limited and the outbreak disease are uncontrollable. Not only this new emerging disease, other infectious diseases are also the problems for shrimp aquaculture. Therefore, to improve the shrimp farming industry in Thailand, the understanding of shrimp immunity and development of agriculture technology should be intensively studied.

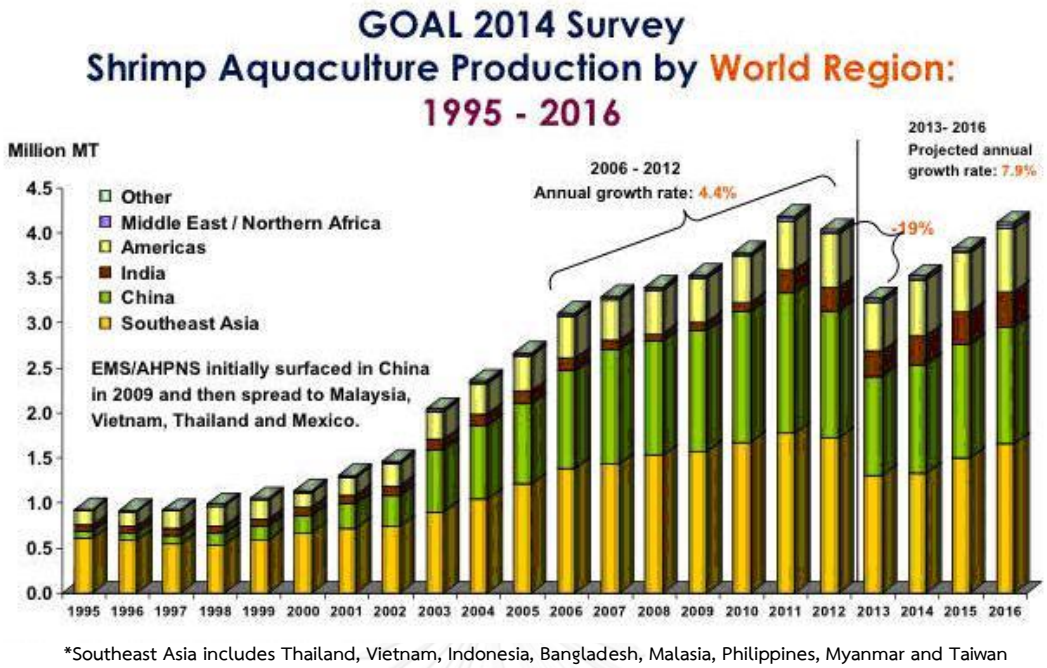

Figure 1.1 The global production of shrimp aquaculture in period from 1995 to 2016 (Sources: FAO (2014) for 1995-2012; GOAL (2014) for 2013-2016).

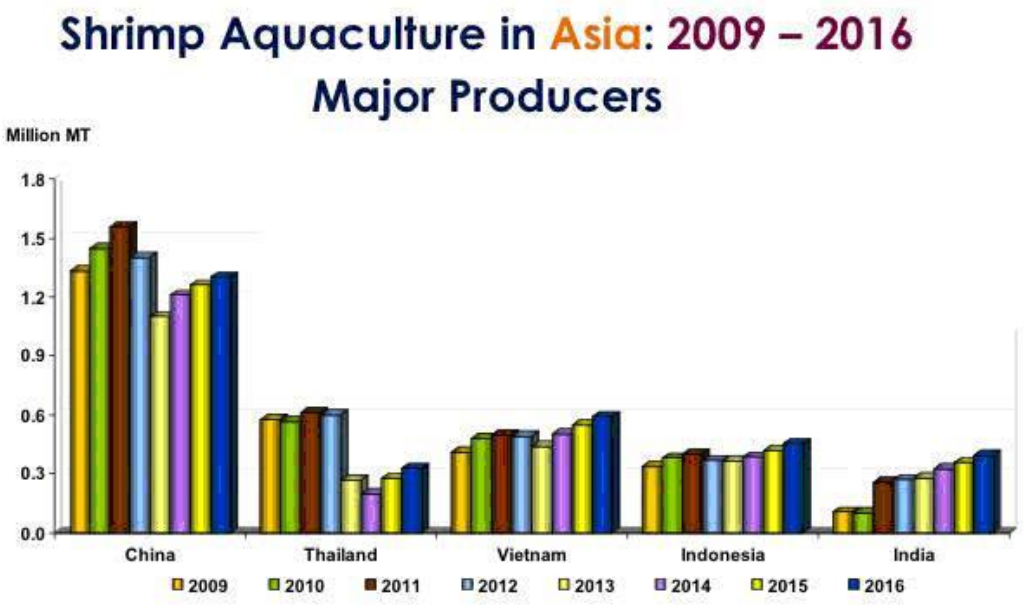

Figure 1.2 The global production of shrimp aquaculture in period from 2009 to 2016 (Sources: FAO (2014) for 2009-2012; GOAL (2014) for 2013-2016).

1.2 Disease emergence in shrimp

In the present day, white spot syndrome virus (WSSV) and bacteria *Vibrio* species (Saulnier et al. 2000, Flegel 2007, Lightner et al. 2012) considered mainly pathogens of infectious diseases in Thailand. The major virulent strains of *Vibrio* in shrimp such as *V. harveyi*, *V. arginolyticus* and *V. parahaemolyticus.* The virulent strains cause extream losses of cultured *P. monodon* in hatcheries and shrimp farm. So, the prevention and control of diseases turned into a priority for shrimp production.

1.2.1 Acute hepatopancreatic necrosis disease (EMS/AHPND)

Since 2009, an emerging disease of farmed Penaeid shrimp, EMS, or known as acute hepatopancreatic necrosis disease (AHPND) has caused significant mortality, up to 100%, in populations of both *P. vannamei* and *P. monodon* cultured in Southeast Asian and in Mexico. In 2010, the range of affected farms in China had expanded, and by 2011, AHPND was confirmed in Vietnam and Malaysia (Lightner et al. 2012, Mooney 2012). AHPND reached Thailand in 2012 (Flegel 2012, Leaño and Mohan 2012). The disease develops quickly, starting approximately 8 days after the ponds are stocked, and severe mortalities occur during the first 20 to 30 days of culture. Infected shrimp shows that the disease cause a significantly pall atrophied hepatopancreas (Fig. 1.3), in which the tubule epithelial cells degenerate, round up, detach from the basement membrane, and then slough into the tubule lumen. At terminal stages, the hepatopancreas shows extensive intertubular, hemocytic aggregations. The affected shrimp die from hepatopancreas dysfunction and from secondary *Vibrio* infections. The causative agent of AHPND has been reported to be *V. parahaemolyticus*, which causes it to release a potent toxin (Tran et al. 2013).

The genome sequences of pathogenic and non-pathogenic strains of *V. parahaemolyticus* revealed that a plasmid contains 2 toxic genes homologous with *Photorhabdus* insect-related (Pir) toxin genes was found in pathogenic AHPND-strains but was absent in non-pathogenic strains (Kondo et al. 2014). The Pir toxins act as binary proteins, which encoded by the PirA and PirB genes, and both proteins are necessary for oral toxicity in moths and mosquitoes (Blackburn et al. 2006, Ahantarig et al. 2009). AHPND-affected shrimp have pathological responses similar to the Pir midgut toxicity in insects that results in severe swelling and shedding of the apical membranes (Blackburn et al. 2006). So far, the knowledge on this new emerging disease is limited. Therefore, the outbreaks are uncontrollable. To maintain the shrimp farming

industry in Thailand, the understanding of shrimp immunity and development of agriculture technology should be intensively studied.

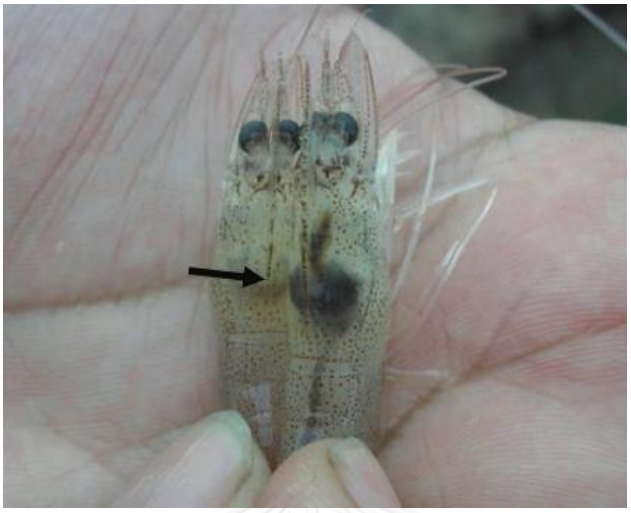

http://www.fao.org/docrep/018/i3422e/i3422e.pdf

Figure 1.3 Juvenile *Penaeus vannamei* from VietNam showing gross signs of EMS/AHPND, specifically a pale atrophied hepatopancreas and an empty stomach and midgut (Source:FAO 2013).

1.2.2 White spot syndrome virus (WSSV)

White spot syndrome virus (WSSV) has spread rapidly to shrimp farming all over the world and become one of the major pathogens causing white spot syndrome (WSD) in cultured shrimp (Lo et al. 1996). WSSV can infect a wide range of aquatic crustaceans especially decapod, including marine, brackish and freshwater prawns, crabs, crayfish and lobsters (Maeda et al. 2000). The major targets of WSSV infection are tissues of ectodermal and mesodermal embryonic origin, especially the cuticular epithelium and subcuticular connective tissues (Inouye et al. 1994, Wonteerasupaya et al. 1995). The gross sign of WSD are white spot on carapace of shrimp and loose cuticle. Several preventive and curative measures have been developed though not successfully implemented in shrimp farms such as vaccination (Rout et al. 2007, Satoh, Nishizawa and Yoshimizu 2008) immunostimulants (Khimmakthong et al. 2013) direct neutralization by antiviral proteins (Dupuy, Bonami and Roch 2004, Tharntada et al. 2009) and RNAi (Ongvarrasopone et al. 2008). In addition, innate immunity in shrimp has been studied intensively to understand the response of shrimp to viral infection (Liu et al., 2009). It is believed that the envelope proteins of virus might be important roles in viral infections (Li et al. 2009).

Figure 1.4 White spot syndrome virus (WSSV)-infected shrimp

1.3 Shrimp immunity

The understanding of innate immune system of penaeid shrimp is greatly motivated by economical requirements, because their culture is limited by the evolution of infectious diseases. Shrimp's natural immunity acts as a fast and efficient defense mechanism against the pathogens. The innate immune response triggers diverse humoral and cellular activities via signal transduction pathways (Fig. 1.5). The major defense responses are carried out in the hemolymph that contains 3 different types of hemocyte including hyalin, granular and semigranular hemocyte (Martin and Grave 1985). Cellular defense components include all those reaction performed direcly by cells. The cellular immune reactions include phagocytosis, nodulation and encapsulation. While the humoral components involve in production of soluble components playing roles in the defense system. The humoral responses include the anticoagulant protein, agglutinin, prophenoloxidase (proPO) system, antimicrobial peptides (AMPs), and proteinase inhibitor (Söderhäll 1999, Jiravanichpaisal, Lee and Soderhall 2006)

The immune responses of innate immunity include immune recognition, signal transduction and effector molecules. Pattern recognition is the first step of innate immunity. Pattern recognition receptors (PRRs) sense the presence of infection and leads to rapid humoral and cellular immune responses. PRRs recognize pathogens by binding to pathogen-associated molecular patterns (PAMPs). These molecular patterns are usually the polysaccharides and glycoproteins on the surface of microbes, such as lipopolysaccharide (LPS) from Gram-negative bacteria, peptidoglycan (PGN) and lipotechoic acid (LTA) from Gram-positive bacteria, and glucans from fungal cells. PRRs, as a set of germline-encoded receptors play very important roles in innate immunity

(Akira, Uematsu and Takeuchi 2006). A series of PRRs including LPS and β-1,3-glucan binding protein (LGBP), Toll-like receptor, lectin, and tetraspanin have been identified in penaeid shrimp (Li and Xiang 2013a).

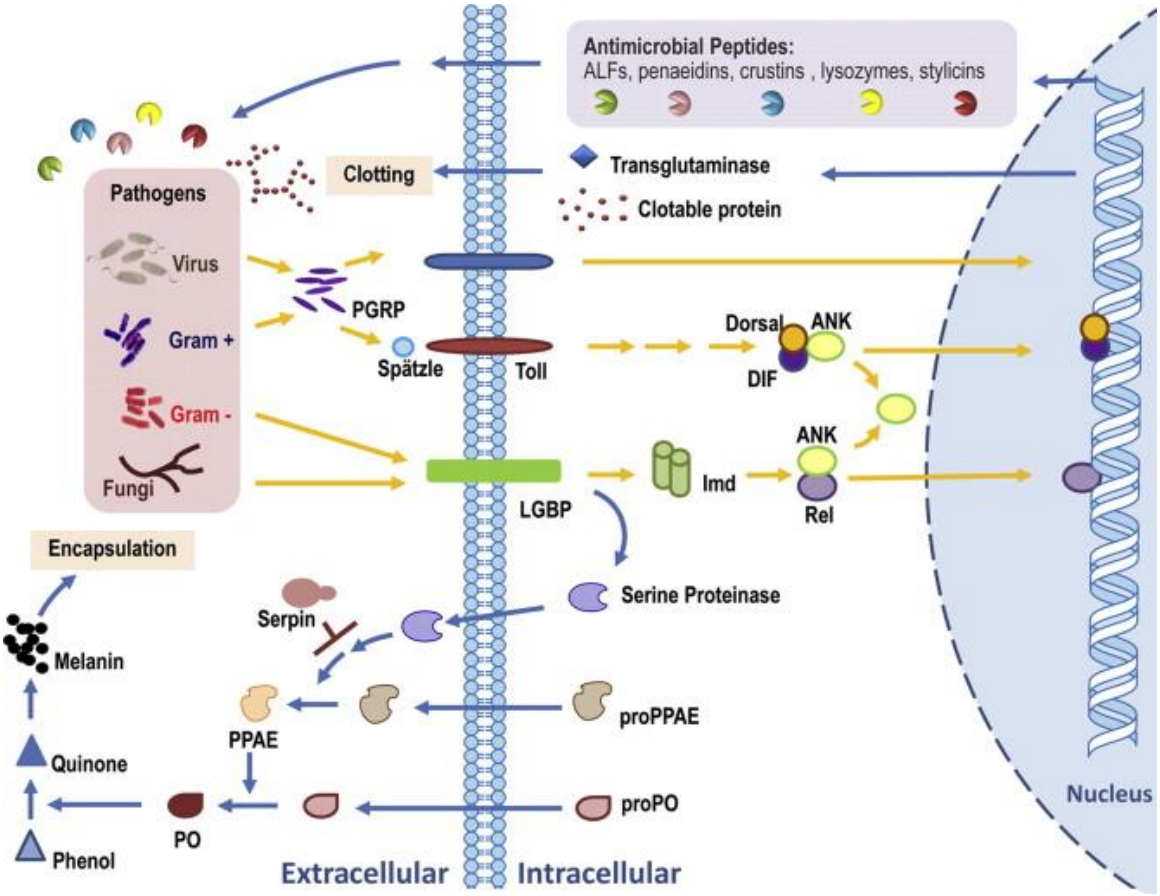

Figure 1.5 A schematic model of the shrimp immune system (Tassanakajon et al. 2013).

1.4 Antimicrobial peptides

Antimicrobial peptides (AMPs), ubiquitously found in all living organisms, are important immune effectors with an ability to neutralize or kill invading microorganisms (Brown and Hancock 2006). AMPs are typically small size, generally less than 150-200 amino acid residues, and have amphipathic structure and cationic property. These peptides are active against a broad spectrum of microorganisms such as bacteria, virus, yeast, parasite, and fungi. AMPs may also exhibit an anti-tumor activity (Cruciani et al. 1991, Hancock and Diamond 2000, Krepstakies et al. 2012). The first AMP family discovered in shrimp is penaeidin of the Pacific white shrimp, *P. vannamei* (Destoumieux et al. 1997) and exhibits antimicrobial activity against Gram-positive bacteria and fungi. Thereafter, other shrimp AMP families had been reported in various shrimp species such as crustins, antilipopolysaccharide factors (ALFs), lysozymes, and stylicins (Amparyup, Donpudsa and Tassanakajon 2008a, Amparyup et al. 2008b, Bartlett et al. 2002, Hikima et al. 2003, Sotelo-Mundo et al. 2003, Supungul et al. 2004).

The antibacterial mechanism of AMPs can be divided into two mechanism including transmembrane pore-forming and intracellular antimicrobial activity (Brogden 2005, Jenssen, Hamill and Hancock 2006). Most of AMPs appear to act on bacteria using a transmembrane pore-forming mechanism via interaction with the cell membrane components leading to pore formation and leakage of the bacterial cytoplasmic contents. The pore forming mechanism was categorized into 4 distinct models including aggregate, barrel-stave, carpet and toroidal-pore models. Moreover, the AMPs may pass through the cell membrane and enter the cells. They might bind to macromolecules and interrupt the synthesis of vital components, such as DNA, RNA and proteins, and resulting in cell death.

Shrimp AMPs are primarily expressed in hemocytes that migrated to infection sites and AMPs are secreted into the circulation as well as site of infection to fight against pathogen invasion (Tassanakajon et al. 2010). AMPs found in *P. monodon* were discovered mainly by means of expressed sequence tag (EST) analysis. These AMP sequences contained major AMPs such as penaeidins, crustins including single WAP domain (SWD) proteins, ALFs and lysozymes. Of these AMPs, crustins were the most abundant followed by penaeidins, ALFs and lysozymes, respectively (Table 1.1)

Table 1.1 Types, number of sequences, diversity and antimicrobial activities of the *Penaeus monodon* AMPs from the EST database (http://pmonodon.biotec.or.th) (Tassanakajon and Somboonwiwat, 2011)

Types	No. of sequences	No. of isoforms	Major isoform	Antimicrobial activities	References
Crustins					
Type II	275	7	Crustin*Pm* 1	Gram +	Supungul *et al.*, 2008
			Crustin*Pm* 5	Gram +	Vatanavicharn *et al.*, 2009
			Crustin-like *Pm*	Gram +	Amparyup *et al.*, 2008a
				Gram +, Gram-	
Type III (SWD)	50	3	SWD*Pm*2	Gram+, anti-subtilisin	Amparyup *et al.*, 2008b
ALFs	208	6	ALF*Pm*3	Gram +, Gram-, fungi	Somboonwiwat *et al.*, 2005
				Anti-virus	Thartada *et al.*, 2009
			ALF*Pm*2	Gram +, Gram-	Tharntada *et al.*, 2008
Penaeidins	284	2	PEN3	ND*	Tassanakajon *et al.*, 2008
			PEN 5	ND*	Tassanakajon *et al.*, 2008
Lysozymes	72	2	C-type	Gram+, Gram-	Supungul *et al.*, 2010
			I-type	Gram+, Gram-	

*ND is no data available.

1.5 Antilipopolysaccharide factor

Antilipopolysaccharide factors (ALFs) are antimicrobial peptides (AMPs) that have been found in horseshoe crabs and crustaceans. ALFs are highly cationic polypeptides of about 100 residues with a hydrophobic N-terminal region. ALFs are composed of 114–124 amino acid residues with a short signal peptide sequence of 16–26 residues. The molecular mass of the mature peptide is about 11 kDa. The theoretical p*I* of the mature peptide and LPS-BD of ALFs ranges from 5.35–10.35 and 4.37–10.95, respectively. The ALF was classified into two groups according to their pI as cationic ALF and anionic ALF (Tassanakajon, Somboonwiwat and Amparyup 2014).

ALFs are amphipathic peptides, which contain two-highly conserved-cysteine residues that form a stable disulfide loop harboring a highly conserved cluster of positively charged (Lys and Arg) residues. Typically, ALFs are highly hydrophobic at the N-terminal region and contain a conserved three-dimensional structure (Fig 1.6). The

3-D structures of ALF from horseshoe crab *Tachypleus tridentatus* and *Limulus polyphemus* (ALF-L) (Tanaka et al. 1982, Muta et al. 1987) and the shrimp *Penaeus monodon* (ALF*Pm*3) (Fig. 1.6) share a similar structure consisting in three α-helices packed against a four-stranded β-sheet (Hoess et al. 1993, Yang et al. 2009). ALFs are amphipathic peptides containing a LPS-binding domain, which is a β-hairpin structure linked by a conserved disulfide bridge. This stable disulfide loop harbors either a highly conserved cluster of positively charged (Lys and Arg) residues for cationic ALF or negatively charged (Glu and Asp) for anionic ALF and hydrophobic residues (Rosa et al. 2013b).

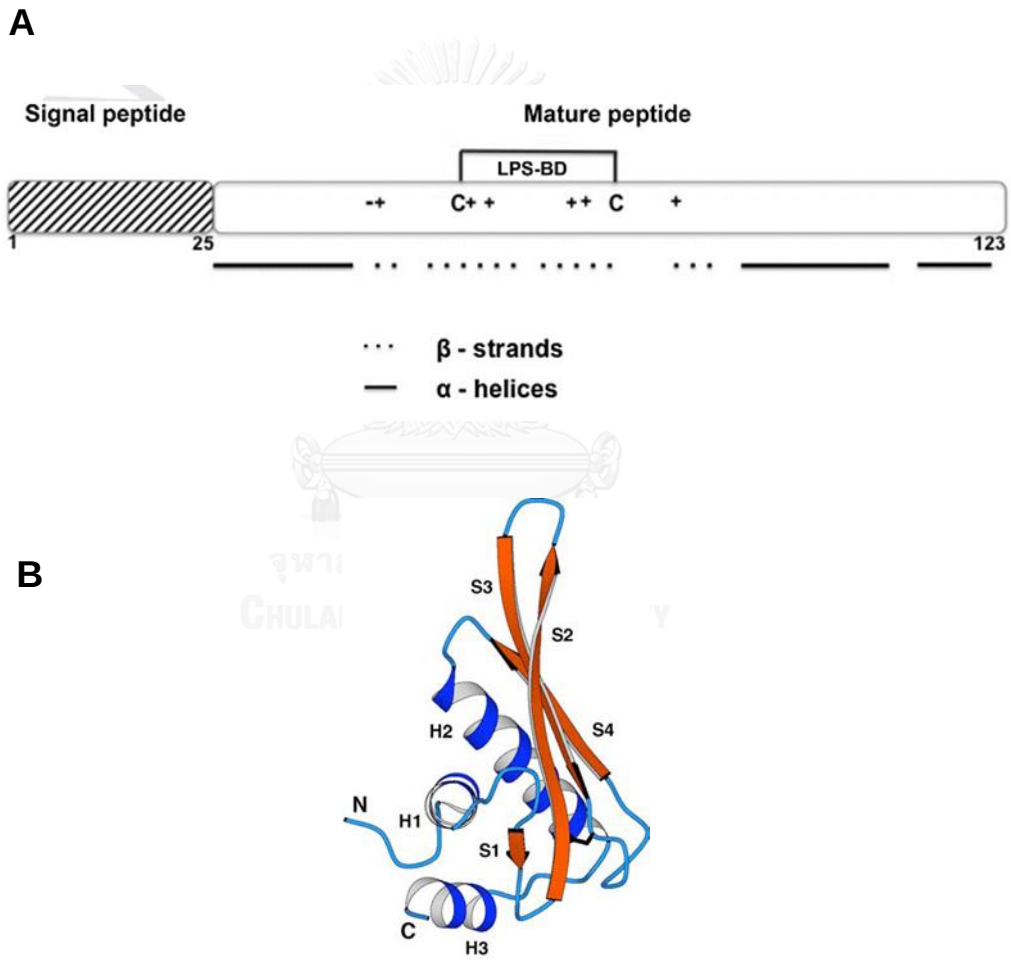

Figure 1.6 The primary and NMR structure of an ALF*Pm*3 from *Penaeus monodon*. A schematic illustration of the primary structure of ALF (A). Based on the resolved 3D-structure of ALF*Pm*3, ALF include three α-helices (solid lines) and a four-stranded ß-sheet (dashed line). ALF has a signal peptide of about 25 amino acid residues and a

mature peptide of 98 amino acid residues. The signature of ALF is the cluster of positive charged amino acids (+) within the disulfide bridge stabilized LPS-BD and the positive charged residues within the flanking ß-strands that are responsible for LPS recognition (Tassanakajon et al. 2014). The NMR-structure resolved by Yang et al, 2009 is shown (B).

Many reports showed that ALFs exhibit a potent antimicrobial activity against a broad range of microorganisms (Tassanakajon et al. 2010). At least 6 different isoforms (ALF*Pm*1-6) (Supungul et al. 2004, Prapavorarat, Pongsomboon and Tassanakajon 2010, Ponprateep et al. 2012) have been identified in the black tiger shrimp *P. monodon*. The difference in LPS-binding domain sequences probably correlates with their antimicrobial activity (Ponprateep et al. 2012). ALF*Pm*3 is the most abundant isoform found in the hemocytes of the black tiger shrimp. ALF*Pm*3 exhibits a broad antimicrobial activity spectrum against filamentous fungi, Gram-positive and Gram-negative including a high potency against the natural shrimp bacterial pathogen, *V. harveyi* (Somboonwiwat et al. 2005). Treating rALF*Pm*3 with *V. harveyi* cause membrane permeabilization and leakage of cytoplasmic components (Jaree, Tassanakajon and Somboonwiwat 2012). The antiviral property of the recombinant ALF*Pm*3 protein (rALF*Pm*3) against WSSV has been also reported inhibits WSSV propagation in crayfish hematopoietic cell culture and in shrimp (Tharntada et al. 2009). Recently, the neutralization effect on WSSV *in vivo* shown that the ALF*Pm*3 performs its anti-WSSV action by binding to the WSSV189 envelope protein and possibly other WSSV proteins (Suraprasit et al. 2014). These results suggested the important role of ALF*Pm*3 protein in the defense mechanism against WSSV infection and vibriosis in *P. monodon*. Although ALF*Pm*3 is found to be the major ALF isoform responsible for fighting against pathogen infection, interestingly, the other ALF*Pm* such as ALF*Pm*6 gene has been shown to be up-regulated in *P. monodon* hemocyte in response to the yellow head virus infection (Prapavorarat et al. 2010) and gene silencing of ALF*Pm*6 led to a significant increase in the cumulative mortality of *V. harveyi*-infected and WSSV-infected shrimp (Ponprateep et al. 2012). These imply that ALF*Pm*6 might be also important in shrimp immunity.

1.6 Signaling pathways regulating AMP gene

In *Drosophila*, the Toll and IMD pathways are clearly the two most important signaling pathways controlling antimicrobial peptide genes (Leclerc and Reichhart 2004, Tanji and Ip 2005, Lemaitre and Hoffmann 2007). The Toll pathway is mainly involved in defense against fungi, Gram-positive bacteria, and viruses (Lemaitre et al. 1996, Rutschmann et al. 2000, Xi, Ramirez and Dimopoulos 2008), while the IMD pathway plays key roles in controlling Gram-negative bacterial and virus infection.

Three Rel/NF-κB transcription factors, Relish, Dorsal and Dif, are involved in both signal transduction pathways of the innate immune response. Relish is required for the IMD pathway to activate the gene expression of antibacterial peptides (Hedengren et al. 1999), while Dorsal and Dif are activated in the successive signaling cascade of Toll pathway for antifungal and antibacterial responses (Belvin and Anderson 1996, Lemaitre, Reichhart and Hoffmann 1997).

The canonical component of the Toll pathway in *Drosophila* contains Spätzle, Toll, Pelle, Tube, MYD88, Cactus, Dorsal, Dorsal-related immunity factor (DIF) (Lemaitre and Hoffmann 2007). In shrimp, most of homologs to the components in Toll pathway of *Drosophila* were identified, including Spätzle, Toll receptor, Pelle, TRAF6, Dorsal, and their function in immune response of shrimp to bacteria or virus are supposed and deduced (Fig. 1.7) (Li and Xiang 2013b).

In mammals suites of 13 Toll-like receptors (TLRs) have been reported with a variety of identified ligands, including PAMPs originating from bacteria, fungi and viruses (West et al., 2006). The first Toll receptor was reported in *Drosophila melanogaster* as a gene whose products control dorsoventral polarity during embryogenesis (Belvin and Anderson 1996, Stein and Stevens 1991). Toll-like receptors have now been identified in *Penaeus monodon* (Arts et al. 2007), *Penaeus japonicus*, (Mekata et al. 2008), *P. vannamei* (Yang et al. 2007) and *P. chinensis* (Yang et al. 2008).

Three types from *P. vannamei* (LvToll1, LvToll2, and LvToll3) were all up regulated after WSSV challenge in gill tissue. LvToll2 could significantly activate the promoters of NF-κB pathway-controlled AMP genes, whereas LvToll1 and LvToll3 had no effect on them (Wang et al. 2012b). These data indicated that three types of TLRs in shrimp played important functions in the immune response of shrimp to bacteria and virus. The Spätzle proteins from *Fenneropenaeus chinensis* (FcSpz) and *P. vannamei* (LvSpz1-3) was identified and showed the up-regulation against *Vibrio* species and WSSV infections. They also affected the expression of certain antimicrobial peptides (Shi et al. 2009, Wang et al. 2012b). The myeloid differentiation factor 88 from *Scylla paramamosain* (SpMyD88) was able bind to SpToll. While FcMyD88 from *F.*

chinensis was up-regulated transcriptionally against bacterial infection (Li et al. 2013b). The Dorsal from *P. vannamei* (LvDorsal) could regulate the transcription of shrimp penaeidin-4 gene (Huang et al. 2010).

In *Drosophila,* IMD pathway is triggered by Gram-negative bacteria via the receptor peptidoglycan recognition protein (PGRP-LC) (Choe et al. 2002, Gottar et al. 2002). The *Drosophila* IMD pathway includes 9 canonical components: IMD, the PGRP-LC receptor, the mitogen-activated protein 3 kinase (TAK1), TAB2, DIAP2 (a member of inhibitor of apoptosis proteins), IKK signalosome (complex of IKKb/ird5 and IKKg/Kenny), the dFADD adaptor, the Dredd caspase, and the transcription factor Relish (Fig 1.8) (Lemaitre and Hoffmann 2007).

IMD encodes a death domain containing protein similar to that of Receptor Interacting Protein (RIP) of the tumor necrosis factor receptor (TNF-R) pathway. Its over-expression triggers the transcription of antibacterial peptide genes in the absence of an infection (Georgel et al. 2001). IMD from *P. vannamei* was able to induce the expression of penaeidin-4 (Wang et al. 2009). IMDs from *F. chinensis* (FcIMD) was involved in regulating the expression of crustins, ALFs and lysozymes in shrimp while PcIMD from *Procambarus clarkia* involved in regulating the expression of AMP gene in crayfish (Lan et al. 2013). The LvRelish could regulate the transcription of penaeidin-4 gene (Huang et al. 2009) while FcRelish from *F. chinensis* was necessary for the expression of penaeidin-5 gene (Li et al. 2009). It has been reported that transcription of other antimicrobial peptides in shrimp including crustin and ALF were also regulated by Relish (Wang et al. 2012a).

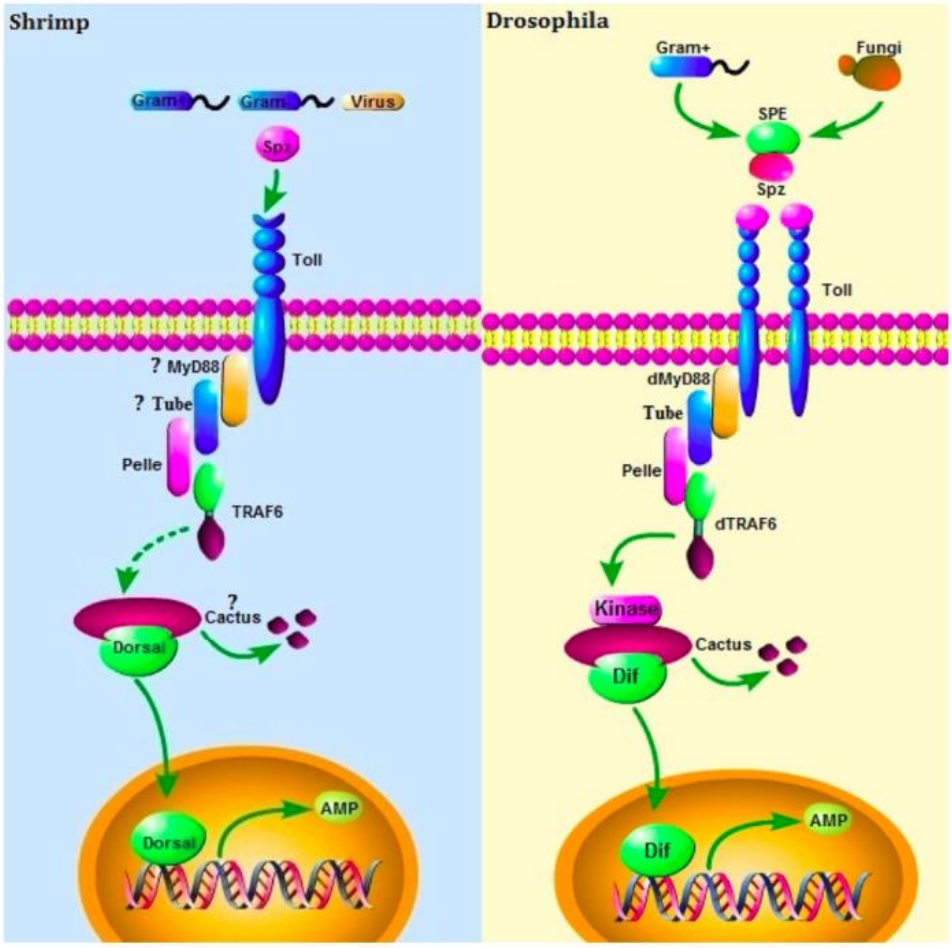

Figure 1.7 Comparison of Toll pathways in shrimp and *Drosophila* (Li and Xiang 2013b).

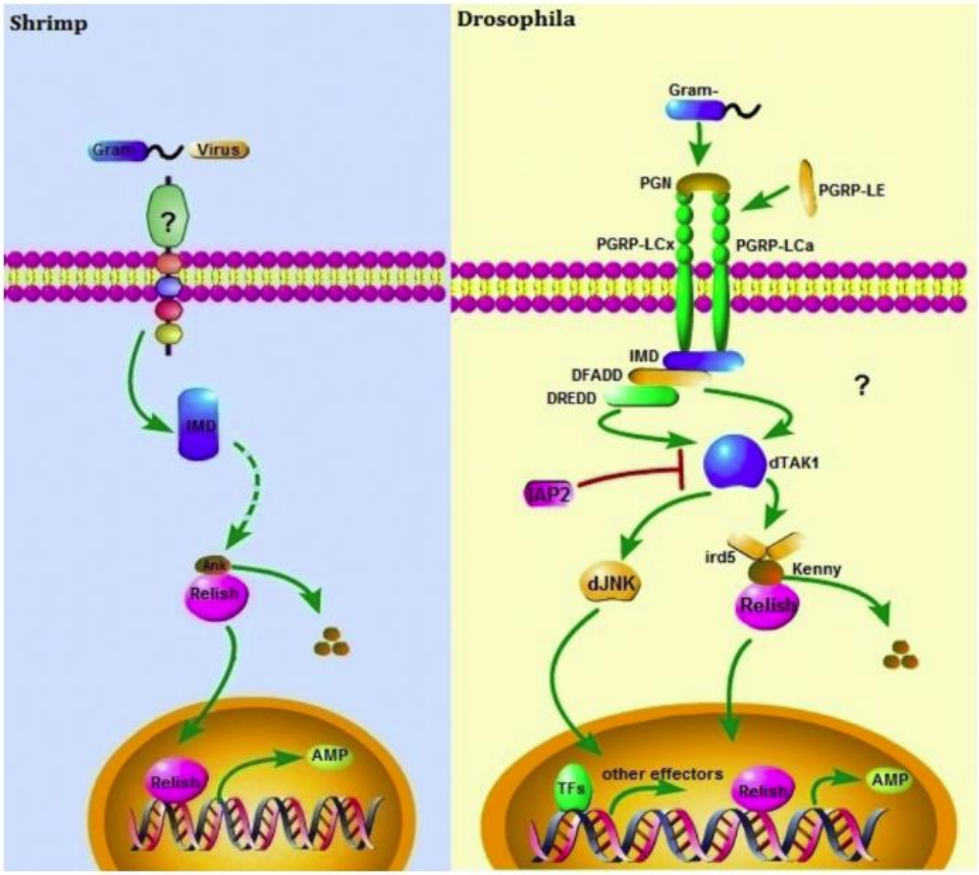

Figure 1.8 Comparison of IMD pathways in shrimp and *Drosophila* (Li and Xiang 2013b).

1.7 Objective of this thesis

ALF*Pm*6 has been shown to be a pathogen infection responsive gene in *P. monodon* hemocyte. However, the antimicrobial activity of ALF*Pm*6 remains uncharactrized. In this study, the recombinant ALF*Pm*6 (rALF*Pm*6) was produced using yeast expression system. The antibacterial activity of crude rALF*Pm*6 protein against *Escherichia coli* 363 and *Bacillus megaterium* was tested. The crude was futher purified by cation exchange chromatography. Also, the synthetic cyclic peptide (cALF*Pm*6#29-52) that is the LPS-binding domain of ALF*Pm*6 was designed. The cALF*Pm*6#29-52 was tested for antimicrobial activity and bacterial agglutination property.

In addition, the expression profiles of ALF*Pm*3 and ALF*Pm*6 genes are different, but the mechanisms that regulated the gene expression of ALF*Pm*3 and ALF*Pm*6 were not revealed. In this study, the genomic regions 5′-upstream of each ALF gene were partially characterized and transcription factor binding sites that might play an important role in controlling gene expression were determined. Also, the signaling pathways that control their transcription are still unclear. Thus, the transcripts of MyD88 and Relish, which are the representative adapter proteins of the Toll and IMD pathways, respectively, were silenced in *V. harveyi*-challenged shrimp in order to determine the signaling pathway involved in regulating ALF*Pm*3 and ALF*Pm*6 gene expression.

CHAPTER II
MATERIALS AND METHODS

2.1 Materials

2.1.1 Equipments

Avanti J-30I high performance centrifuge (Beckman coulter)

Amicon Ultra concentrators (Millipore)

Autoclave model # MLS-3750 (SANYO E&E Europe (UK Branch) UK Co.)

Automatic micropipette P10, P20, P100, P20 and P1000 (LioPette/ Select BioProduct/ Gilson Medical Electrical)

ÄKTA Prime Plus FPLC Purification System (GE Healthcare)

Balance PB303-s (Mettler Teledo)

Biophotometer (Eppendof)

Centrifuge 5804R (Eppendof)

Centrifuge AvantiTM J-301 (Beckman Coulter)

-20°C Freezer (Whirlpool)

-80°C Freezer (Thermo Electron Corporation)

Force mini centrifuge (Select BioProducts)

Gel Documention System (GeneCam FLEX1, Syngene)

GelMate2000 (Toyobo)

Gene pulser (Bio-RAD)

0.45 mm glassbeads

Incubator 30°C (Heraeus)

Incubator 37°C (Memmert)

Innova 4080 incubator shaker (New Brunswick Scentific)

Laminar Airflow Biological Safety Cabinets ClassII Model NU-440-400E (NuAire, Inc., USA)

Microcentrifuge tube 0.6 ml and 1.5 ml (Axygen®Scientific, USA)

Minicentrifuge (Costar, USA)

Minipulser electroporation system (Bio-RAD)

Mini-PROTEAN® 3 Cell (Bio-RAD)

Nipro disposable syringes (Nissho)

Optima™L-100 XP Ultracentrifuge (Beckman Coulter)

Orbital shaker SO3 (Stuart Scientific, Great Britain)

PCR Mastercycler (Eppendof AG, Germany)

PCR thin wall microcentrifuge tubes 0.2 ml (Axygen®Scientific, USA)

PD-10 column (GE Healthcare)

pH-meter pH 900 (Precisa, USA)

Pipette tips 10, 100 and 1000 µl (Axygen®Scientific, USA)

Power supply, Power PAC3000 (Bio-RAD Laboratories, USA)

Refrigerated incubator shaker (New Brunswick Scientific, USA)

Refrigerated microcentrifuge MIKRO 22R (Hettich Zentrifugen, Germany)

SpectraMax M5 Multi-Mode Microplate Reader (Molecular Devices)

Water bath (Memmert)

Whatman® 3 MM Chromatography paper (Whatman International Ltd., England)

96-well cell culture cluster, flat bottom with lid (Costar)

2.1.2 Chemicals and Reagents

100 mM dATP, dCTP, dGTP and dTTP (Promega)

5-bromo-4-chloro-3-indolyl-b-D-galactopyranoside (X-Gal) (Fermentas)

Absolute alcohol, C_2H_5OH (Hayman)

Acetic acid glacial, CH_3COOH (Merck)

Acrylamide, C_3H_5NO (Merck)

Agarose, low EEO, Molecular Biology Grade (Research Organics)

Agar powder, Bacteriological (Hi-media)

Alkaline phosphatase-conjugated rabbit anti-mouse IgG (Jackson ImmunoResearch Laboratories, Inc.)

Ammonium persulfate, $(NH_4)_2S_2O_8$ (Bio-Rad)

Benchmark™ Pre-stained Protein Ladder (Invitrogen)

Benchmark™ Unstained Protein Marker (Invitrogen)

Bovine serum albumin (Fluka)

Bromophenol blue (Merck, Germany)

Casein Enzyme Hydrolysate, Type-I, Tryptone Type-I (Hi-media)

Casein Peptone (Hi-media)

Chloroform, $CHCl_3$ (Merck)

D-Glucose anhydrous (Ajax)

Diethyl pyrocarbonate (DEPC), $C_6H_{10}O_5$ (Sigma)

Ethylene diamene tetraacetic acid disodium salt, EDTA (Ajax)

Ethidium bromide (Sigma)

GeneRuler™ 100bp DNA ladder (Fermetas)

GeneRuler™ 1kb DNA ladder (Fermetas)

Glycerol, $C_3H_8O_3$ (Ajax)

Glycine, USP Grade, NH_2CH_2COOH (Research organics)

Hybond™-ECL membrane (GE Healthcare)

Hydrochloric acid (HCl) (Merck)

HiTrap SP Sepharose™ Fast Flow column (GE Healthcare)

Imidazole (Fluka)

Isopropanol, C_3H_7OH (Merck)

Isopropyl-ß-D-thiogalactoside (IPTG), $C_9H_{18}O_5S$ (USBiological)

Magnesium chloride, $MgCl_2$ (Merck)

Methanol, CH_3OH (Merck)

0.22 µM and 0.45 µM Millipore membrane filter (Millipore)

N, N, N´, N´-tetramethylethylenediamene (TEMED) (BDH)

N, N´-methylenebisacrylamide, $C_7H_{10}N_2O_2$ (USB)

Ni Sepharose 6 Fast Flow (GE Healthcare)

Nitroblue tetrazolium (NBT) (Fermentas)

Paraformaldehyde (Sigma)

Phenol:chloroform:isoamyl alcohol (Sigma)

Phosphoric acid (Labscan)

Prestained protein molecular weight marker (Fermentas)

Skim milk powder (Mission)

Silver nitrate (Merck)

Sodium carbonate anhydrous (Carlo Erba)

Sodium chloride, NaCl (Ajax)

Sodium citrate, $Na_3C_6H_5O_7$ (Carlo Erba)

Sodium dodecyl sulfate, $C_{12}H_{25}O_4SNa$ (Vivantis)

Sodium hydrogen carbonate, $NaHCO_3$ (BDH)

Sodium dihydrogen orthophosphate, $NaH_2PO_4.H_2O$ (Ajax)

di-Sodium hydrogen orthophosphate anhydrous, NaH_2PO_4 (Ajax)

Sodium hydroxide, NaOH (Merck)

Triton® X-100 (Merck)

TriReagent® (Molecular Research Center)

Tris (Vivantas)

Tryptic soy broth (Difco)

Tween™-20 (Fluka)

Unstained protein molecular weight marker (Fermentas)

Urea (Affy Metrix USB)

2.1.3 Kits

High-speed plasmid mini kit (Geneaid)

Nucleospin® Extract II kit (Macherey-Nagel)

RevertAID™ first strand cDNA synthesis kit (Fermentas)

RQ1 RNase-free DNase (Promega)

SsoFast™ EvaGreen® Supermix (Biorad)

T&A cloning vector kit (RBC Bioscience)

pGEM-T easy vector system (Promega)

T7 RiboMAX™ Express RNAi System (Promega)

Yeastmaker™ Yeast Transformation System 2 (Clontech)

Effectene transfection reagent (Qiagen)

Dual-luciferase® Reporter assay (Promega)

2.1.4 Enzymes

Advantages® 2 Polymerase Mix (Clontech)

*Bgl*II (Biolabs)

*Eco*RI (Biolabs)

*Hind*III (Biolabs)

*Nhe*I (Biolabs)

*Sac*I (Biolabs)

KOD *Taq* polymerase (TOYOBO)

Phusion® Hot Start High-Fidelity DNA polymerase (Finnzymes)

Taq DNA polymerase (RBC Bioscience)

Ligation High Ver.2 (TOYOBO)

T4 DNA ligase (Biolabs)

2.1.5 Antibiotics

Amplicillin (BioBasic)

Kanamycin (BioBasic)

100x Penicillin-Streptomycin (Gibco, Life technology)

Tetracycline (BioBasic)

2.1.6 Bacterial, yeast and virus strains

Aerococcus viridans

Bacillus megaterium

Enterobacter cloacae

Erwinia carotovora

Escherichia coli strain XL-1-Blue

E. coli strain 363

E. coli strain BL21(DE3)

E. coli strain TOP10

Klebsiella pneumoniae

Micrococcus luteus

Pichia pastoris strain KM71

Staphylococcus aureus

Staphylococus haemolyticus

Vibrio harveyi strain 639

2.1.7 Softwares

BlastN, BlastX (http://www.ncbi.nlm.nih.gov/blast/Blast.cgi)

ClustalW (http://www.ebi.ac.uk/Tools/msa/clustalw2/)

ExPASy ProtParam (http://au.expasy.org/tools/protparam.html)

GENETYX version 7.0 program (Software Development Inc.)

SECentral (Scientific & Educational Software)

SignalP (http://www.cbs.dtu.dk/serveces/SignalP/)

SPSS statistic 17.0 (Chicago, USA)

2.1.8 Vectors

pBAD/Myc-His A (Invitrogen)

pET-16b (Novagen®, Germany)

phRL-null (Promege)

pGBKT7 (Clontech, USA)

pGEMT-easy vector (Promege)

pGL3-basic (Promega)

2.2 Expression and characterization of antilipopolysaccharide factor isoform 6 (ALF*Pm*6)

2.2.1 Transformation of pALF*Pm*6 into *Pichia pastoris* KM71

In this study, to characterize function of ALF*Pm*6, the recombinant ALF*Pm*6 (r ALF*Pm*6) was produced using yeast expression system. The *P. pastoris* strain KM71 electro-competent cells were prepared for transformation. A single colony of yeast, *P. pastoris,* was cultured overnight in YPD medium (1% yeast extract, 2% peptone, 2% dextrose) at 280 rpm, 30 °C. Twenty microliters of the overnight culture starter were inoculated into 100 ml of fresh YPD medium in a 1-liter flask and incubated at 30 °C until the OD_{600} reached 1-2. The cells were collected by centrifugation at 3,000 rpm, 5 min at 4 °C. The cell pellet was washed with 100 ml of cold sterile water followed by 50 ml of cold sterile water and 4 ml of ice-cold 1 M sorbitol, gently mixed and then centrifuged. The cells were then pelleted, resuspended in 200 µl of ice-cold 1 M sorbitol. The cell suspension was aliquoted into 80 microliters and stored at -80 °C until used.

The expression plasmid, pALF*Pm*6, was linearized using restriction enzyme, *Sac*I (New England BioLabs®) and analyzed using 1.0% agarose gel electrophoresis to

confirm the completely digestion plasmid. Then the linearized plasmid was purified by ethanol precipitation.

The linearized expression plasmid, pALF*Pm*6, was transformed into *P. pastoris* KM71 competent cells. The yeast competent cells were mixed with 5 μg of *Sac*I-linearized plasmid and placed on ice for 5 min. The mixture was subsequently transfered into cold 0.2 cm electroporation cuvette. The electroporating pulse was applied at 1.5 kV, 25 μF, 200 Ω using the Gene pulser apparatus (Bio-RAD). One ml of ice-cold 1 M sorbitol was immediately added to electroporated cell. The cell suspension was spread on the MD plate, the histidine-deficient medium (1.34% YNB, 4×10^{5}% biotin, 2% dextrose) and incubated at 30 °C for 2-5 days. The plasmid containing the *HIS4* gene allowed the transformed yeast carrying the plasmid integrated into the yeast genome to grow on histidine-deficient medium.

2.2.2 Screening for the transformants with multiple copy inserts

In *Pichia* expression system, the transformant containing high copy number integrate cassette, which can be selected by high G418-sulfate resistance, was referred to as the clone with high protein expression level. To obtain the clone with high copy number, the transformants were screened for G418-sulphate resistance. The transformants yeast cells on MD plate were resuspended in sterile water and pooled. The number of cells was calculated according to the formula 1 OD_{600} = 5 × 10^{7} cells/ml. The suspension 10^{7} cells were spread onto the YPD plates with G418-sulphate at a final concentration of 1 and 2 mg/ml. The plates were incubated at 30 °C for 3-5 days until the G418-sulphate resistance colonies appeared. Although the number of copies of the expression cassette, pALF*Pm*6 constructs, integrated to *Pichia* genome has not yet been determined, the transformants which can grow on YPD plate containing 2 mg/ml G418-sulphate, were considered as high-copy-number transformants. The hyper-resistance clone that could grow on YPD plate containing 2 mg/ml G418-sulfate were randomly selected. Then, transformants were re-streaked on YPD plates containing 2 mg/ml G418-sulphate to isolate the single colonies and to confirm G418-sulphate resistance.

2.2.3 Determination of the integrated ALF*Pm6* gene in *P. pastoris* genome by PCR technique

To check the presence of integrated ALF*Pm6* gene in transformants, the single colony was resuspended in 10 µl of water. The cells were lysed by adding 5 µl of a 5U/µl lyticase (Sigma). The reaction was incubated at 30 °C for 10 min and freezed at -80 °C for 10 min. The cell lysate (1 µl) was mixed with 48 µl of hot start PCR reaction mixture containing 5 µl of 10x reaction buffer, 1 µl each of the 10 µM α-factor and 3′-AOX primers, 5 µl of 25 mM $MgCl_2$, 1 µl of 25 mM dNTP mixture and 36 µl of sterile ultrapure water. The mixture were incubated at 95 °C, 5 min. Then 1 µl of Phusion DNA polymerase (New England BioLabs®) was added. The PCR was perfomed for 30 cycles as follows: denaturation at 95 °C for 1 min, annealing at 54 °C for 1 min, and extension at 72 °C for 1 min, The resulting PCR product was analyzed by 1.2% agarose gel electrophoresis to determine whether the DNA fragment was successfully amplified. As a negative control, the pPIC9K vector was used as a template where the expected size of PCR product was 195 bp. The positive clone was expected to give 539 bp PCR product (195 bp of parental plasmid plus 344 bp of ALF*Pm6* gene fragment).

2.2.4 Expression of recombinant clone

The hyper-resistant clone was selected for the protein expression analysis. The single colony was grown in YPD broth medium at 30 °C for overnight. Then, the overnight culture was inoculated into 100 ml of fresh BMGY medium (1% yeast extract, 2% peptone, 100 mM potassium phosphate, pH 6.0, 1.34% YNB, biotin, and 1% glycerol) in a 1 liter flask and grown at 30 °C in a shaking incubator with 300 rpm until OD_{600} reaches 4-6. The cells were harvested by centrifugation at 1,500 ×g for 5 min at room temperature and resuspended in 20 ml BMMY medium (1% yeast extract, 2% peptone, 100 mM potassium phosphate, pH 6.0, 1.34% YNB, biotin, and 0.5% methanol). After that, the protein production was induced by adding 100% methanol every 24 h to maintain the final concentration at 0.5%. After 3 day of methanol induction, the expression of the recombinant ALF*Pm6* (rALF*Pm6*) in the culture

medium supernatant was collected by centrifugation at 8,000 rpm for 10 min at 4 °C and analyzed by 15% SDS-PAGE and the protein bands were detected with silver staining. The crude rALF*Pm6* protein was tested antimicrobial activity against Gram-negative bacterium, *E. coli 363*, and a Gram-positive bacterium, *B. megaterium* by liquid growth inhibition assays. 20 µl of the crude rALF*Pm6* protein, or sterile deionised water as a control, were incubated in sterile microtitration plates with 100 µl of a suspension of mid-logarithmic growth phase culture of bacterial diluted in culture medium to OD_{600}=0.001. Bacteria were grown overnight under vigorous shaking at 30 °C. After 16 h, the inhibition bacterial growth was observed. The transformant that could over-produce rALF*Pm6* at the highest level and highest antibacterial activity were selected.

2.2.5 Optimization of the condition for the rALF*Pm6* production

To obtain the high level of rALF*Pm6* production, the small-scale expression was performed to identify the optimal condition such as temperature, cell densities and time of methanol induction.

2.2.5.1 Effect of cell density on the rALF*Pm6* protein production

In *Pichia* expression system, the culture can be grown at very high densities to obtain the large amount of the recombinant protein. To determine the optimum cell density, the highest expressed clone was cultured in BMGY medium at 30 °C in a shaking incubator with 280 rpm until OD_{600} reached 10, 15 and 20. Then, the cells were harvested by centrifugation at 1,500 ×g for 5 min at room temperature and resuspended in 20 ml BMMY medium and induced by adding 100% methanol every 24 h to maintain the final concentration at 0.5% for 3 days. Every 24 hours after induction, the culture supernatant was collected by centrifugation at 8,000 rpm for 10 min at 4 °C. The rALF*Pm6* protein was analyzed by 15% silver-stained SDS-PAGE.

2.2.5.2 Effect of induction time on the rALF*Pm6* protein production

The days after induction, required for induction, were optimized. The rALF*Pm6* highest expressed clone was cultured in BMGY medium at 30 °C in a shaking incubator with 280 rpm until OD_{600} reached 15. Then, the cells were harvested by centrifugation

at 1,500 ×g for 5 min at room temperature and resuspended in 20 ml BMMY medium and induced by adding 100% methanol every 24 h to maintain the final concentration at 0.5% for 3 days. Every 24 hours after induction, the culture supernatant was collected by centrifugation at 8,000 rpm for 10 min at 4 °C. The rALF*Pm6* expression at day 0 to day 3 induction was detected by 15% silver-stained SDS-PAGE.

2.2.5.3 Effect of temperature on the rALF*Pm6* protein production

Temperature is a key environmental factor known to affect protein expression. To optimize the temperature used for culture, the culture were grown in BMGY medium in a shaking incubator with 280 rpm at 28 °C or 30 °C until OD_{600} reached 15. Then, the cells were harvested by centrifugation at 1,500 ×g for 5 min at room temperature and resuspended in 20 ml BMMY medium and induced by adding 100% methanol every 24 h to maintain the final concentration at 0.5% for 1 day. The culture supernatant was collected by centrifugation at 8,000 rpm for 10 min at 4 °C. The rALF*Pm6* protein before (day 0) and after induction was detected by 15% silver-stained SDS-PAGE.

2.2.6 Purification of the rALF*Pm6* protein

Upon methanol induction, the rALF*Pm6* protein secreted into culture supernatant was harvested after centrifugation at 8000 xg, 4 °C for 15 min. The supernatant containing rALF*Pm6* was desalted and exchanged buffer by using Vivaflow 50 (Sartorius AG) or dialysis. After that, the SP Sepharose High Performance column (GE Healthcare) was equilibrated with the binding buffer. The recombinant protein was loaded into the column with flowrate 1 ml/min. The column was washed with binding buffer to remove unbound protein until A_{280} near zero. After washing step, the bound protein was eluted with elution buffer. Five purification conditions are shown in table 2.1. The purified fractions were analyzed by 15% silver-stained SDS-PAGE.

Table 2.1 The purification condition for rALF*Pm6* protein

Condition	Sample preparation	Purification Buffer
I	The crude protein rALF*Pm6* was mixed with binding buffer by equal volumn.	**Binding buffer :** 20 mM Tris-HCl, pH 7.0 **Elution buffer :** 20 mM Tris-HCl, pH 7.0 with various concentration of NaCl (500 mM, 1 M)
II	The crude protein rALF*Pm6* was mixed with binding buffer by equal volumn.	**Binding buffer :** 20 mM sodium phosphate, pH 6.0 **Elution buffer :** 20 mM sodium phosphate, pH 6.0 with various concentration of NaCl (100 mM, 300 mM, 500 mM, 1 M)
III	The crude protein rALF*Pm6* was concentrated and exchanged buffer to binding buffer by ultrafiltration system.	**Binding buffer :** 50 mM sodium phosphate, pH 6.0 **Elution buffer :** 50 mM sodium phosphate, pH 6.0, 500 mM NaCl
IV	The crude protein rALFPm6 was dialyzed against binding buffer	**Binding buffer :** 50 mM MES, pH 6.0 **Elution buffer :** 50 mM MES, pH 6.0 with various concentration of NaCl (50 mM, 200 mM, 300 mM, 500 mM, 1 M)
V	The crude protein rALF*Pm6* was dialyzed against binding buffer	**Binding buffer :** 50 mM MES, pH 5.6 **Elution buffer :** 50 mM MES, pH 5.6, 500 mM NaCl

2.2.7 Antibacterial activity assay

The bacterial strains including Gram-negative bacteria; *Escherichia coli* 363, *Klebsiella pneumoniae, Enterobacter cloacae, Vibrio harveyi,* non-vilurent *Vibrio parahaemolyticus,* vilurent *Vibrio parahaemolyticus* (AHPND) and *Erwinia carotovora*, and Gram-positive bacteria; *Bacillus megaterium*, *Aerococcus viridans, Micrococcus luteus, Staphylococus haemolyticus* and *Staphylococcus aureus,* were used to study the antibacterial activity.

In this study, the antibacterial activity of crude rALF*Pm*6 protein against *Escherichia coli* 363 and *Bacillus megaterium* was tested. Also, the synthetic cyclic peptide (cALF*Pm*6#29-52) that is the LPS-binding domain of ALFPm6 was designed and then subjected to synthesis service by BIO BASIC INC., Canada. The lyophilized cALF*Pm*6#29-52 resuspend in ultrapure-water and an aliquot was kept at -20°C until used.

Antimicrobial activity of crude rALF*Pm*6 against *Escherichia coli* 363 and *Bacillus megaterium* was performed by liquid growth inhibition assay according to Somboonwiwat et al., 2005. Briefly, 20 µl aliquots of the crude rALF*Pm*6 were incubated in 96-well plate with 100 µl of a suspension of mid-logarithmic phase culture of bacteria at OD_{600} = 0.001. Poor-broth nutrient medium (1% bactotryptone, 0.5% NaCl, w/v, pH 7.5) was used for standard bacterial culture. The negative and positive controls for checking the desired outcome of experiment were sterile water (instead of tested protein) in the culture medium with and with out tested bacteria, respectively. The bacterial culture was grown at 30°C in a shaking incubator at 120 rpm and measured the bacterial growth at 600 nm after 16-18 h. The A_{600} values of the test and control were compared.

The liquid growth inhibition assay as above were performed to test the antibacterial activity of cALF*Pm*6#29-52 peptide. Then, 20 µl aliquots of the bacterial culture incubated with the synthetic cALF*Pm*6#29-52 peptide was plated on the LB agar plates. The bacterial culture was grown at 30°C for 16 h. The positive control were sterile water (instead of tested peptide) in the culture medium with tested bacteria. The remaining bacterial colony on the LB agar plates of the test and control were

compared. The minimum bactericidal concentrations (MBCs) of the synthetic cALF*Pm6*#29-52 peptide were determined by counting the remaining bacterial colony on the LB agar plates. The MBC is defined as the range between the highest concentration of the peptide where bacterial growth was observed and the lowest concentration of the peptide that reduces the viability of the initial bacterial inoculum.

2.2.8 Bacterial agglutination assay

Bacterial strians including *E. coli* 363, *B. megaterium*, *A. viridans,* and *M. luteus* were tested for bacterial agglutination property. The 20 µl aliquots of the synthetic cyclic ALF*Pm6*#29-52 peptide (cALF*Pm6*#29-52) at 25 and 50 µM final concentration were incubated in 96-well plate with 100 µl of a suspension of mid-logarithmic phase culture of bacteria at OD_{600} = 0.001. Poor-broth nutrient medium (1% bactotryptone, 0.5% NaCl, w/v, pH 7.5) was used for standard bacterial culture. The negative and positive controls were designed for checking the desired outcome of experiment. The bacterial culture was grown at 30°C in a shaking incubator at 120 rpm for 16 h. After incubation, one drop of the mixture was placed on a microscope slide and bacterial sample were then Gram-stained and observed under a 100X magnification light microscope (Olympus CX31) and images were taken using a Nikon DS-Fi1.

2.3 Characterization of the ALF*Pm* gene regulation

2.3.1 Identification of the promoter of ALF*Pm* gene

Due to the potential of ALFs in crustaceans, previous research has focused on the antimicrobial activity, but knowledge of the regulation of ALFs is limited. To better understand how ALF genes are regulated, the sequences and activity of ALF*Pm*3 and ALF*Pm*6 promoter were characterized since the expression profiles of ALF*Pm*3 and ALF*Pm*6 were different.

In this experiment, the 5′ upstream sequences of ALF*Pm*3 and ALF*Pm*6 genes were identified by genome walking technique. The restriction enzyme-digested *P. monodon* genomic DNA were used as template. The primary PCR using the outer adaptor primer (AP1) and the first gene-specific primer (GSP1) was amplified. PCR product was diluted for 50 fold and used as template for the secondary or nested PCR

with the nested adaptor primer (AP2) and a nested gene specific primer (GSP2). The GSP1 and GSP2 primer designed from the known genomic sequence of ALF*Pm*3 and ALF*Pm*6 are shown in Table 2.2.

To identify the 5′ upstream sequences of ALF*Pm*3, three libraries derived from *P. monodon* DNA digested with *Dra*I, *Pvu*II and *Stu*I were used as template. For ALF*Pm*6, four libraries containing *Eco*RV, *Dra*I, *Pvu*II and *Stu*I were used as template. For primary PCR, 1 µl of DNA template was used in a 50 µl total reaction volume containing 1 µl of 50x Advantage® 2 Polymerase Mix, 5 µl of 10x Advantage® 2 PCR buffer, 1 µl of 10 mM dNTP mix, 1 µl of each AP1 and GSP1 primer and 40 µl of sterile deionized H_2O. The PCR condition was initial denaturation at 94 °C for 2 min, followed by 5 cycles of 94 °C for 25 sec and 72 °C for 3 min; 20 cycles of 94 °C for 25 sec and 67 °C for 3 min; and 67 °C for an additional 7 min. The primary PCR products were analyzed by 1.2% agarose/EtBr gel electrophoresis. Then, each primary PCR product was diluted 50 fold with sterile deionized H_2O and used as secondary PCR template. In the secondary (nested PCR), the 50 µl PCR reaction contained 1 µl of 50x Advantage® 2 Polymerase Mix, 5 µl of 10x Advantage® 2 PCR buffer, 1 µl of 10 mM dNTP, 1 µl of AP2 and GSP2 and sterile deionized H_2O. The PCR condition began with initial denaturation at 94 °C for 2 min, followed by 5 cycles of 94 °C for 25 sec and 72 °C for 3 min; 20 cycles of 94 °C for 25 sec and 67 °C for 3 min; and 72 °C for 7 min. The nested PCR products were analyzed by 1.2% agarose/EtBr gel electrophoresis. The largest size of DNA fragment from nested PCR of ALF*Pm*3 and ALF*Pm*6 genes were purified by Nucleospin® Extract II kit (Macherey-Nagel). The purified DNA fragments were cloned into pGEM®-T easy vector (Promega) and analyzed by DNA sequencing sevice (Macrogen Inc., Korea). The promoter of ALF*Pm*3 and ALF*Pm*6 genes were predicted by Promoter 2.0 Prediction Server and BDGP (Neural Network Promoter Prediction) program. The transcription start site and TATA box of both genes were identified.

Table 2.2 List of primers used for genome walking experiment

Primer name	Sequence (5'⟶3')
GSP1_ALF3_primary	5' CTTGCACTCGTGGCCGAGAAGTTCAGTT 3'
GSP2_ALF3_nested	5' AGCACCAGGCTTACCAGCACGGACACA 3'
GSP1_ALF6_primary	5' AGTTTGTTCGCAATGGCTGGCACCAAT 3'
GSP2_ALF6_nested	5' CACCACCACCACGAGGATCATGCTGAA 3'

2.3.2 Prediction of transcription factor binding site on ALF*Pm*3 and ALF*Pm*6 promoter fragments by bioinformatic analysis

The 5′ upstream sequences of ALF*Pm*3 and ALF*Pm*6 gene were analysed for the putative cis-regulatory elements by using TF search Version 1.3 (TRANSFAC® Public database), Match 1.0 (TRANSFAC® Public database) and Alibaba 2 analysis program (TRANSFAC® Public database). The results were compared with JASPAR database to confirm the putative transcription factor binding sites.

2.3.3 Construction of the luciferase reporter plasmid containing the ALF*Pm* promoter

The 5′ upstream sequences of ALF*Pm*3 gene from -1478 to +324 position were cloned into pGL3-basic reporter plasmid (Promega) which contained firefly luciferase gene to produce the parental constructs, p(-1478/+324). For The 5′ upstream sequences ALF*Pm*6 gene from -419 to +85 position was cloned into pGL3-basic reporter plasmid to produce the parental constructs, p(-419/+85). The recombinant plasmid p(-1478/+324) and p(-419/+85) were confirmed by double digestion with restriction enzyme *Nhe*I and *Bgl*II and sequenced (Macrogen Inc., Korea).

To identify the promoter active sequences of ALF*Pm*3 and ALF*Pm*6, the promoter sequences were narrowed down using PCR technique. ALF*Pm*3 promoter were randomly narrowed down into various fragment sizes including the nucleotide position region of (-1478/+324), (-814/+324), (-719/+324), (-265/+324) and (-71/+324). For ALF*Pm*6 promoter, the various fragment size contained the nucleotide position regions of (-419/+85), (-282/+85), (-162/+85) and (-80/+85) were constructed. Each

promoter fragment was amplified using the parental constructs p(-1478/+324) for ALF*Pm*3 and p(-419/+85) for ALF*Pm*6, respectively, as a template and specific primer containing restriction sites *Nhe*I and *Bgl*II at the 5′-end of forward and reverse primers, respectively (Table 2.3). The PCR reaction contained 1 µl of 50x Advantage® 2 Polymerase Mix, 5 µl of 10x Advantage® 2 PCR buffer, 1 µl of 10 mM dNTP mix, 1 µl of forward and reverse primers and sterile deionized H_2O to final concentration volume of 50 µl. The PCR condition was 95 °C for 1 min, followed by 35 cycles of 95 °C for 30 sec, 60 °C for 30 sec, and 68 °C for 30 sec, and then a final extension at 68 °C for 10 min. The PCR product were analyzed by 1.2% agarose/EtBr gel electrophoresis and purified by Nucleospin® Extract II kit (Macherey-Nagel). The purified product were digested with *Nhe*I and *Bgl*II and cloned into pGL3-basic vector. For each construct, 10 µl of ligation mixture contained 50 ng of *Nhe*I/*Bgl*II digested pGL3-basic vector, *Nhe*I/*Bgl*II digested ALF*Pm*3 or ALF*Pm*6 promoter fragment, 5 µl of Ligation High Ver. 2 (TOYOBO). The reaction was incubated at 16 °C for 2 h and 5 µl of the ligation mixture was transformed into *E. coli* strain XL-1 blue by electroporation and selected on LB agar plate with 100 µg/ml ampicillin. The recominant plasmids were extracted using High-speed plasmid mini kit (Geneaid). The plasmids were double digested with *Nhe*I and *Bgl*II and analyzed by 1.2% agarose/EtBr gel electrophoresis to confirm the insertion fragment. The pGL3 plasmid containing ALF*Pm*3 promoter region; p(-1478/+324), p(-814/+324), p(-719/+324) p(-265/+324), and p(-71/+324) and The pGL3 plasmid containing ALF*Pm*6 promoter; p(-419/+85), p(-282/+85), p(-162/+85) and p(-80/+85) were confirmed the sequence of insert by DNA sequencing (Macrogen Inc., Korea).

Table 2.3 List of primers used to amplify ALF*Pm*3 and ALF*Pm*6 promoter fragments

Primer name	Sequence (5'-3')
ALF3promo+324BglII_R	5' AGGCGCAGATCT-CTTCTGCAAGGGAAATAAAGATAAC 3'
ALF3promo-1478NheI_F	5' ATGAGCTAGCGCTGGTCCTGTGGTAAG 3‘
ALF3promo-814NheI_F	5' AGTAGCTAGC-GAAGCAGAGCCTCGCTAT 3'
ALF3promo-719NheI_F	5' ATCTGCTAGC-TGAGGAAGAATGTGCGAGTG 3'
ALF3promo-265NheI_F	5' GCCTGCTAGC-GGAAATACGCGTTGCTGT 3'
ALF3promo-71NheI_F	5' TACGGCTAGC-ATAGGCTCCTGGCAACT 3'
ALF6promo+85BglII_R	5' ACTGAGATCT-GATGGACGTGAAGTGAAG 3'
ALF6promo-419NheI_F	5' TTACGCTAGC-CCCGGGCTGGTAAATG 3'
ALF6promo-282NheI_F	5' ATCGGCTAGC-GGCTGGTATTCCCAAGTCT 3'
ALF6promo-162NheI_F	5' AGCGGCTAGC-ACATGTATGAATGCCGAAAACG 3'
ALF6promo-80NheI_F	5' CAGCGCTAGC-ACATTTATGCACCCATCTCC 3'

2.3.4 Promoter activity assay

Drosophila Schneider 2 (S2) cell was seeded into a 24-well plate at density 8 x 10^5 cells/well and cultured in the complete Schneider's *Drosophila* Medium containing 10% heat-inactivated FB5 and antibiotic (50 units penicillin G and 50 µg/ml streptomycin sulfate, Invitrogen) at 27 °C for overnight. The 200 ng of pGL3-Basic (control plasmid) or pGL3 plasmid containing ALF*Pm*3 and ALF*Pm*6 promoter fragments were co-transfected with 50 ng of the pRL-TK plasmid containing *Renilla* luciferase gene into the S2 cells by using the Effectene transfection reagent (Qiagen) according to manufacturer's protocol. On the day of transfection, 8×10^5 cell were seed in 300 µl complete Schneider's *Drosophila* Medium. 200 ng DNA was diluted with Buffer EC to a total volume of 60 µl and 1.6 µl Enhancer was added then mix by

vortexing for 1 s. The mixture was incubated at room temperature for 5 min then 25 µl Effectene Reagent was added to the DNA-Enhancer solution then mix by vortexing for 10 s. The mixture was incubated for 10 min at room temperature to allow transfection-complex formation. Complete Schneider's *Drosophila* Medium 200 µl were added to the tube containing the transfection complex. The transfection complexes were added drop-wise onto the cells in the 24-well plate and gently swirl the dish to ensure uniform distribution of the complexes. The pRL-TK plasmid were used as an internal control and for transfection efficiency determination. Cells were collected at 48 h after transfection. The promoter activity was determined using Dual®-Luciferase Reporter Assay (Promega). Briefly, After 48 h post transfection, S2 cell was collected by centrifugation at 1000 x g for 5 min at room temperature, then the cell pellet were collected and discarded the supernatant. The cell was lyzed with 1X PLB (Passive lysis buffer) and 100 µl transferred to 96 well plate. The 20 µl substrate of firefly luciferase activity was added and the luminescence signal was determined in Relative Luminescence Units (RLU) using SpectraMax M5 Multi-Mode Microplate Reader (Molecular device). After that Stop & Glo solution was added to stop the *Firefly* luciferase activity and measure the luminescence signal of the *Renilla* luciferase activity. The RLU value of *Firefly* luciferase activity was normalized to that of the *Renilla* luciferase to correct the transfection efficiency. The data was reported as the relative luciferase activity. Independent triplicate experiments were performed for each construct and standard deviation (SD) was calculated.

2.3.5 Determination of the regulatory element involved in ALF*Pm*3 and ALF*Pm*6 gene regulation

2.3.5.1 Deletion assay

To determine the involvement of the 21 units of GAAAGAGAGTAAGAG[T/C] tandem repeat regulating ALF*Pm*3 gene expression, the deletion of the 21 units of GAAAGAGAGTAAGAG[T/C] tandem repeat were construct. The gene specific primers including the deletion of the the 21 units of GAAAGAGAGTAAGAG[T/C] tandem repeat were designed. The deletion construct, del(-693/-358)/p(-1478/+302), was preparing by

rolling PCR using p(-1478/+324) as a template and a primer pair; del(-693/-358)/p(-1478/+324)F and del(-693/-358)/p(-1478/+324)R (Table 2.4). The PCR condition were 94 °C for 2 min, followed by 35 cycles of 98 °C for 10 s, 60 °C for 30 s, and 68 °C for 7 min, using KOD *Taq* polymerase (TOYOBO). The PCR product were analyzed by 1% (w/v) agarose gel electrophoresis and purified by Nucleospin® Extract II kit (Macherey-Nagel). The 10 µL ligation mixture containing purified PCR product of del(-693/-358)/p(-1478/+324) and 5 µL of Ligation High Ver.2 (TOYOBO) were prepared and incubated at 16 °C, overnight. The 5 µL of ligation mixture were transformed into *E. coli* XL-1 blue by electopolation. The transformants were selected on LB agar plate containing 100 µg/ml ampicillin. The del(-693/-358)/p(-1478/+302) plasmids were extracted using High-speed plasmid mini kit (Geneaid). The deletion of the 21 units of GAAAGAGAGTAAGAG[T/C] tandem repeat was confirmed by DNA sequencing (Macrogen Inc., Korea). The promoter activity of the mutant was measured as described in section 2.2.4 and compared with wild type using Dual-Luciferase Reporter Assay (Promega).

2.3.5.2 Site-directed mutagenesis technique

Site-directed mutagenesis technique was performed to identify the transcription factor regulating ALF*Pm* gene. The gene specific primers including the mutation of the conserved nucleotide on transcription binding site were designed (Table 2.4). For the -719/-265 ALF*Pm*3 promoter region, the mutation of transcription factor binding site of NF-κB (-280/-270) and deletion of 21 units of GAAAGAGAGTAAGAG[T/C] tandem repeat were performed using p(-1478/+324) as a template. For the -162/-80 ALF*Pm*6 promoter region, the mutation of transcription factor binding site of ICSBP (-147/-136) and C/EBP beta (-78/-88) were performed using p(-419/+85) as a template. The mutated constructs of these transcription factor-binding sites were prepared by rolling PCR using the conserved nucleotides of the interested TF-binding site were identified by JASPAR (an open-access database for eukaryotic TF-binding profiles) and their specific primers (Table 2.4). The PCR were performed using KOD *Taq* polymerase (TOYOBO). The PCR condition were 94 °C for 2 min, followed by 35 cycles of 98 °C for 10 s, 60 °C for 30 s, and 68 °C for 7 min, using KOD *Taq* polymerase (TOYOBO). The PCR product were analyzed by 1.2% agarose/EtBr gel and

purified by Nucleospin Extract II kit (Macherey-Nagel). The 10 µL ligation mixture containing mutated-ALF*Pm* promoter fragment and 5 µL of Ligation High Ver.2 (TOYOBO) were incubated at 16 °C for overnight. 5 µL of ligation mixture were transformed into *E. coli* XL-1 blue by electopolation. The transformants were selected on LB agar plate containing 100 µg/ml ampicillin. The mutant plasmids were extracted using High-speed plasmid mini kit (Geneaid). The mutated-transcription factor-binding sites were confirmed by DNA sequencing (Macrogen Inc., Korea). The promoter activity of the mutant was measured as described in section 2.2.4 and compared with wild type using Dual-Luciferase Reporter Assay (Promega).

Table 2.4 List of primers used for site-directed mutagenesis of transcription factor binding sites on ALF*Pm* promoter region

Primer name	**Sequence (5'-3')**
del(-693/-358)/p(-1478/+324)F	5' AGAGAGGGGGGGGGAGAGG 3'
del(-693/-358)/p(-1478/+324)R	5' CTTTCACTCGCACATTCTTCCTCACTC 3'
p(-814/+324)muNF-kB_F	5' CGTTGCTGTTACTATAGTTTCCACGTCG 3'
p(-814/+324)muNF-kB_R	5' CGTATTTCCAGCTGAGAAAGATACTGCC 3'
p(-282/+85)muICSBP_F	5' ACATGTATGAATGCCGCACACTCCAACTGAGCTG 3'
p(-282/+85)muICSBP_R	5' ATATCTATACATAATGGACTTTGG 3'
p(-282/+85)muC/EBPbeta_F	5' AATGTATAAAGTAACATTTATGCACC 3'
p(-282/+85)muC/EBPbeta_R	5' ATTCACACATTATATGTTATTCTCA 3'

2.4 Effect of MyD88 and Relish gene knockdown on the ALF*Pm*3 and ALF*Pm*6 gene expression

2.4.1 Preparation of double strand RNA (dsRNA)

The dsRNA specific to MyD88, Relish and GFP were prepared according T7 RiboMAX™ Express RNAi System (Promega) kit's instruction using MyD88-pGEM, Relish-pGEM and GFP-pGEM recombinant plasmid as a template for producing sense and antisense DNA templates of *in vitro* transcription. DNA template containing the T7 promoter sequence at 5'-end were generate by PCR using specific primer (Table 2.4). The PCR condition were 94 °C for 2 min, followed by 35 cycles of 94 °C for 30 s, 58 °C for 30 s, and 72 °C for 30 s, using RBC *Taq* polymerase (RBC Bioscience). The PCR products were analyzed by 1.2% agarose/EtBr gel and purified by Nucleospin® Extract II kit (Macherey-Nagel).

The dsRNA synthesis reaction contained 8 µl of 1 µg linear DNA template of each target gene, the 10 µl of T7 RiboMAX™ Express 2x buffer and 2 µl of Enzyme Mix T7 Express in the final volume of 20 µl per reaction. Then, the reaction of DNA fragments was incubated at 37 °C for 1 h. The equal amounts of each complementary ssRNA were mixed and incubated at 70 °C for 10 min and slowly cool down to room temperature. DNA template was removed by addition of 2 µl of RQ1 RNase-free DNase (1U/ µg of DNA template) and incubation at 37 °C for 30 min. Total RNA was extracted using TriReagent® and the final aquaphase was precipitated by mixing with 4 µl of 3 M sodium acetate and 45 µl of isopropanol. After thoroughly mixed, the solution was frozen at -20 °C for 20 min and then centrifuged at 13,500 xg for 15 min at 4 °C. The upper phase was discarded and the pellet was washed with 1 ml of 75% ethanol. Then, the same was centrifuged at 13,500 xg for 15 min at 4 °C and the ethanol was discarded. The pellet was air-dried for 5 min. Finally, 40 µl of Nuclease-free water was used to dissolve the pellet and the purified dsRNA was stored at -80 °C until used. The dsRNA was measured at A_{260} using spectrophotometer. The concentration of total RNA was determined using the formular: [RNA] = A_{260} × dilution factor × 40. The purified dsRNA was also run on 1.2% agarose gel electrophoresis to confirm the integrity before use.

Table 2.5 List of primers used for RNA interference

Primer name	**Sequence (5'-3')**
PmMyD88 dsRNA	
Sense strand template T7-MyD88-F	5'TAATACGACTCACTATAGGG-CCTCAGCAAAGGTCTTGAAC 3'
MyD88-R	5' CAGTCCACCAATTAGGTCTC 3'
Anti-sense strand template MyD88-F	5' CCTCAGCAAAGGTCTTGAAC 3'
T7-MyD88-R	5' TAATACGACTCACTATAGGG-CAGTCCACCAATTAGGTCTC 3'
PmRelish dsRNA	
Sense strand template T7-Relish-F	5'TAATACGACTCACTATAGGG-CTCGTGGTCAGGAAGACTCAAT 3'
Relish-R	5' GACTGGAGATGGAGACTGAATG 3'
Anti-sense strand template Relish-F	5' CTCGTGGTCAGGAAGACTCAAT 3'
T7-Relish-R	5'TAATACGACTCACTATAGGG-GACTGGAGATGGAGACTGAATG 3'
GFP dsRNA	
Sense strand template T7-GFP-F	5' TAATACGACTCACTATAGGG-ATGGTGAGCAAGGGCGAGGA 3'
GFP-R	5' TTACTTGTACAGCTCGTCCA 3'
Anti-sense strand template GFP-F	5' ATGGTGAGCAAGGGCGAGGA 3'
T7-GFP-R	5' TAATACGACTCACTATAGGG-TTACTTGTACAGCTCGTCCA 3'

2.4.2 Total RNA extraction

Hemolymph was individually collected and briefly mixed with 500 µl of TriReagent® (Molecular Research Center). Then, 200 µl of chloroform were added. Each sample was vortexed for 15 sec and let it stand at room temperature for 10 min before centrifugation at 12,000 × g for 15 min at 4 °C. The colorless upper aqueous phase was transferred to a fresh 1.5 ml microcentrifuge tube. The total RNA was precipitated with 500 µl of cold isopropanol. The mixture was left at room temperature for 10 min and then centrifuged at 12,000 × g for 15 min at 4 °C. The supernatant was removed and the pellet of total RNA was washed in 1 ml of 75% ethanol in diethyl pyrocarbonate (DEPC)-treated water and centrifuged at 13,500 × rpm for 15 min at 4 °C. The ethanol was completely removed by pipetting. The RNA pellet was briefly air-dried for 10 min. The total RNA was dissolved with an appropriate amount of DEPC-treated water and kept on ice until it was completely dissolved. The purified total RNA was kept at -80 °C until used.

2.4.3 Determination of the quantity and quality of RNA samples

The quantity of total RNA was measured by spectrophotometer at A_{260} nm. The concentration of total RNA was determined using the formular:

$$[RNA] = A_{260} \times \text{dilution factor} \times 40$$

One A_{260} corresponds to 40 µg/ml of RNA (Sambrook 1989). The relative purity of RNA samples was examined by measuring the ratio of $A_{260/280}$. The maximum absorption of nucleic acid, and protein is at 260, and 280 nm, respectively. The ratio of absorbance at 260 nm and 280 nm is used to assess the purity of RNA. An approximately ratio above 1.7 is generally accepted as pure RNA. If the ratio is appreciably lower, it may indicate the presence of protein, phenol or other contaminants that absorb strongly at or near 280 nm. The quality was further investigated through 1.2% (w/v) agarose gel electrophoresis. The gel was stained with EtBr and visualized under UV light, respectively.

2.4.4 DNase treatment of total RNA samples

The obtained total RNA was further treated with RQ1 RNase-free DNase (Promega). The reaction contains 5 µg of total RNA in 1× RNase-free DNase buffer and 1 unit of RQ1 RNase-free DNase. The DNase treatment reactions were incubated at 37 °C for 30 min to remove the contaminating chromosomal DNA. Then, the total RNA was purified by TriReagent® as described in section 2.4.2. The quantity and quality of total RNA was examined as described in section 2.4.3.

2.4.5 First-strand cDNA synthesis

The first strand cDNA was synthesized from 1 µg of the total RNA using the RevertAid™ First Strand cDNA Synthesis Kit (Thermo Scientific). According to the kit's instruction, the reaction was performed by mixing 1 µg of the total RNA, 0.5 µg of the oligo$(dT)_{18}$ primer and adjusted the volume to 12 µl by DEPC-treated water. The reaction was incubated at 65 °C for 5 min and spin down and chilled on ice for 5 min to allow the primer to anneal to RNA. After that, 4 µl of 5X reaction buffer, 1 µl of RiboLock™ RNase inhibitor (20U/µl), 2 µl of 10 mM dNTP mix and 1 µl (200U/µl) of RevertAid™ M-MuLV reverse transcriptase were added and gently mixed. The reaction mixture (20 µl) was incubated 42 °C for 1 h and finally heated at 70 °C for 15 min to terminate the reaction. The cDNA was stored at -20 °C until used.

2.4.6 Silencing efficiency of MyD88 dsRNA and Relish dsRNA

To test the efficiency of MyD88 dsRNA and Relish dsRNA in silencing the expression of MyD88 or Relish genes in shrimp, the expression of MyD88 and Relish mRNA, respectively, was determined after injection of 10 µg/g shrimp of the MyD88 dsRNA, Relish dsRNA, GFP dsRNA or 0.85% NaCl into shrimp. At time point 0, 24, 48 and 72 hpi, hemolymph of individual shrimp were collected and total RNA was extraction as described in section 2.4.2. The first strand cDNA was synthesized from 1 µg of the total RNA using the RevertAid™ First Strand cDNA Synthesis Kit as described in section 2.4.3. The elongation factor-1α (EF-1α) gene was generally used as an internal control. The PCR reaction in a 12.5 µl total volume was carried out. The reaction contained 1 µl of 5-fold diluted cDNA template, 1.25 µl of 10× PCR buffer, 0.125 µl of

10 mM dNTP mix, 0.125 µl of 10 µM forward primer, 0.125 µl of 10 µM reverse primer, 8.8125 µl of sterile ultrapure water, and 0.0625 µl of 5 U/µl RBC *Taq* polymerase (Bioscience). For MyD88 gene, the PCR condition was pre-denaturation at 94 °C for 1 min followed by 30 cycles of denaturation at 94 °C for 30 sec, annealing at 60 °C for 30 sec and extension at 72 °C for 30 sec, and the final extension at 72 °C for 10 min. For Relish gene, the PCR condition was pre-denaturation at 94 °C for 1 min followed by 35 cycles of denaturation at 94 °C for 30 sec, annealing at 60 °C for 30 sec and extension at 72 °C for 30 sec, and the final extension at 72 °C for 10 min. The PCR condition for EF-1α gene was pre-denaturation at 94 °C for 1 min followed by 27 cycles of denaturation at 94 °C for 30 sec, annealing at 58 °C for 30 sec and extension at 72 °C for 30 sec, and the final extension at 72 °C for 10 min. The PCR products were analyzed by 1.5% (w/v) agarose gel electrophoresis.

Table 2.6 Primer pairs used for quantitative realtime RT-PCR amplification

Gene	**Primer**	**Sequence (5'-3')**	**PCR product**
EF-1α	EF-F	5'-GGTGCTGGACAAGCTGAAGGC-3'	149 bp
	EF-R	5'-CGTTCCGGTGATCATGTTCTTGATG-3'	
PmMyD88	PmMyD88-RT_F	5' GTGCACCAGAGTCATTGTAG3'	170 bp
	PmMyD88-RT_R	5' GGGAGTGGCAGAAACTTATC 3'	
PmRelish	PmRelish-RT_F	5' TCTCCAGGTGAGCACTCAGTTG 3'	157 bp
	PmRelish-RT_R	5' GCTGTAGCTGTTGCTGTTGTTGAG 3'	

2.4.7 Preparation of *Vibrio harveyi* infected shrimp

A single colony of *V. harveyi* was inoculated in the tryptic soy broth (TSB) supplemented with 2%(w/v) NaCl at 30 °C for 12-16 h, The overnight culture was diluted (1:100) in the same medium and grown at 30 °C for 2 h. The culture was then diluted 1:100 with a sterile 0.85% (w/v) NaCl. The titer of this dilution (10^8 CFU/ml) was

monitored by a plate count method in tryptic soy agar (TSA) supplemented with 2% (w/v) NaCl (modified from Austin, 1988). *V. harveyi* approximately 10^6 CFU/ml was intramuscularly injected into the forth abdominal segment, whereas the control group was injected with 100 µl of 0.85% (w/v) NaCl solution.

2.4.8 MyD88 dsRNA and Relish dsRNA mediated gene knockdown in *V. harveyi* infected shrimp

To investigate the effect of MyD88 and Relish gene knockdown upon *V. harveyi* infection on the ALF*Pm*3 and ALF*Pm*6 transcripts, shrimp were divided into 3 groups including MyD88 dsRNA, Relish dsRNA or GFP dsRNA gene silencing. The 10 µg/g shrimp of the MyD88 dsRNA, Relish dsRNA or GFP dsRNA into shrimp. After the first dsRNA injection for 12 h, shrimp were challenged with 10^6 CFU of *V. harveyi* mixed with 10 µg/g shrimp dsRNA. At 0, 6 and 24 h post *V. harveyi* infection, shrimp hemolymph was collected for total RNA extraction, cDNA synthesis and RT-PCR analysis. Transcription levels of ALF*Pm*3 and ALF*Pm*6 genes in each sample were analyzed by quantitative real-time PCR.

To confirm that the MyD88 dsRNA and Relish dsRNA could also suppress the MyD88 and Relish transcripts in *V. harveyi*-infected shrimp, the expression of MyD88 and Relish gene in *V. harveyi*-infected shrimp injected with MyD88 dsRNA, Relish dsRNA or GFP dsRNA was determined by RT-PCR. At 0, 6 and 24 h post *V. harveyi* infection, shrimp hemolymph was collected for total RNA extraction, cDNA synthesis and RT-PCR analysis. The PCR product was analyzed by 2% agarose gel electrophoresis and EtBr staining.

Quantitative realtime RT-PCR analysis was performed on the BioRad CFX96™ Real-Time PCR system. For ALF*Pm*3, ALF*Pm*6 and EF-1α gene amplification, gene specific primer were used (Table 2.6). EF-1α gene was generally used as an internal control. Reactions were prepared in a total volume of 15 µl containing 7.5 µl SsoFast™ EvaGreen Supermix (Bio-Rad), 1 µl cDNA template, 1 µl each of 10 µM forward and reverse primers. Amplification profile consisted of 94 °C for 5 min, and 40 cycles of 94 °C for 30 s, 60 °C for 30 s and 72 °C for 30 s. The $2^{-\Delta\Delta_{ct}}$ method was used to calculate

the relative expression ratio (Pfaffl 2001). Expression of each gene was normalized relatively to EF-1α gene in the same sample.

PCR amplification efficiency, E, is calculated from the slope of the standard curve and expressed as the percentage of the efficiency or % efficiency (%E). The conversion of percentage efficiency to E used the formula (Pfaffl, 2001):

$$E = (\%\ \text{Efficiency} \times 0.01) + 1$$

Table 2.7 Primer pairs used for PCR amplification

Gene	**Primer**	**Sequence (5'-3')**
EF-1α	EF-F	5'-GGTGCTGGACAAGCTGAAGGC-3'
	EF-R	5'-CGTTCCGGTGATCATGTTCTTGATG-3'
ALF*Pm*3	qRT-ALF*Pm*3_F	5'-CCCACAGTGCCAGGCTCAA-3'
	qRT-ALF*Pm*3_R	5'-TGCTGGCTTCTCCTCTGATG-3'
ALF*Pm*6	qRT-ALF*Pm*6_F	5'-AGTCAGCGTTTAGAGAGGTT-3'
	qRT-ALF*Pm*6_R	5'-GCTCGAACTCTCCACTCTC-3'

CHAPTER III
RESULTS

3.1 Expression and characterization of ALF*Pm6*

3.1.1 Transformation of pALF*Pm6* into *P. pastoris*

Previously, a gene fragment coding for mature peptide of ALF*Pm6* was cloned into pPIC9K vector. To characterize ALF*Pm6* protein, the recombinant protein of ALF*Pm6* (rALF*Pm6*) was produced in *Pichia pastoris* expression system. The recombinant expression plasmid, pALF*Pm6*, that has been checked for the correction of sequences coding for rALF*Pm6* has the deduced amino acid sequences, predicted molecular mass and pI, as shown in Table 3.1. The pALF*Pm6* was linearized with *Sac*I (Fig. 3.1) and transformed into *P. pastoris* by electroporation. The transformants were selected on MD plates before screening for G418-sulfate resistance on YPD plates containing 1 and 2 mg/ml G418-sulfate antibiotic. The G418-sulfate resistant clones were determined for the presence of the integrated ALF*Pm6* expression cassette in *Pichia* genome by colony PCR (Fig. 3.2). The parental plasmid, pPIC9K, and the recombinant plasmids, pALF*Pm6*, should give a specific band of 195 bp and 344 bp, respectively. The result indicated that all selected transformants contained the ALF*Pm6* expression cassette integrated into *Pichia* genome. Although the number of copies of the expression cassette, pALF*Pm6* construct integrated into *Pichia* genome has not yet been determined, the transformants which could grow on YPD plate containing 2 mg/ml, were considered as high-copy-number transformants and screened for rALF*Pm6* expression.

Table 3.1 The deduced amino acid sequence, predicted molecular weight and pI of rALF*Pm6*

Recombinant protein	**rALF*Pm6***
Amino acid sequence	YVSGWEALVPAIANKLTSLWESGEFELLGHYCSFNVTPKFKRW QLYFRGRMWCPGWTTIRGQAETRSRSGVVGRTTQDFVRKAFR AGIITESEAQAWLNN
Amino acid length (residues)	100
pI	9.62
Molecular weight (dalton)	11520.10

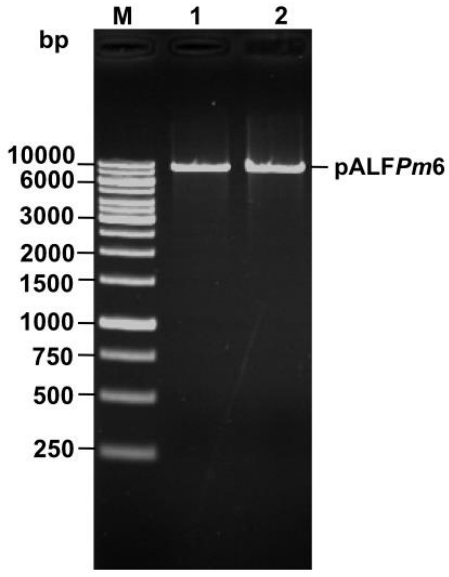

Figure 3.1 Preparation of *Sac*I-linearized pALF*Pm6* plasmid for *Pichia pastoris* KM71 transformation. The recombinant plasmid, pALF*Pm6*, was linearized with *Sac*I and run on 1.2% agarose gel electrophoresis to confirm the complete digestion before

transformation into *P. pastoris* KM71 by electroporation to produce recombinant yeast expressing rALF*Pm6.*

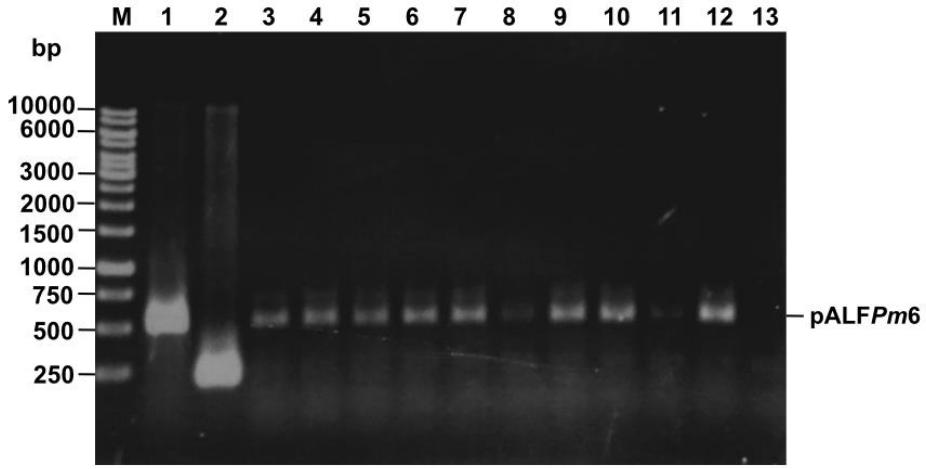

Figure 3.2 Screening for recombinant yeast containing multi-copy of ALF*Pm6*-expression cassette. The yeast transformants were screened on YPD containing 1 mg/ml and 2 mg/ml of G418-sulfate. Ten hyper-resistant clones that could grow on YPD plate containing 2 mg/ml G418-sulfate considering as high-copy-number transformants were randomly selected and checked for integrated ALF*Pm6* expression cassette in genome by colony PCR.

Lane M : 1 kb DNA Ladder

Lane 1 : PCR product of plasmid pALF*Pm6*

Lane 2 : PCR product of plasmid pPIC9K

Lane 3-12 : PCR product of 2 mg/ml G418-sulfate resistant transformants

Lane 13 : negative control

3.1.2 Screening of the recombinant clones expressing rALF*Pm6*

To obtain clone with the highest level of rALF*Pm6* protein expression, small-scale screening was performed. Eight hyper-resistant recombinant clones for rALF*Pm6* expression (rALF*Pm6* no. 1-8) were grown in BMGY medium until A_{600} reached 6 and induced for expression by maintaining methanol induction for 3 days. Using α-factor signal, rALF*Pm6* was secreted into the culture medium. The culture supernatant was collected and the rALF*Pm6* protein was analyzed by 15% silver-stained SDS-PAGE (Fig. 3.3). Six clones including clone number 1, 2, 3, 6, 7 and 8 were successfully produced rALF*Pm6* protein with the expected size of about 12 kDa from day 1 to day 3 after induction. The preliminary antibacterial assay of the day 3 crude culture supernatant was performed against a Gram-negative bacterium, *E. coli* 363, and a Gram-positive bacterium, *B. megaterium*, using liquid broth assay. The rALF*Pm6* no. 1, 2, 3, 6, 7 and 8 could inhibit growth of both tested strains (Fig. 3.4). These results indicated that the active rALF*Pm6* were produced. The rALF*Pm6* no. 1 showing the highest antibacterial activity was selected for a large-scale production.

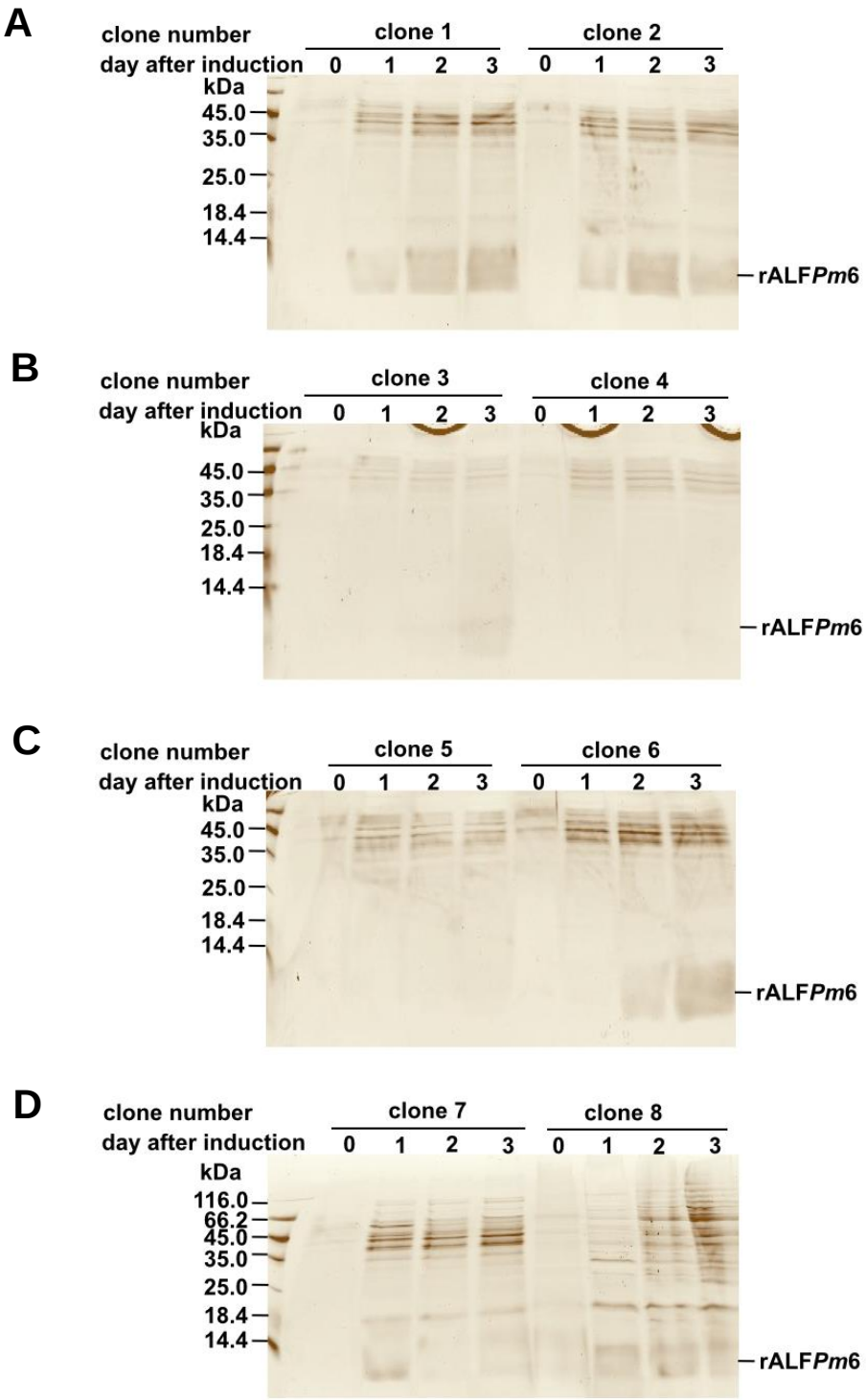

Figure 3.3 Analysis of rALF*Pm6* expression from *P. pastoris* transformants by 15% silver-stained SDS-PAGE. Eight hyper-resistant clones that could grow on YPD plate containing 2 mg/ml G418-sulfate were random selected and tested for rALF*Pm6* protein

expression. The culture supernatant was collected before (day 0) and after methanol induction for 1, 2 and 3 days and the rALF*Pm*6 protein expression was analyzed. The expected band of the rALF*Pm*6 protein, whose size of about 12 kDa is indicated.

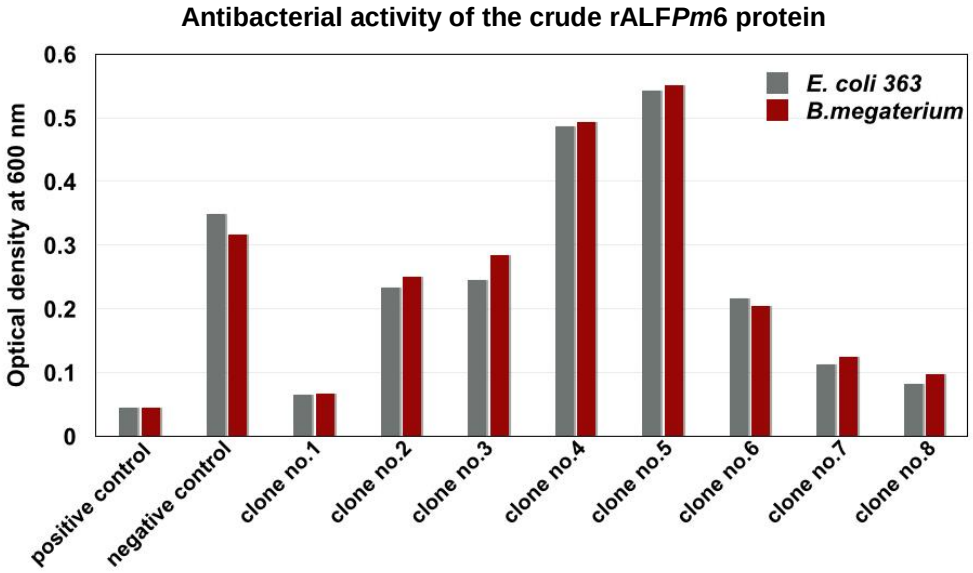

Figure 3.4 Antibacterial activity assay of the crude rALF*Pm*6 protein. The crude rALF*Pm*6 (day 3), which over-produced by eight hyper-resistant clones, was performed against a Gram-negative bacterium, *E. coli* 363, and a Gram-positive bacterium, *B. megaterium*, using liquid broth assay. The diluted bacterial culture (A_{600}=0.001) was incubated with the crude rALF*Pm*6 proteins at 30˚C in a shaking incubator at 120 rpm and measured the bacterial growth at 600 nm after 16-18 h. The inhibition bacterial growth was observed comparing with negative and positive control, which the diluted bacterial culture or poor-broth (PB) medium, respectively, was incubated with sterile water.

3.1.3 Optimization of the rALF*Pm6* protein production

3.1.3.1 Effect of cell density and induction time on the rALF*Pm6* protein production

ALF homologues have been characterized in many crustacean species. Many reports showed that ALFs exhibit a potent antimicrobial activity against a broad range of microorganisms (Tassanakajon et al. 2010). The positive-charged cluster in LPS-binding site of ALF mainly contributes to antimicrobial activity. To further characterize ALF*Pm6* antimicrobial activity, the rALF*Pm6* no.1 was selected for large-scale production and purification.

The optimum conditions (cell density, methanol induction time and temperature) for rALF*Pm6* expression were investigated. In *P. pastoris* expression system, the culture can grow to very high densities, which is useful for the large-scale production of the recombinant protein. To determine the optimum cell density and induction time, the rALF*Pm6* clone no. 1 was cultured in BMGY medium at 30 °C until OD_{600} reached 10, 15 and 20 and induced rALF*Pm6* expression by maintaining methanol at 0.5% final concentration for 3 days. Every 24 hours after induction, the culture supernatant was collected. The rALF*Pm6* protein was analyzed by 15% silver-stained SDS-PAGE. The result showed that the rALF*Pm6* protein was produced from day 1 to 3 after methanol induction. At OD_{600} of about 15, the rALF*Pm6* protein was expressed at the highest level according to the band density observed when compared to at OD_{600} of 10 and 20 (Fig. 3.5). Also, the result showed no difference in band intensity from day 1 to 3 after induction indicating that only 1 day induction is required for the rALF*Pm6* protein expression. Therefore, to obtain high quantity of rALF*Pm6* protein, the yeast transformant was grown to optimum cell density at OD_{600} of about 15 before methanol induction and induced with 0.5% methanol for 1 day.

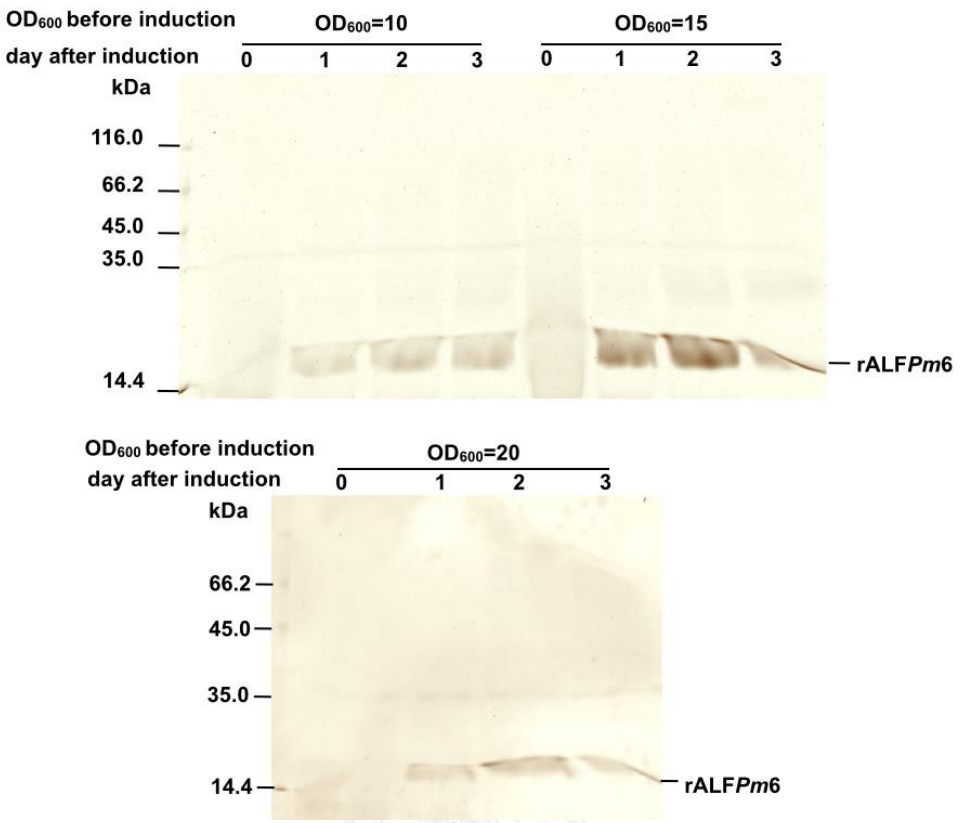

Figure 3.5 Effect of cell density and induction time on the rALF*Pm*6 protein expression level. Yeast transformant rALF*Pm*6 no. 1 was grown at 30 °C to OD_{600} of 10, 15 and 20 and induced by 0.5% methanol for 3 days. The culture supernatant was collected before (day 0) and after methanol induction for 1-3 days and analyzed for the level of rALF*Pm*6 protein production by 15% silver-stained SDS-PAGE.

3.1.3.2 Effect of temperature on the rALF*Pm6* protein production

Temperature is a key environmental factor known to affect protein expression. To optimize the temperature used for culture, the culture was grown at 28 °C or 30 °C until OD_{600} reached 15 and induced for rALF*Pm6* expression for 1 day. The culture supernatant was collected and the rALF*Pm6* protein was detected by 15% silver-stained SDS-PAGE (Fig. 3.6). The result showed that culturing the transformant at 28 °C could produce higher level of rALF*Pm6* expression than at 30 °C.

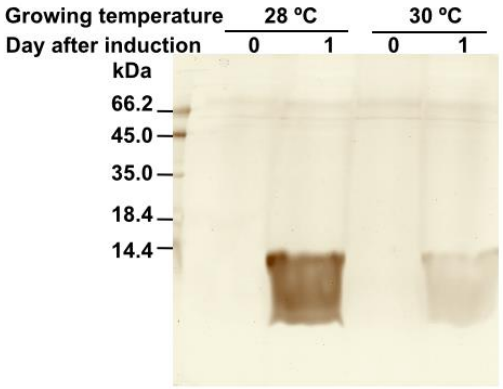

Figure 3.6 Effect of temperature on the rALF*Pm6* protein expression. Yeast transformant was grown at 28 °C and 30 °C until OD_{600} reached 15. The culture supernatant was collected before (day 0) and after methanol induction for 1 day and analyzed for the level of rALF*Pm6* protein production by 15% silver-stained SDS-PAGE.

3.1.4 Purification of the rALF*Pm*6 protein

In order to obtain the purified rALF*Pm*6 protein for further analysis, cation exchange chromatography was used because of the high cationic property of rALF*Pm*6 (pI=9.62). Various conditions for the rALF*Pm*6 protein purification have been tried (Table 2.2). The crude rALF*Pm*6 protein was purified as described in section 2.1.6 and the elution fractions were analyzed by 15% SDS-PAGE.

For the first condition, the crude rALF*Pm*6 protein was purified by 5 ml HiTrap SP HP column (GE Healthcare) on the AKTA Prime Plus Purification System (GE Healthcare). The crude protein was diluted 1:1 with the start buffer (20 mM Tris-HCl, pH 7.0). The purification was controlled at flow rate of 1 ml/min. After equilibration with 20 column volume of the start buffer, the rALF*Pm*6 protein was loaded into the column and washed with the start buffer to remove unbound proteins until A_{280} decreased to zero. The rALF*Pm*6 protein was eluted by elution buffer (20 mM Tris-HCl, pH 7 supplemented with 500 mM and 1 M NaCl). The fractions collected were analyzed by 15% silver-stained SDS-PAGE. The result showed that the rALF*Pm*6 was detected only in flow-through fraction but not in the elution fractions indicating that the rALF*Pm*6 protein could not bind to the column (Fig. 3.7). Testing for the antibacterial activity against *Escherichia coli* 363 and *Bacillus megaterium,* the crude protein and flow-through fractions showed the antibacterial activity against *E. coli* 363 and *B. megaterium*. These results confirmed the existence of rALF*Pm*6 in both fractions.

In the second condition, using the same buffer system as the first condition but pH was changed from pH 7.0 to pH 6.0. The crude protein was diluted 1:1 with the start buffer (20 mM phosphate buffer pH 6.0). The bound rALF*Pm*6 protein was eluted by a series of elution buffer (20 mM phosphate buffer pH 6.0 supplemented with 100 mM, 300 mM, 500 mM and 1 M NaCl). The band corresponding to the rALF*Pm*6 was detected in crude and flow-through fractions as a major band and it was also found as a faint band in the elution fractions of elution buffer with 1 M NaCl (Fig. 3.8). These results suggested that the decrease of pH of purified buffer resulted in improving the binding of rALF*Pm*6 to the column. The crude protein, flow-through and elution fractions were tested for the antibacterial activity against *E. coli* 363 and *B. megaterium.*

The crude protein and flow-through fractions showed the antibacterial activity against *E. coli* 363 and *B. megaterium* while elution fraction did not show any antibacterial activity.

Because high salt concentration in the culture medium can affect the binding capacity of protein to the column, in the third condition, the crude protein was concentrated and desalted using Vivaflow50 (Sartorius AG). Then, the column was equilibrated with 20-column volume of the start buffer (50 mM phosphate buffer, pH 6.0). The rALF*Pm*6 protein was loaded onto the column and washed with the start buffer to remove unbound proteins until A_{280} decreased to zero. The purified rALF*Pm*6 protein was eluted by 50 mM phosphate buffer, 500 mM NaCl, pH 6.0. The rALF*Pm*6 protein containing fractions was collected and analyzed by 15% silver-stained SDS-PAGE. The result showed that rALF*Pm*6 was detected in crude and flow-through fractions as a major band. The rALF*Pm*6 protien and the other impurity proteins was found as a faint band in the elution fractions (Fig. 3.9). The crude protein and flow-through fractions showed the antibacterial activity against *E. coli* 363 and *B. megaterium* while the elution fractions containing the band corresponding to rALF*Pm*6 did not exhibit antibacterial activity.

In the fourth condition, the purified buffer was changed from 50 mM phosphate buffer, pH 6.0 to 50 mM MES buffer, pH 6.0. The crude protein was dialyzed against binding buffer (50 mM MES buffer, pH 6.0). The column was equilibrated with the start buffer and the rALF*Pm*6 protein was loaded into the column. The bound protein was eluted by the elution buffer containing 300 mM NaCl and 500 mM NaCl. The rALF*Pm*6 protein containing fractions were collected and analyzed by 15% silver-stained SDS-PAGE. The result showed the expected band of purified rALF*Pm*6 in the elution fractions at 500 mM NaCl (Fig. 3.10). The crude protein and flow-through fractions showed the antibacterial activity against *E. coli* 363 and *B. megaterium* while this activity was not found on the elution fractions.

In the fifth condition, using the same buffer system as the fourth condition but pH of binding buffer and elution buffer were changed from pH 6.0 to pH 5.6. The crude protein was dialyzed against binding buffer (50 mM MES buffer, pH 5.6). The column

was equilibrated with the start buffer and the rALF*Pm6* protein was loaded into the column. The bound protein was eluted by the elution buffer containing 300 mM NaCl and 500 mM NaCl. The rALF*Pm6* protein-containing fractions were collected and analyzed by 15% silver-stained SDS-PAGE. The result showed the expected band of purified rALF*Pm6* in the elution fractions at 500 mM NaCl (Fig. 3.11). The crude protein showed the antibacterial activity against *E. coli* 363 and *B. megaterium* while this activity was not found on the elution fractions and flow-through fractions.

In conclustion, the purification of rALF*Pm6* protein was not successful because only small amount of rALF*Pm6* protein could bind to 5 ml HiTrap SP HP column in different condition (condition 2-5). The loss of antibacterial activity of this elution fraction was probably due to low quantity of rALF*Pm6*.

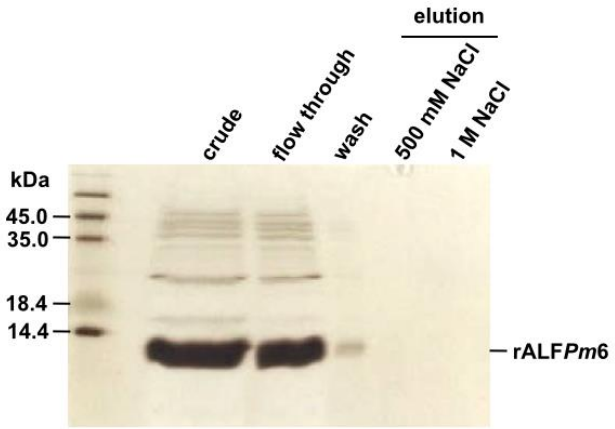

Figure 3.7 The crude rALF*Pm6* protein was purified by using 5 ml HiTrap SP HP column (Condition 1). The crude protein was diluted 1:1 with the start buffer; 20 mM Tris-HCl, pH 7.0. The rALF*Pm6* protein was loaded into the column and washed with the start buffer to remove unbound proteins. The purified rALF*Pm6* protein was eluted with 20 mM Tris-HCl, pH 7.0 supplement with 500 mM and 1 M. The rALF*Pm6* protein fractions were analyzed by 15% silver-stained SDS-PAGE.

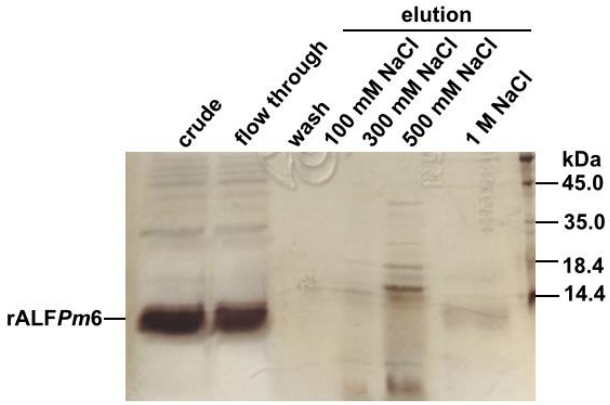

Figure 3.8 The crude rALF*Pm6* protein was purified by using 5 ml HiTrap SP HP column (Condition 2). The crude protein was diluted 1:1 with the start buffer; 20 mM Tris-HCl, pH 6.0. The rALF*Pm6* protein was loaded into the column and washed with the start buffer to remove unbound proteins. The purified rALF*Pm6* protein was eluted with 20 mM Tris-HCl, pH 6.0 supplement with 100 mM, 300 mM, 500 mM and 1 M. The rALF*Pm6* protein fractions were analyzed by 15% silver-stained SDS-PAGE.

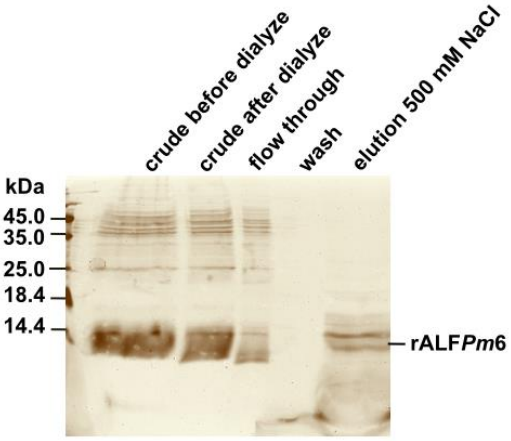

Figure 3.9 The crude rALF*Pm6* protein was purified by using 5 ml HiTrap SP HP column (Condition 3). The crude protein was concentrated and desalted by using Vivaflow50 (Sartorius AG). The rALF*Pm6* protein was loaded into the column and washed with the start buffer to remove unbound proteins. The purified rALF*Pm6* protein was eluted with 50 mM phosphate buffer, pH 6.0, 500 mM NaCl. The rALF*Pm6* protein fractions were analyzed by 15% silver-stained SDS-PAGE.

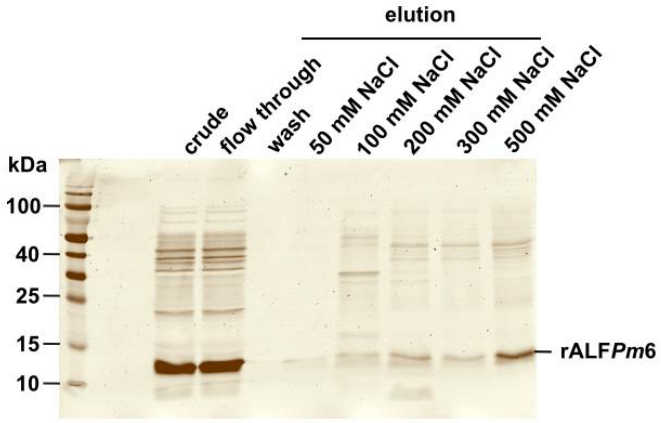

Figure 3.10 The crude rALF*Pm*6 protein was purified by using 5 ml HiTrap SP HP column (Condition 4). The crude protein was dialyzed in 50 mM MES buffer, pH 6.0. The rALF*Pm*6 protein was loaded into the column and washed with the start buffer to remove unbound proteins. The purified rALF*Pm*6 protein was eluted with 50 mM MES buffer, pH 6.0 supplement with 50 mM, 200 mM, 300 mM, 500 mM and 1 M. The rALF*Pm*6 protein fractions were analyzed by 15% silver-stained SDS-PAGE.

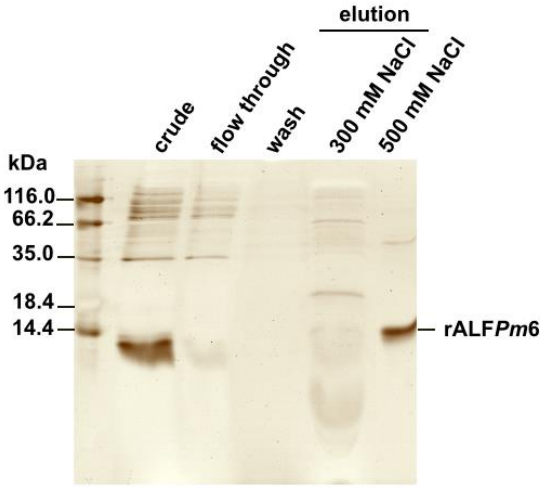

Figure 3.11 The crude rALF*Pm*6 protein was purified by using 5 ml HiTrap SP HP column (Condition 5). The crude protein was dialyzed in 50 mM MES buffer, pH 5.6. The rALF*Pm*6 protein was loaded into the column and washed with the start buffer to remove unbound proteins. The purified rALF*Pm*6 protein was eluted with 50 mM MES buffer, pH 5.6, 500 mM NaCl. The rALF*Pm*6 protein fractions were analyzed by 15% silver-stained SDS-PAGE.

3.1.5 Antimicrobial activity of ALF*Pm*6-derived synthetic peptide

According to previous report, the antimicrobial activity of ALFs depends on the binding capacity to pathogen cell wall, which is mediated mainly via a positively charged cluster within LPS-binding domain of ALFs peptide (Rosa et al. 2013a). Although, purification of rALF*Pm*6 protein was unsuccessful, the peptide sequence corresponding to the LPS-binding domain of ALF*Pm*6 was synthesized and tested for the antibacterial activity.

The amino acid sequence (YCSFNVTPKFKRWQLYFRGRMWCP) corresponding to the cyclic LPS-binding domain of ALF*Pm*6 (accession number: AER45468) with a flanking amino acid residue in both N and C terminal end was designed and synthesized, in which a disulfide bond was formed between two cysteine residues. The synthetic cyclic peptide, cALF*Pm*6#29-52, was examined for antimicrobial activity against various strains of Gram-negative bacteria including *E. coli* 363, *K. pneumoniae, E. cloacae*, *V. harveyi,* non-vilurent *V. parahaemolyticus,* vilurent *V. parahaemolyticus* (AHPND) and *E. carotovora*, and Gram-positive bacteria including *B. megaterium*, *A. viridans, M. luteus, S. haemolyticus* and *S. aureus*. The complete killing of bacteria of cALF*Pm*6#29-52 peptide was observed when compared with positive control. It could kill a Gram-negative bacterium, *E. coli* 363, and some Gram-positive bacteria *B. megaterium*, *A. viridans,* and *M. luteus* with MBC value of 25-50 μM (Table 3.2).

Table 3.2 Range of bactericidal activity of the synthetic peptide ALF*Pm*6 against various strains of microorganisms using liquid growth inhibition assay

Microorganisms	**MBC value*** **ALF*Pm*6#29-52 (μM)**
Gram-positive bacteria	
Aerococcus viridans	25-50
Bacillus megaterium	25-50
Micrococcus luteus	25-50
Staphylococus haemolyticus	>100
Gram-negative bacteria	
Enterobacter cloacae	>100
Erwinia carotovora	>100
Escherichia coli 363	25-50
Klebsiella pneumoniae	>100
Virulent Vibrio haemolyticus	>100
Non-virulent Vibrio haemolyticus	>100
Vibrio harveyi	>100

*MBC value is expressed as the interval *a-b,* where *a* is the highest concentration tested at which microorganisms are growing and *b* the lowest concentration tested to kill particular bacterium.

3.1.6 Bacterial agglutination property

From previous studies, some antimicrobial proteins and peptides have been found to agglutinate bacteria cells. Interestingly, rcrustin*Pm*1 and rcrustin*Pm*7 could inhibit the growth of bacteria and also induced bacterial agglutination (Krusong et al. 2012).

In this study, bacterial binding property of the synthetic cyclic peptide, ALF*Pm*6#29-52 (cALF*Pm*6#29-52), was tested in soluble phase by monitoring bacterial agglutination property. Bacterial strians including *E. coli* 363, *B. megaterium*, *A. viridans,* and *M. luteus* were grown at exponential phase and incubated with the synthetic cALF*Pm*6#29-52 in 96-wells plates for 16 h at 30°C in a shaking incubator at 150 rpm. After incubation, one drop of the mixture was placed on a microscope slide and bacterial sample were then Gram-stained and observed under a light microscope. The result showed that the synthetic cALF*Pm*6#29-52 induced bacterial agglutination in *E. coli* 363, *B. megaterium*, *A. viridans,* and *M. luteus* at 25 μM final concentration. At 50 μM ALF*Pm*6#29-52 where the bacterial growth was completely inhibited, only cell debris could be noticed under microscopic observation (Fig. 3.12).

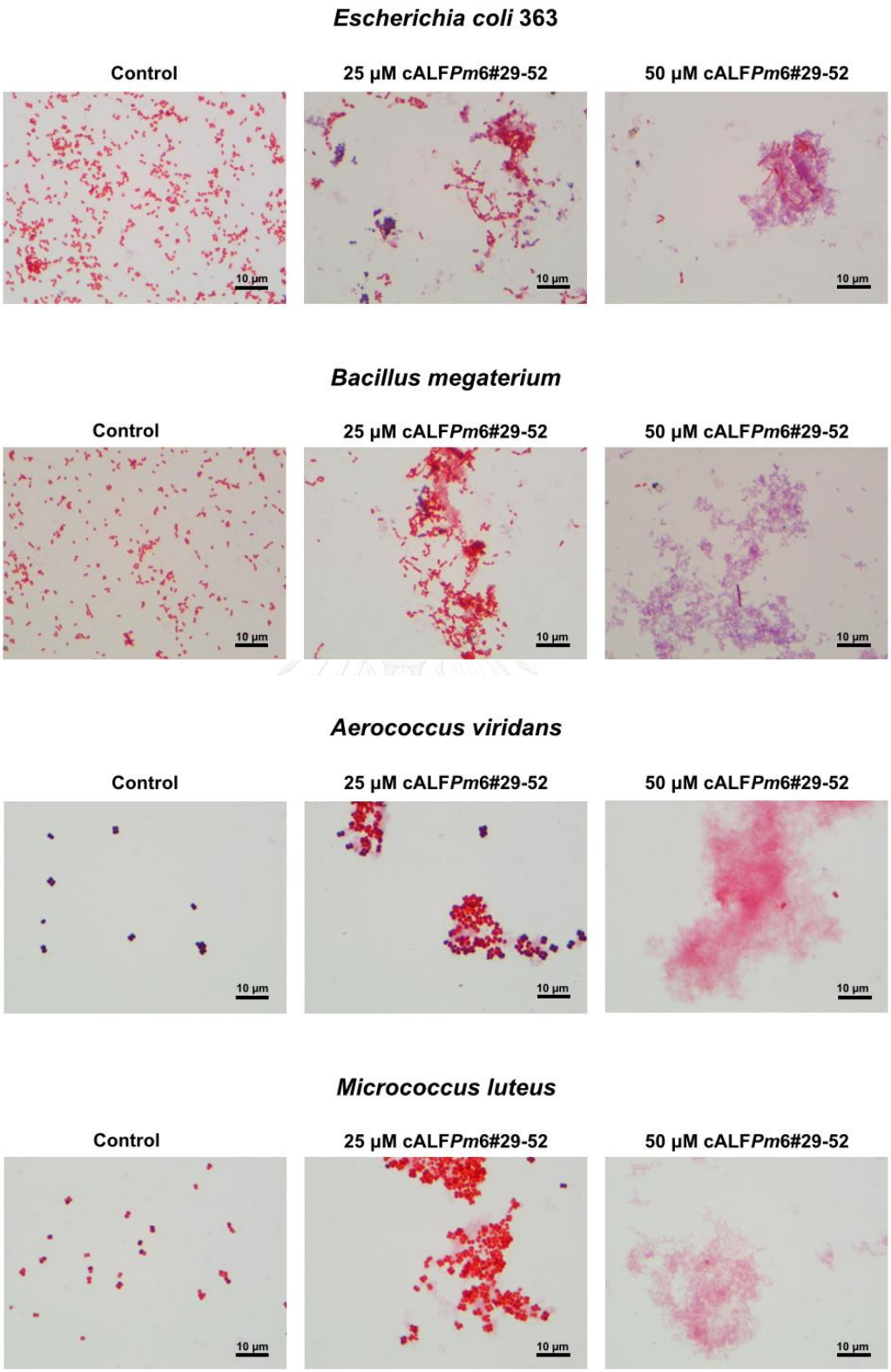

Figure 3.12 Bacterial agglutination mediated by the synthetic cyclic peptide ALF*Pm*6#29-52 (cALF*Pm*6#29-52). (A) *Escherichia coli* 363, (B) *Bacillus megaterium*, (C) *Aerococcus viridans*, and (D) *Micrococcus luteus* was incubated with the synthetic

cALF*Pm*6#29-52 at 25 and 50 µM final concentration. The agglutination was under a 100X magnification of light microscope (Olympus CX31) and images were taken using a Nikon DS-Fi1.

3.2 Characterization of the ALF*Pm*3 and ALF*Pm*6 gene regulation

3.2.1 Promoter sequence identification of ALF*Pm*3 and ALF*Pm*6 gene

It is the fact that the expression profiles of ALF*Pm*3 and ALF*Pm*6 genes upon infection of shrimp pathogens are different (Ponprateep et al. 2012). To better understand how both genes are regulated, the sequences and activity of their promoter were identified and characterized.

From the previous study, approximately 600 bp of ALF*Pm*3 5′ upstream sequences from the transcription start site was obtained by genome walking technique. The putative promoter of ALF*Pm*3 was identified at the position -29 of 5′ upstream sequences. Several transcription factor-binding sites, including octamer (Oct-1), GATA, CCAAT box and GAAA motifs, were predicted in the 5′ upstream sequences (Tharntada et al., 2007). However, the promoter activity has not been tested.

In this experiment, the 5′ upstream genomic sequences of ALF*Pm*3 and ALF*Pm*6 were identified by genome walking technique. For ALF*Pm*3 promoter, three genomic libraries derived from *P. monodon* DNA digested with *Dra*I, *Pvu*II and *Stu*I were used as template. While the 5′ upstream genomic sequences of ALF*Pm*6 were obtained using *Dra*I, *Eco*RV, *Pvu*II and *Stu*I libraries as template. The PCR products of primary and nested PCR were analyzed by 1.0% agarose gel electrophoresis (Fig. 3.13). The adapter primer (AP2/AP2) was also used for amplification as a control for detecting any false positive results. The product of the nested PCR for ALF*Pm*3 and ALF*Pm*6 genome walking whose size of about 1700 bp and 600 bp, respectively, were detected, purified, cloned into pGEM-T easy vector, and analyzed for the nucleotide sequences by DNA sequencing. The obtained sequences were analyzed by Promoter 2.0 Prediction Server and BDGP (Neural Network Promoter Prediction). The position of transcription start site (+1) of ALF*Pm*3 and ALF*Pm*6 genes located on the nucleotide positions -302 and -85, respectively, 5′-upstream from the start codon (ATG) and TATA box of ALF*Pm*3 and

ALF*Pm*6 genes located on -31 to -23 and -29 to -24 5′-upstream from transcription start site (+1), respectively (Fig. 3.14).

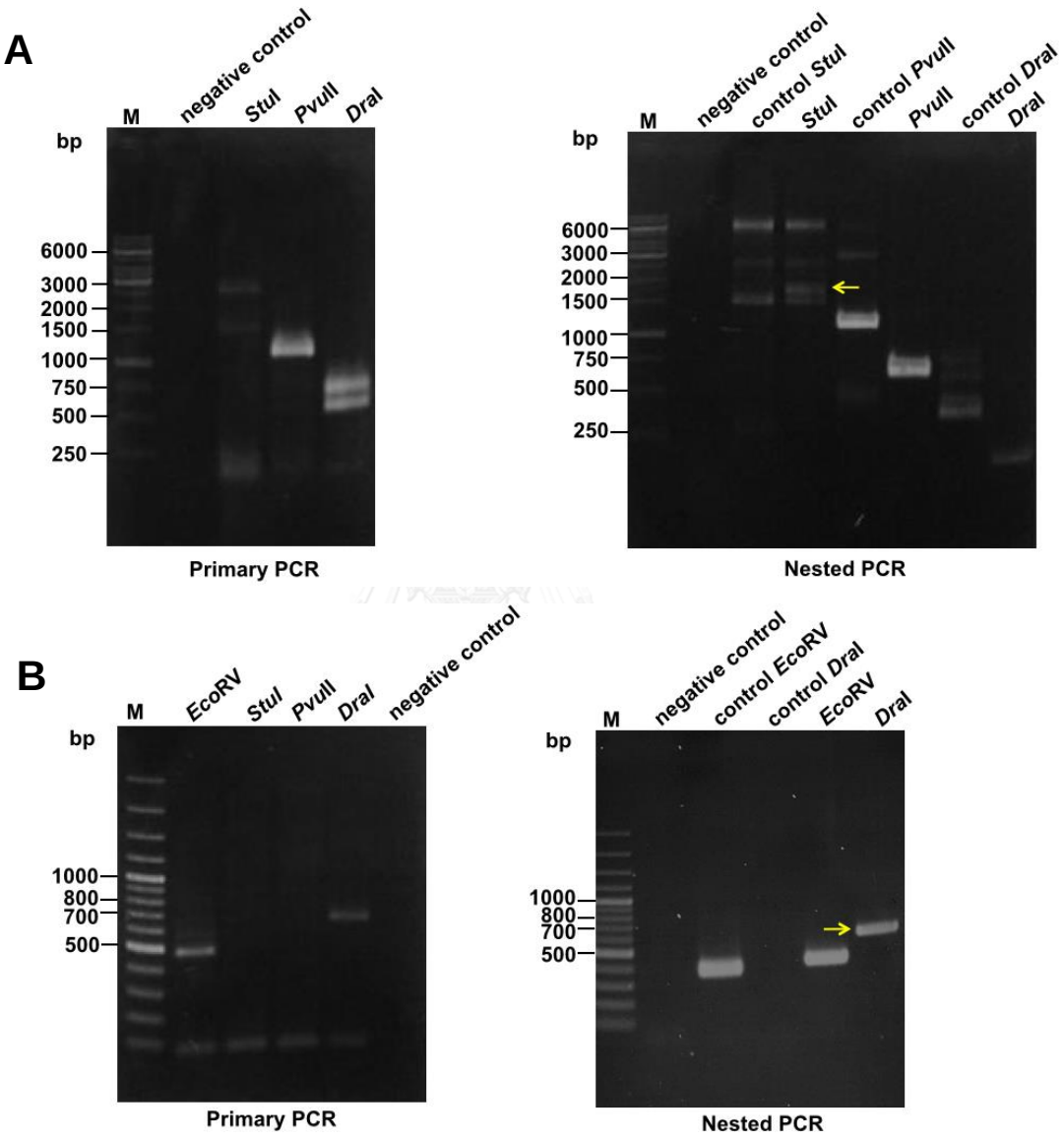

Figure 3.13 Identification of 5′-upstream sequences of ALF*Pm*3 and ALF*Pm*6 genes by Genome walking technique. Genome walking reactions of ALF*Pm*3 (A) and ALF*Pm*6 gene (B) were analyzed by 1.0% agarose gel electrophoresis. Three genomic libraries, *Stu*I, *Pvu*II and *Dra*I were used as template for ALF*Pm*3 and four genomic libraries of *EcoR*V, *Stu*I, *Pvu*II and *Dra*I were used as template for ALF*Pm*6. PCR reactions were

amplified using a gene specific primer and an adapter primer. In each library, the adapter primer only (AP2/AP2) was used in the control reaction for detecting any false positive results in the nested PCR reactions. The arrows show the major band of nested PCR product.

3.2.2 Determination of regulatory elements of ALF*Pm*3 and ALF*Pm*6 gene by bioinformatic analysis

The 5′ upstream sequences were analyzed for the putative cis-regulatory elements by using Match and Alibaba 2 analysis program (TRANSFAC® Public database). The putative promoter of ALF*Pm*3 and ALF*Pm*6 genes were identified at position -30 and -32, respectively, 5′ upstream sequences from the start site. Several transcription factor-binding sites were predicted (Fig. 3.14).

For ALF*Pm*3 gene, several transcription factor-binding sites such as specificity protein 1 (Sp-1), activator protein 1 (AP-1), nuclear factor (NF)-kappaB binding sites, CCAAT-enhancer-binding proteins beta (C/EBPbeta), CCAAT-enhancer-binding proteins alpha (C/EBPalpha), octamer (Oct-1), GATA, Hepatocyte nuclear factors-1 (HNF-1), Hepatocyte nuclear factors-1C (HNF-1C), D1, cytoplasmic polyadenylation element binding protein (CPE bind) and interferon consensus sequence-binding protein (ICSBP), were predicted (Fig. 3.14A).

For ALF*Pm*6 gene, many transcription factor-binding sites were predicted including specificity protein 1 (Sp-1), octamer (Oct-1), GATA, CCAAT-enhancer-binding proteins beta (C/EBPbeta), and interferon consensus sequence-binding protein (ICSBP), were predicted (Fig. 3.14B).

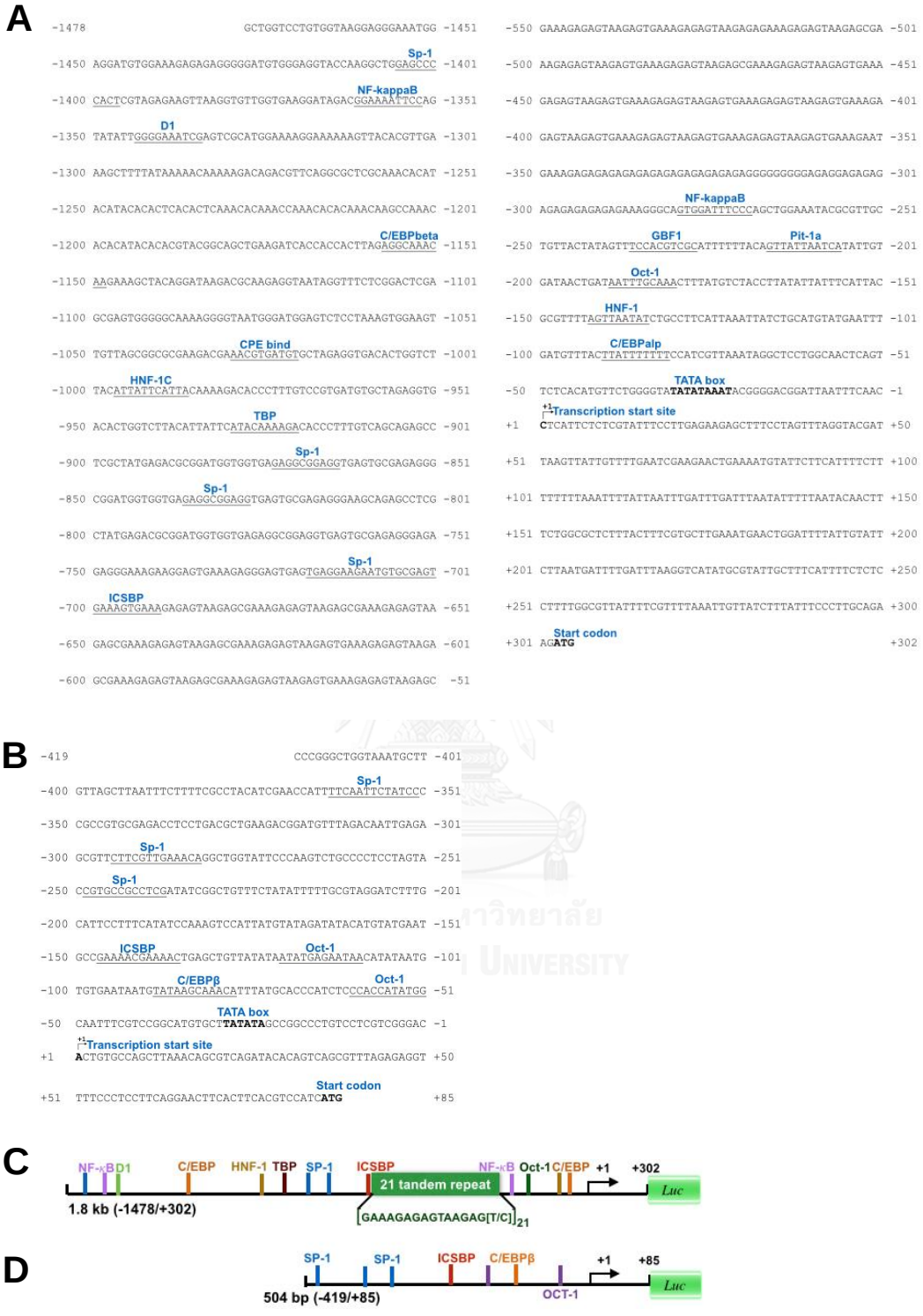

Figure 3.14 Genomic sequence of the 5′-upstream region of ALF*Pm*3 (A) and ALF*Pm*6 (B) genes. The putative cis-regulatory elements in the 5′-flanking promoter region are

underlined. The transcription start site (+1) is indicated by the arrow labeled +1. Start codon and TATA box are also indicated and their sequences are bolded. Schematic diagrams of the ALF*Pm*3 (C) and ALF*Pm*6 (D) promoter constructs used to delineate the TF-binding sites are shown.

3.2.3 Narrow down assay of ALF*Pm*3 and ALF*Pm*6 promoter activity in *Drosophila* S2 cell

From the obtained 5′ upstream sequences of both ALF*Pm* genes, the DNA sequence of ALF*Pm*3 promoter at position (-1478/+302) and of ALF*Pm*6 promoter at position (-419/+85) that contained TATA box and transcription factor binding site to translation start site (ATG, start codon) were cloned into pGL3-basic vector containing the firefly luciferase gene for promoter activity assay. The schematic diagrams showing ALF*Pm*3 and ALF*Pm*6 promoter constructs are shown in Fig. 3.14C and 3.14D, respectively.

The important part of ALF*Pm*3 and ALF*Pm*6 promoter sequences that involved in regulation of ALF*Pm*3 and ALF*Pm*6 gene expression were identified by narrow down assay. In first set, ALF*Pm*3 promoter sequences were randomly narrowed down from (-1478/+302) into 2 additional fragments of (-814/+302) and (-265/+302) and cloned into pGL3-basic vector. The reporter plasmids containing the ALF*Pm*3 promoter including p(-1478/+302), p(-814/+302) and p(-265/+302) were co-transfected with pRL-TK vector that contained the renella luciferase gene (internal control) into *Drosophilla* S2 cell. The promoter activities of each ALF*Pm*3 promoter fragment were determined. The promoter activity of each ALF*Pm*3 fragment was then compared to the control. The results showed that the promoter fragment -814/+302 had the highest promoter activity whereas the promoter fragment -265/+302 had the lowest activity but higher than the basal level (Fig. 3.15A), suggesting that the region -814/+302 might take part in controlling ALF*Pm*3 gene expression. To determine whether the promoter region from -265 to +302 was involved in ALF*Pm*3 gene regulation, the promoter fragment -814/+302 was further narrowed down to (-71/+302). The reporter plasmid p(-71/+302) together with p(-814/+302) and p(-265/+302) were tested for the promoter activity. The result indicated that the promoter sequence between position -265 to -72 was

not involved in regulation of ALF*Pm*3 gene expression because the promoter activity of p(-71/+302) as compared with p(-265/+302), which had the minimum promoter activity, was not significantly different (Fig. 3.15B). Next, the promoter active region was further determined by construction of p(-719/+302) and analysis for promoter activity in comparison with that of p(-814/+302) and p(-265/+302). The promoter activity of p(-814/+302) was at the highest level whereas that of p(-719/+302) was slightly decrease and the activity of p(-265/+302) was lowest (Fig. 3.15C). Therefore, the promoter sequence position -814 to -266 might has the activator-binding site. The DNA sequence at position -814 to -266 of ALF*Pm*3 promoter region contained many TF-binding sites such as Sp-1 at the position -719 to -701, ICSBP at the position -700 to -691, 21 units of GAAAGAGAGTAAGAG[T/C] tandem repeat at the position -693 to -358 and NF-κB at the position -280 to -270.

ALF*Pm*6 promoter were randomly narrowed down from (-419/+85) into 2 additional parts of (-282/+85) and (-80/+85). Each promoter fragment was amplified and cloned into pGL3-basic vector. The reporter plasmid containing various size of ALF*Pm*6 promoter including p(-419/+85), p(-282/+85) and p(-80/+85) were co-transfected into *Drosophilla* S2 cell with pRL-TK control plasmid. The promoter activity of each ALF*Pm*6 promoter fragment was determined. As compare to the control, the promoter fragment (-282/+85) had the highest promoter activity whereas the promoter fragment (-80/+85) showed the lowest promoter activity (Fig. 3.16). These results suggested that the ALF*Pm*6 promoter sequences at position -282 to -81 might be involved in ALF*Pm*6 gene regulation. The DNA sequence at position -282 to -81 of ALF*Pm*6 promoter region contained many transcription factor binding sites such as Sp-1 at the position -249 to -238, ICSBP at the position -146 to -135, Oct-1 at the position -121 to -112 and C/EBPβ at the position -88 to -80.

In conclusion, the ALF*Pm*3 promoter region between -814 to -266 and the ALF*Pm*6 promoter region between -282 to -81 nucleotide positions 5′ upstream from start site might contain the activator-binding site suggested by the significant decrease of promoter activity after the deletion of promoter region (-814/-265) and (-262/-162), respectively.

A

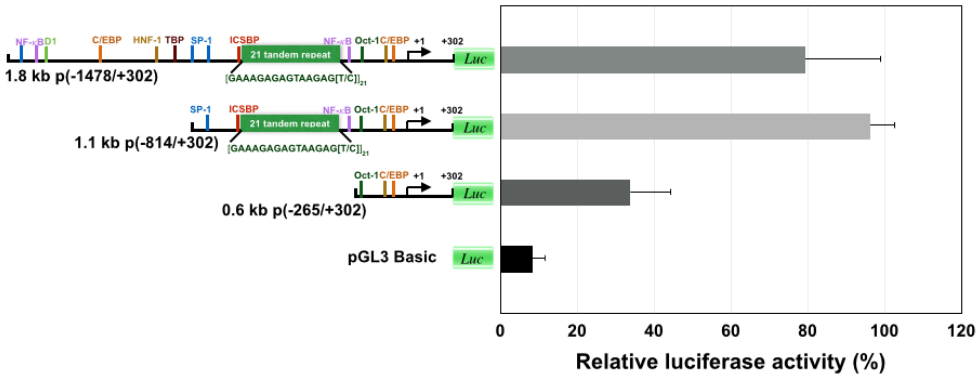

	pGL3	pGL3-promoter ALF*Pm*3		
		p(-265/+302)	p(-814/+302)	p(-1478/+302)
Relative luciferase activity (%) (mean±SD)	8.39±3.32	33.88±10.64	96.23±6.53	79.37±19.75

B

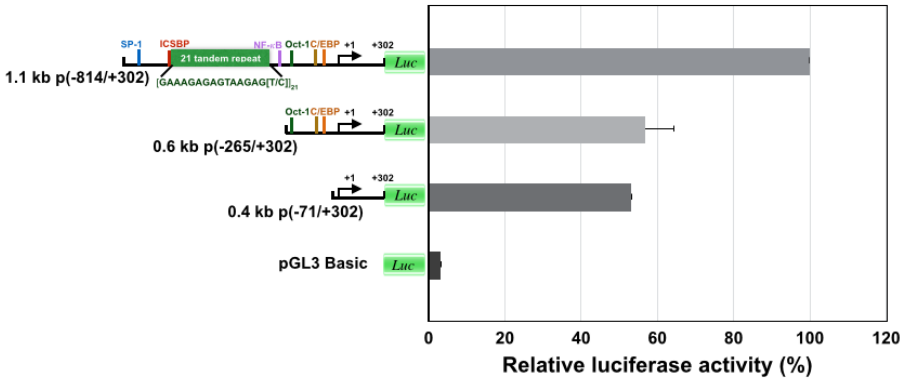

	pGL3	pGL3-promoter ALF*Pm*3		
		p(-71/+302)	p(-265/+302)	p(-814/+302)
Relative luciferase activity (%) (mean±SD)	3.36±0.31	53.03±0.38	56.69±7.73	100±0.00

C

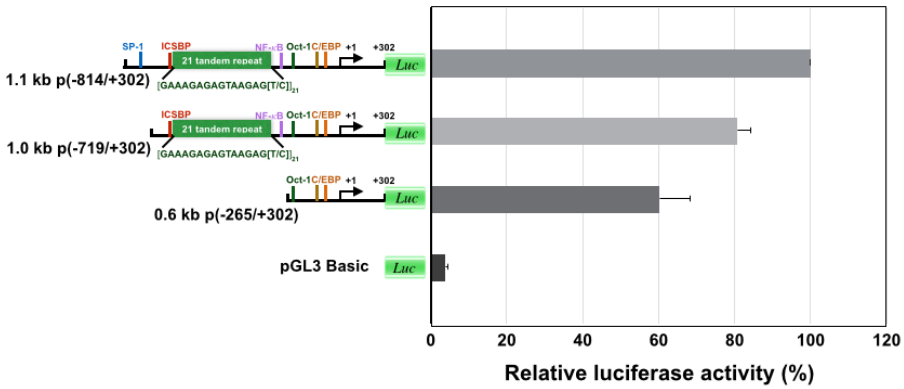

	pGL3	pGL3-promoter ALF*Pm*3		
		p(-265/+302)	p(-719/+302)	p(-814/+302)
Relative luciferase activity (%) (mean±SD)	3.92±0.61	60.29±8.03	80.75±3.72	100±0.00

Figure 3.15 Functional mapping of the deletion ALF*Pm*3 promoter. To study ALF*Pm*3 promoter, various promoter fragments were cloned into pGL3 basic vector and co-transfect with pRL-TK control vector into *Drosophila* S2 cell. Luciferase activity was tested at 48 h post-transfection. (A) For promoter region -1478 to -265, the reporter vector containing ALF*Pm*3 promoter fragments of (-1478/+302), (-814/+302) and (-265/+302) were constructed. (B) For promoter region -814 to -71, the reporter vector containing ALF*Pm*3 promoter fragments of (-814/+302), (-265/+302) and (-71/+302) were constructed. (C) For promoter region -814 to -265, the reporter vector containing ALF*Pm*3 promoter fragments of (-814/+302), (-719/+302) and (-265/+302) were constructed. The relative luciferase activity of each construct has been normalized to that of p(-814/+302) which is arbitrarily set to 100%. The percentage of relative luciferase is presented as horizontal bars with an arbitrary scale, and the error bars represent ± SD from triplicate assays. A schematic illustration showing the predicted TF binding sites of each promoter-luciferase reporter construct is shown on left. The plasmid numbers in parentheses specify the beginning and end position of the promoter fragments. The arrow labeled +1 marks the transcription start site.

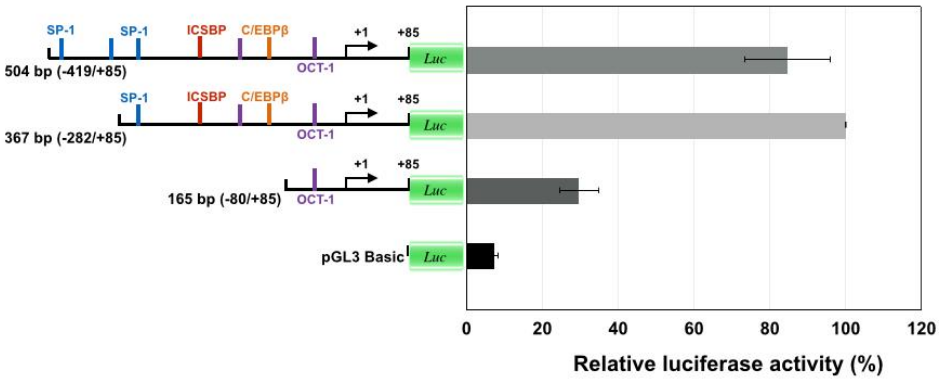

	pGL3	pGL3-promoter ALF*Pm6*		
		p(-80/+85)	p(-282/+85)	p(-419/+85)
Relative luciferase activity (%) (mean±SD)	7.27±1.13	29.69±5.19	100±0.00	84.6±11.46

Figure 3.16 Functional mapping of the deletion ALF*Pm6* promoter sequence from position -418 to -80. The fragments of ALF*Pm6* promoter such as (-419/+85), (-282/+85) and (-80/+85), in pGL3 basic vector (firefly luciferase) were assay for promoter activity in *Drosophila* S2 cell. Luciferase activity was tested at 48 h post-transfection. The relative luciferase activity of each construct has been normalized to that of p(-282/+85) which is arbitrarily set to 100%. The percentage of relative luciferase is presented as horizontal bars with an arbitrary scale, and the error bars represent ± SD from triplicate assays. A schematic illustration showing the predicted TF-binding sites of each promoter-luciferase reporter construct is shown on left. The plasmid numbers in parentheses specify the beginning and end position of the promoter fragments. The arrow label +1 marks the transcription start site.

3.2.4 Determination of the regulatory element involved in ALF*Pm*3 gene regulation

According to promoter activity assay above, the ALF*Pm*3 promoter region between -814 to -266 nucleotide position, including 21 units of GAAAGAGAGTAAGAG[T/C] tandem repeat at the position -693 to -358 and other transcription factor binding sites, NF-κB and ICSBP, might be involved in ALF*Pm*3 gene regulation. This promoter region probably has the activator-binding site suggested by the decrease of the promoter activity after promoter region (-814/-265) deletion. In order to further investigate which element is responsible for ALF*Pm*3 gene regulation, deletion assay for 21 units of GAAAGAGAGTAAGAG[T/C] tandem repeat as well as site-directed mutagenesis at the transcription factor binding site, NF-κB were performed.

To determine the involvement of the 21 units of GAAAGAGAGTAAGAG[T/C] tandem repeat regulating ALF*Pm*3 gene expression, the 21 units of GAAAGAGAGTAAGAG[T/C] tandem repeat deletion construct, del(-693/-358)/p(-1478/+302) was cloned and assay for the promoter activity. Note that, due to the limitation of primer design both ICSBP transcription factor binding site and 21 units of GAAAGAGAGTAAGAG[T/C] tandem repeat were deleted. At 48 h post-transfection, the promoter activity of was assayed using Dual-Luciferase® assay kit. The promoter activity of del(-693/-358)/p(-1478/+302) was not significantly different when compare with the control p(-1478/+302) (Fig. 3.17). The result suggested that the 21 units of GAAAGAGAGTAAGAG[T/C] tandem repeat as well as ICSBP transcription factor binding site were not involved in ALF*Pm*3 gene regulation.

Site-directed mutagenesis technique was performed to determine whether NF-κB transcription factor binding site is involved in regulating ALF*Pm*3 gene. The gene specific primers containing the mutated nucleotides at the conserved position of each transcription binding site were designed (Fig. 3.18). For the -814/-265 ALF*Pm*3 promoter active region, The mutated version of reporter plasmid at the transcription factor binding site of NF-κB (-280/-270) was constructed by rolling PCR using p(-814/+302) as a template and p(-814/+302)muNF-κB_F/p(-814/+302)muNF-κB_R primers. The mutated plasmid ΔNF-κB/p(-814/+302) was confirmed for the correction of nucleotide

sequence then assayed for the promoter activity in comparison with wild type plasmid p(-814/+302). Mutation at the NF-κB binding site caused about 64.4% decrease in promoter activity as compared with the wild type plasmid p(-814/+302) (Fig. 3.19).

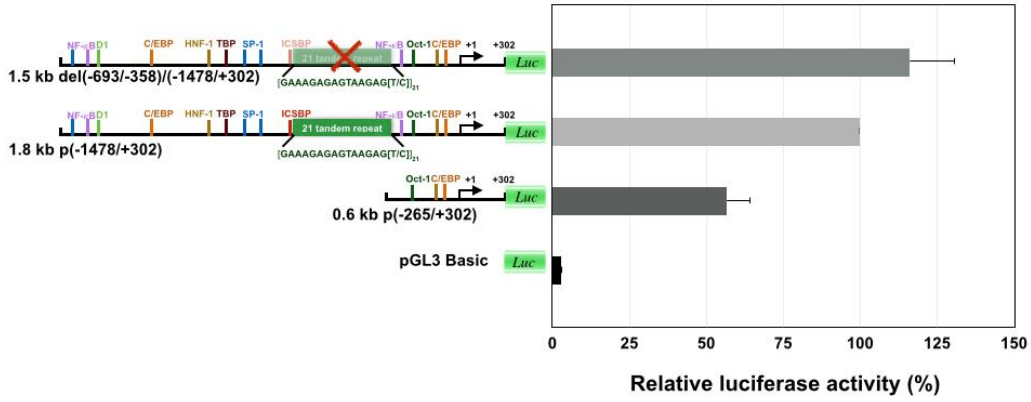

	pGL3	pGL3-promoter ALF*Pm3*		
		p(-265/+302)	p(-1478/+302)	del(-693/-358)/ p(-1478/+302)
Relative luciferase activity (%) (mean±SD)	3.02±0.31	56.69±7.73	100±0.00	116.22±14.74

Figure 3.17 Effect of deleting the 21 units of [GAAAGAGAGTAAGAG(T/C)] tandem repeat on the position -693 to -358 from the ALF*Pm*3 promoter region. The deletion plasmid, del(-693/-358)/p(-1478/+302), was assayed for the promoter activity in *Drosophila* S2 cell in comparison with the parental plasmid p(-1478/+302). The relative luciferase activity of del(-693/-358)/p(-1478/+302) was normalized to that of p(-1478/+302). The percentage of relative luciferase is presented as horizontal bars with an arbitrary scale, and the error bars represent ± SD from triplicate assays. A schematic illustration of the promoter-luciferase reporter constructs is shown on left. The plasmid numbers in parentheses specify the beginning and end position of the promoter fragments. The arrow label +1 marks the transcription start site.

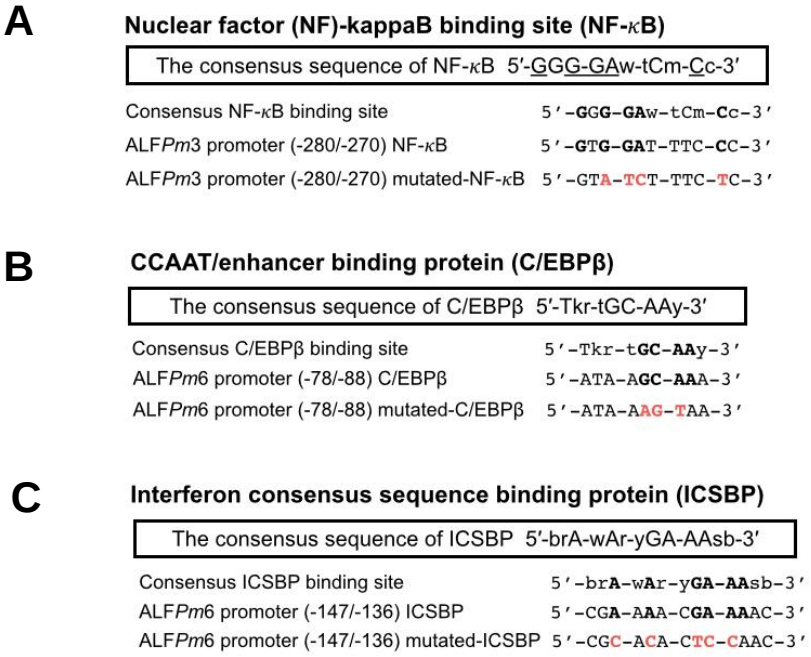

Figure 3.18 The consensus and mutated sequences of transcription factor binding sites on the activator-binding region of ALF*Pm*3 and ALF*Pm*6 promoter. The mutated nucleotide (red letters) of the transcription factor binding sites such as NF-κB (A) for the ALF*Pm*3 promoter as well as C/EBPβ (B) and ICSBP (C) for the ALF*Pm*6 promoter were designed based on consensus and wild-type sequences.

3.2.5 Determination of the regulatory element involved in ALF*Pm6* gene regulation

The promoter activity assay revealed that ALF*Pm6* promoter active region (-282/-81) might contain the activation-binding site. The predicted transcription factor-binding sites identified here were SP1, C/EBPβ and ICSBP.

For the -162/-80 ALF*Pm6* promoter active region, the mutated version of reporter plasmids at the transcription factor binding site of ICSBP (-146/-135) and C/EBPbeta (-88/-80) were constructed by rolling PCR using p(-282/+85) as a template and p(-282/+85)muICSBP_F/p(-282/+85)muICSBP_R and p(-282/+85)muC/EBPbeta_F/ p(-282/+85)muC/EBPbeta_R primers, respectively. The mutated plasmids **Δ**ICSBP/p(-282/+85) and **Δ**C/EBPβ/p(-282/+85) were confirmed for the correction of nucleotide sequence then assayed for the promoter activity in comparison with wild type plasmid p(-282/+85). Mutation at the C/EBPβ binding site caused about 76.1% decrease in promoter activity as compared with the wild type plasmid p(-282/+85) while mutation at the ICSBP binding site resulted in a slightly decrease in promoter activity (%28.5) when compared with the wild type plasmid p(-282/+85) (Fig. 3.20).

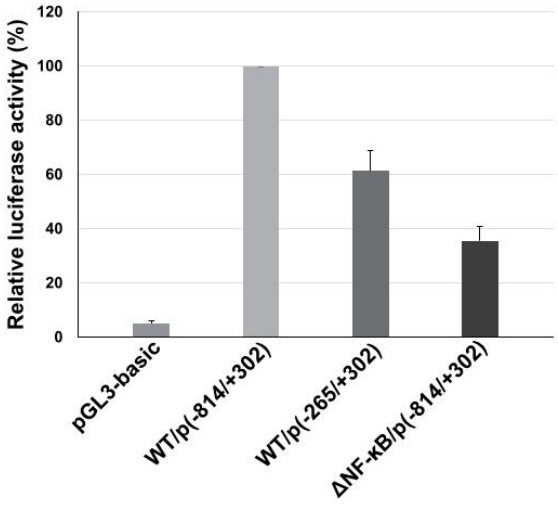

	pGL3	WT/ p(-814/+302)	WT/ p(-265/+302)	ΔNF-κB/ p(-814/+302)
Relative luciferase activity (%) (mean±SD)	4.95±1.19	100±0.00	61.37±7.84	35.57±5.64

Figure 3.19 Site-directed mutagenesis of transcription factor binding site NF-κB on the ALF*Pm*3 promoter active region (-814/-265). The transcription factor binding site of NF-κB (-280/-270) was mutated by rolling PCR using p(-814/+302) as a template. Mutated plasmid ΔNF-κB/p(-814/+302) was assayed for the promoter activity in comparison with wild type plasmid p(-814/+302). The percentage of relative luciferase activity of ALF*Pm*3 p(-814/+302) promoter construct to wild-type or mutated transcription factor binding site, NF-κB, is shown. Data represents the means ± SD from three independent experiments.

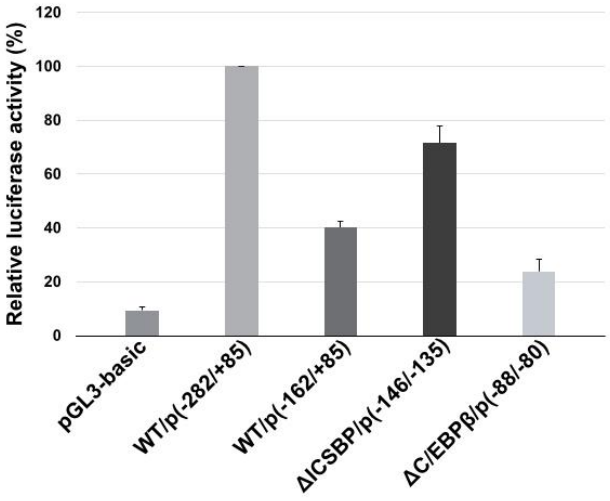

	pGL3	WT/ p(-282/+85)	WT/ p(-162/+85)	ΔICSBP/ p(-282/+85)	ΔC/EBPβ/ p(-282/+85)
Relative luciferase activity (%) (mean±SD)	9.46±1.30	100±0.00	40.11±2.37	71.49±6.42	23.87±4.80

Figure 3.20 Site-directed mutagenesis of transcription factor binding sites on the ALF*Pm6* promoter active region (-282/+85). The transcription factor binding sites such as ICSBP (-146/-135) and C/EBPβ (-88/-80) were mutated by rolling PCR using p(-282/+85) as a template. The mutated plasmid ΔICSBP/p(-282/+85) and ΔC/EBPβ/p(-282/+85) were assayed for the promoter activity in comparison to wild type plasmid p(-282/+85). The percentage of relative luciferase activity of ALF*Pm6* p(-282/+85) promoter construct to wild-type or mutated transcription factor binding sites, ICSBP and C/EBPβ, is shown. Data represents the means ± SD from three independent experiments.

3.3 Effect of knocking-down MyD88 and Relish gene on the transcript level of ALF*Pm*3 and ALF*Pm*6 in the *V. harveyi*-infected *P. monodon*

ALFs are important AMP in shrimp innate immunity. Previous studies suggested that ALF*Pm*3 and ALF*Pm*6 plays important role in the protection of shrimp against microbial infections. Interestingly, the expression profiles of ALF*Pm*3 and ALF*Pm*6 are different, but the mechanisms that regulated the gene expression of ALF*Pm*3 and ALF*Pm*6 were not revealed. Also, pathways that control their transcription are still unclear. In this study, MyD88 and Relish, which are the representative adapter proteins of the Toll and IMD pathways, respectively, were silenced in *V. harveyi*-challenged shrimp in order to determine which signaling pathway plays role in regulating ALF*Pm*3 and ALF*Pm*6 gene expression.

3.3.1 Silencing efficiency of MyD88 dsRNA and Relish dsRNA

To test the efficiency of MyD88 dsRNA or Relish dsRNA in silencing the expression of MyD88 or Relish gene in shrimp, the expression of MyD88 and Relish mRNA, respectively, was determined after injection of 10 μg/g shrimp of the specific dsRNA into shrimp at 0, 24, 48 and 72 h. Semi-quantitative RT-PCR analysis was performed using EF1α as an internal control. Normal saline- and GFP dsRNA-injected shrimp were used as negative controls. The result showed that MyD88 gene expression was suppressed at 0-72 h post-MyD88 dsRNA injection (Fig. 3.21C). While the expression of Relish gene was suppressed at 0-48 h post-Relish dsRNA injection and slightly recovered at 72 h post dsRNA-Relish injection (Fig. 3.21D).

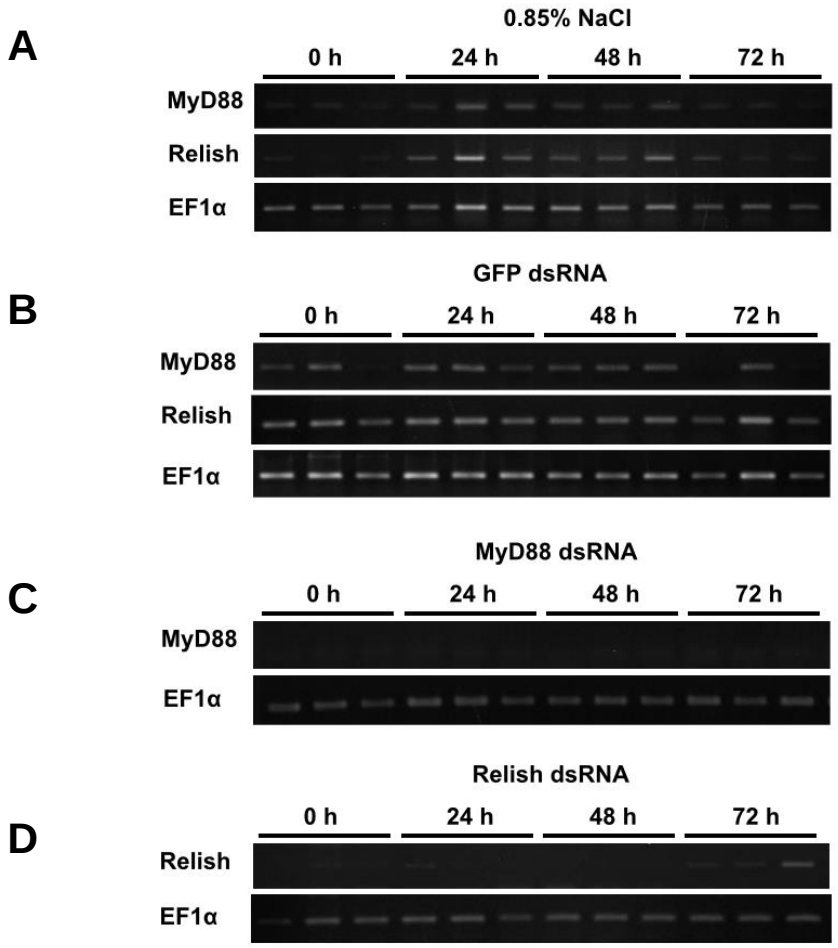

Figure 3.21 Efficiency of MyD88 and Relish gene silencing mediated by dsRNA in shrimp. Control groups were injected with 0.85% NaCl (A) or GFP dsRNA (B). The experimental groups were shrimp injected with 10 μg/g shrimp MyD88 dsRNA (C) and Relish dsRNA (D). At 0, 24, 48 and 72 h post-dsRNA injection, hemolymph was collected from 3 individual shrimp and the transcription level of MyD88 or Relish was analyzed using semi-quantitative RT-PCR. Elongation factor-1α (EF1α) was used as an internal control.

3.3.2 Effect of MyD88 and Relish gene knockdown on the ALF*Pm*3 and ALF*Pm*6 gene expression

To confirm that the MyD88 dsRNA and Relish dsRNA could also suppress the MyD88 and Relish transcripts in *V. harveyi*-infected shrimp, the expression of MyD88 and Relish gene in *V. harveyi*-infected shrimp injected with either MyD88 dsRNA, Relish dsRNA or GFP dsRNA was determined. After the first dsRNA injection for 12 h, shrimp were challenged with 10^{-6} colony forming unit (CFU) *V. harveyi* mixed with 10 µg/g shrimp dsRNA. At 0, 6 and 24 h post *V. harveyi* infection, shrimp hemolymph was collected for total RNA extraction, cDNA synthesis and RT-PCR analysis. The result showed that MyD88 or Relish gene transcipt levels were significantly decreased in the MyD88 and Relish knockdown shrimp whereas GFP dsRNA had no effect on Relish and MyD88 mRNA expression levels (Fig. 3.22).

To investigate the effect of MyD88 and Relish gene knockdown upon *V. harveyi* infection, the level of expression of ALF*Pm*3 and ALF*Pm*6 transcripts in hemocytes of *V. harveyi*-challenged shrimp was determined by quantitative real-time PCR assay.

After challengeing MyD88- and Relish-silenced shrimp with *V. harveyi,* the expression of ALF*Pm*3 was decreased at 6 h post *V. harveyi* infection when normalize to dsGFP knockdown shrimp at 0 hpi in both of MyD88 and Relish dsRNA knockdown shrimp (Fig. 3.23A). It is likely that ALF*Pm*3 was regulated by Toll and IMD pathway. The expression of ALF*Pm*6 gene in MyD88 knockdown shrimp was decreased at 6 h when normalize to dsGFP knockdown shrimp at 0 hpi. Whereas the increase of ALF*Pm*6 gene expression was detected at 6 and 24 hpi in Relish knockdown shrimp (Fig. 3.23B). Therefore, silencing MyD88 might down regulate ALF*Pm*6 transcription and it was Toll rather than IMD pathway that might be more responsible for the transcription of ALF*Pm*6.

In this study, RNAi knockdown of MyD88 and Relish showed the different influence between Toll pathway and IMD pathway on ALF*Pm*3 and ALF*Pm*6 transcription.

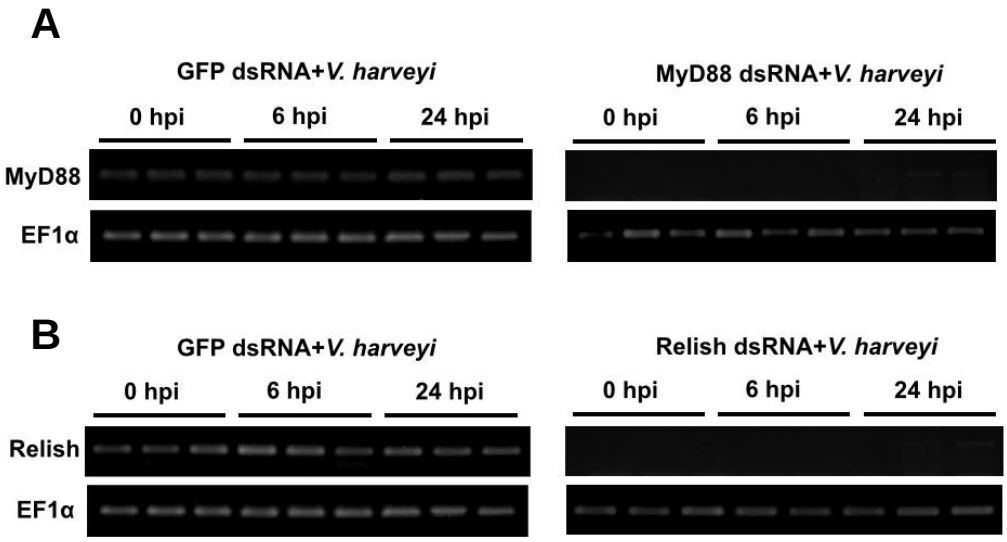

Figure 3.22 The MyD88 and Relish gene silencing in *Vibrio harveyi*-infected shrimps. (A) Transcriptional level of MyD88 gene in the hemolymph at 0, 6 and 24 h post-*V. harveyi* infection was determined. (B) Transcriptional level of Relish gene in hemolymph at 0, 6 and 24 h post-*V. harveyi* infection was determined. The control was shrimp that was injected with GFP dsRNA. EF1α was used as the internal control gene.

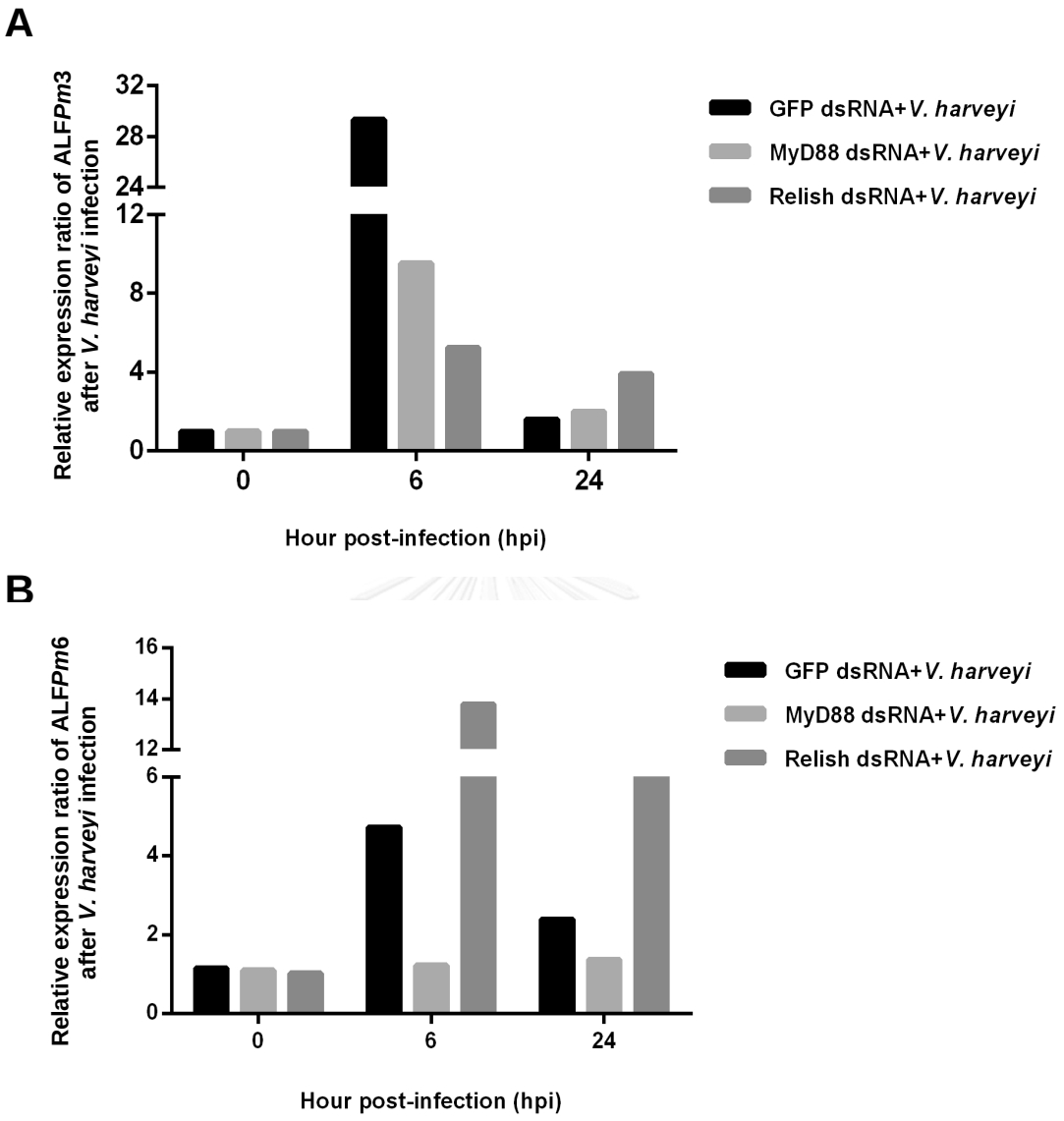

Figure 3.23 Expression of ALF*Pm*3 (A) and ALF*Pm*6 (B) genes in the MyD88 and Relish gene-silenced shrimp upon *V. harveyi* challenge was determined by qRT-PCR. The control was shrimp that was injected with GFP dsRNA. The ALF*Pm*3 and ALF*Pm*6 gene expression levels were normalized to EF1α. The expression of ALF*Pm*3 and ALF*Pm*6 gene of the *V. harveyi*-infected group at 6 and 24 hpi was normalized to that of control group at 0 hpi. The graph shows the mean of relish expression ratio of 2 independent sets of pooled sample from 2 individuals.

CHAPTER IV
DISCUSSIONS

ALF is a group of antimicrobial peptide that has been identified and characterized in shrimp and other crustaceans. Six isoforms of ALF has been discovered in *P. monodon*. ALF*Pm*6 is the most recent and the second most abundant isoform identified from the *P. monodon* EST database (http://pmonodon.biotec.or.th) (Tassanakajon et al. 2006). The previous report indicated that ALF*Pm*6 gene is up-regulated upon YHV infection (Prapavorarat et al. 2010). Moreover, silencing of ALF*Pm*6 gene revealed that ALF*Pm*6 is essential for shrimp survival and plays protection roles in shrimp from *Vibrio harveyi* and WSSV infections (Ponprateep et al. 2012). These suggest a potential role of ALF*Pm*6 in the shrimp immunity. However, there is no report on ALF*Pm*6 characterization. In this study, the rALF*Pm*6 was over-produced using the *P. pastoris* expression system. This system is chosen because *P. pastoris* is an eukaryotic yeast and possess many advantages of higher eukaryotic expression system such as protein processing, protein folding and posttranslational modification. The yeast transformant expressing rALF*Pm*6 was selected based on the level of G418-sulfate resistance indicating multiple copies of the expression cassette. The production yield of rALF*Pm*6 depended on the copy number of expression cassette integrated into yeast genome, which correlated to level of G418-sulphate resistance. The higher concentration of G418-sulphate the recombinant yeast can resist, the higher yield of recombinant protein can be produced. In this study, the transformants that could resist 2 mg/ml G418-sulphate were selected. The selected transformants were induced for rALF*Pm*6 production by methanol induction. The obtained rALF*Pm*6 protein had the expected size of 12 kDa. This crude preparation also exhibited antimicrobial activity against *E. coli* 363 and *B. megaterium.* The crude rALF*Pm*6 protein was further purified using cation exchange chromatography because of the high cationic property of rALF*Pm*6 (pI=9.62). Various conditions for the rALF*Pm*6 protein purification have been tried. Unfortunately, purification of rALF*Pm*6 protein was unsuccessful because only

small amount of rALF*Pm*6 protein could bind to column. The ALFs structure consists of three α-helices packed against a four-stranded ß-sheet. ALFs contain a LPS-binding domain, which is a ß-hairpin structure linked by a conserved disulfide bridge. In horseshoe crab, positively-charged residues within LPS-binding site recognizing the lipid A moiety of LPS located in the ß-hairpin stabilized by the disulfide bridge (Hoess et al. 1993). Hydrophobic residues at position 44 and 46 of the horseshoe crab ALF sequence playing a crucial role in stabilizing the hydrophobic face of the ß-hairpin (Mora et al. 2008). In penaeid shrimp, this stable disulfide loop harbors either a highly conserved cluster of positively charged (Lys and Arg) residues or negatively charged (Glu and Asp) and hydrophobic residues (Hoess et al. 1993, Yang et al. 2009). Based on 3-D structure, the recombinant shrimp ALF*Pm*3 binds to Lipid A and the LPS-binding site involves six positively-charged residues and one negatively-charged amino acid located in the cysteine-stabilized ß-hairpin and in the two neighboring ß-strands, respectively (Yang et al. 2009). Interestingly, the synthetic peptide of ALF LPS-binding domain could interact with LPS *in vitro* (Nagoshi et al. 2006). Also, the synthetic cycled loop peptide designed based on LPS-binding domain of *P. monodon, Scylla paramamosain*, and *Scylla serrata* showed inhibition effects on the growth of Gram-negative bacteria such as *V. harveyi*, *Pseudomonas aeruginosa*, *E. coli* and a Gram-positive bacterium *M. luteus* (Imjongjirak et al. 2007, Pan et al. 2007, Sharma et al. 2011). Antibacterial activities of synthetic peptides corresponding to the LPS-binding domain of ALFs were also reported in SALF from *P. monodon*, which can act against *M. luteus* (Pan et al. 2007) and cSsALF from *S. serrata*, which exhibits activity against *E. coli* (Sharma et al. 2011). In this research, the antimicrobial activity of the synthetic cyclic LPS-binding domain peptide, cALF*Pm*6#29–52, exhibited antimicrobial activity against a Gram-negative bacterium with MBC ranging from 25 to 50 mM for *E. coli* 363 and Gram-positive bacteria including *B. megaterium, M. luteus* and *A. viridan* with MBC ranging from 25 to 50 mM. However, the cALF*Pm*6#29–52 showed less antimicrobial activity than the synthetic peptide of ALF*Pm*3#35–51, which could act against a broder range of the Gram-negative and Gram-positive bacteria (Somboonwiwat et al. 2005). It is noteworthy that the amino acid composition of the LPS-binding domain of ALF*Pm*3 and ALF*Pm*6 differs somewhat. The total numbers of positively charged amino acid

residues (Arg and Lys) of both ALF*Pm*s are different. LPS-binding domain of ALF*Pm*3 had 4 Lys and 2 Arg while ALF*Pm*6 contains 3 Arg and 2 Lys with the net charge of LPS-binding domain of 6 and 5, respectively. In terms of sequences and range of theoretical isoelectric point (p*I*) of the whole protein, ALF*Pm*3 is a highly cationic peptide (pI=9.96) while ALF*Pm*6 has lower cationic property (pI=9.81) (Rosa et al. 2013b). The difference in net charge implied the unequal antibacterial activity of ALF*Pm*3 and ALF*Pm*6.

It is already known that ALF*Pm*3 exhibited the antibacterial activity by binding to bacterial cell wall components and permeabilized bacterial membrane causing loss of membrane intigrity and cell lysis (Jaree et al. 2012). Unlikely, the cALF*Pm*6#29-52 caused bacterial agglutination against *E. coli* 363, *B. megaterium, M. luteus* and *A. viridan.* Previously, rcrustin*Pm*1 and rcrustin*Pm*7, a family of antimicrobial peptide from *P. monodon,* was shown to be able to inhibit the growth of bacteria and also induced bacterial agglutination (Krusong et al. 2012). In mud crab, *Scylla serrata,* hemocyanin could bind to bacterial cells and mediated agglutination through recognition of OmpA and Ompx proteins in bacteria (Yan et al. 2011). rEs-DWD1 from the Chinese mitten crab (*Eriocheir sinensis*) caused significant aggregation of *B. subtilis* and *P. pastoris* (Li, Langenegger and Haner 2013). The synthetic peptide, GL13NH2, derived from the parotid secretory protein, agglutinated both Gram-negative and Gram-positive bacteria, including the oral pathogen *Aggregatibacter actinomycetemcomitans* and the oral commensal *Streptococcus gordonii* but not showed bactericidal activity. To achieve bactericidal activity, three amino acid residue of GL13NH2 peptide were replaced with positive charge amino acids to increase the calculated net charge from +1 to +5. These results in the loss ability of bacterial agglutinate but gained bactericidal activity against against *Pseudomonas aeruginosa*, *S. gordonii* and *E. coli* (Abdolhosseini et al. 2012).

It is well known that ALFs plays important role in protection shrimp against microbial infections. Therefore, the understanding of the gene regulation of ALFs might be useful for improving shrimp immunity. Previously, approximately 600 bp of ALF*Pm*3 5′-upstream sequences from the transcription start site was obtained by genome walking technique. The putative promoter of ALF*Pm*3 was identified at the position -

29 of 5′-upstream sequences. Several transcription factor (TF)-binding sites, including octamer (Oct-1), GATA, CCAAT box and GAAA motifs, were predicted in the 5′-upstream sequences (Tharntada et al. 2009). However, the promoter activity has not been tested. In ALFFc from *F. chinensis*, the immune-related TF-binding sites such as one AP4, one NF-kB, one SP-1, two GAAA, three Oct-1, and three GATA, were identified in the region of -702 to +1. Analysis of ALFFc promoter activity in insect Sf9 cell lines showed that the putative promoter region from +33 to -702 was induced by lipopolysaccharide or (1,3)-ß-D-glucan, but the shorter promoter sequence pALF-318 (from +33 to -318) could be induced only by (1,3)-ß-D-glucan (Ting et al. 2014). However, the important TF that control ALFs transcription are still uncharacterized. In this study, the TF-binding site involved in regulating ALF*Pm*3 and ALF*Pm*6 gene expression was identified by narrow down technique.

Narrow down assay of the 5′-flanking promoter sequence was used to identify the promoter active region. From our analysis, we concluded that ALF*Pm*3 promoter region at the position (-814/-266) contained the activator-binding site. The DNA sequence at position -814 to -266 of ALF*Pm*3 promoter region contained many TF-binding sites such as Sp-1, ICSBP, 21 units of GAAAGAGAGTAAGAG[T/C] tandem repeat and NF-**κ**B. Tandem repeats (TR's) of DNA are prevalent and hypervariable in higher eukaryotic genomes**.** TR's of DNA represent a section of the genomic that may be highly evolvable, as repeat numbers can change with frequencies 100-10000 higher than point mutation (Lynch et al. 2008). The numbers of TR's present in coding regions and promoters, and introns have demonstrated functional roles in modulating protein activity and gene expression and are correlated with disease (Hannan 2010, Vinces et al. 2009, Verstrepen et al. 2005). However, the functional role of intergenic TR's that are found far away from coding regions is unclear. Deletion assay for 21 units of GAAAGAGAGTAAGAG[T/C] tandem repeat as well as ICSBP suggested that this tandem repeat and ICSBP were not involved in ALF*Pm*3 gene regulation. While SP-1 and NF-**κ**B might be activator binding sites on ALF*Pm*3 promoter.

Rel/NF-**κ**B family genes play a central role in the transcription of innate immune effectors (Hoffmann et al. 2002). The NF-**κ**B binding sites were found in

different antimicrobial peptide (AMP) genes, including Penaeidin (O'Leary and Gross 2006), Crustin (Amparyup et al. 2008b) and ALF*Pm*2 (Tharntada et al. 2008). In this study, NF-κB binding sites of ALF*Pm*3 was also found at nucleotide position -280 to -270 from the transcription start sites. The NF-κB family genes, *Relish* and *Dorsal*, could regulate the transcription of *Pen4* (Huang et al. 2009, Huang et al. 2010) and *Pen5* (Li et al. 2009). The transcription of other antimicrobial peptides in shrimp including crustin and ALF was also regulated by Relish (Wang et al. 2012a). In this study, using site-directed mutagenesis, nuclear factor-kappa B of Rel domain (Rel/NF-κB) at position (-280/-270) was identified as the activator-binding site that regulated the ALF*Pm*3 gene regulation.

Like ALF*Pm*3, The promoter active region of ALF*Pm*6 was identified by narrow down assay. After deletion of the promoter region at position (-162/-80), the promoter was decreased. From this result, we concluded that ALF*Pm*6 promoter region on the position (-162/-80) contained the activator-binding site. The predicted transcription factor-binding sites identified here were SP1, C/EBPβ and ICSBP. The transciprtion factor binding sites, C/EBPβ and ICSBP, regulating ALF*Pm*6 gene were confirmed by site-directed mutagenesis. C/EBPβ binding site at position (-88/-80) was identified as the activator-binding site. C/EBPβ is one of family members of transcription factors involved in important physiological processes, such as cellular proliferation and differentiation, regulation of energy homeostasis, inflammation, and hematopoiesis. Previously, LPS-induced C/EBPβ was shown to specifically bind to the C/EBP response element in the SerpinB2 proximal promoter in murine, and loss of C/EBPβ abrogates constitutive SerpinB2 gene transcription and the response to LPS (Ekemini et al., 2013). C/EBPβ has been reported to physically interact with AP-1, and NF-κB to promote gene expression of inflammatory mediators (Tsukada et al. 2011). Previously, C/EBPβ binding site was identified as one member of transcription factor binding motif of crustinPm7 gene (Amparyup et al. 2008b).

Sp1 is a ubiquitous nuclear factor that plays a key role in maintaining basal transcription of house-keeping genes (Samson and Wong 2002). According to previous reports, SP-1 and NF-κB were key transcription factors in the regulation of CD40 gene.

SP-1 was a key transcription factor that control basal expression of CD40. In LPS-stimulated cells, the transcription factor NF-κB up-regulated CD40 expression. On the other hand, SP-1 was phosphorylated and its DNA binding activity was reduced after LPS stimulaton (Tone et al. 2002). Therefore, it could be hypothesized that SP-1 also involved in ALF*Pm*3 and ALF*Pm*6 gene regulation. However, further investigation is need.

In summary, our studies showed that Rel/NF-κB at nucleotide position (-280/-270) and C/EBPβ at nucleotide position (-88/-80) in ALF*Pm*3 and ALF*Pm*6 promoter active region, respectively, are necessary for regulation the gene expression by act as activator.

Toll and IMD pathways are the important NF-κB signaling pathways controlling expression of antimicrobial peptide genes (Leclerc and Reichhart 2004, Tanji and Ip 2005, Lemaitre and Hoffmann 2007). Previously, ALF*Pm*3 showed diffirential expression profile against microbial infections. In this study, the signaling pathway that plays role in regulating the ALF*Pm*3 and ALF*Pm*6 gene expression was identified in *V. harveyi*-infected shrimp by RNAi technique. Knockdown of the adaptor protein, MyD88, and the transcription factor, Relish, which are molecule of Toll and IMD pathway, respectively, was used to investigate which pathway is resposible for controlling each ALF gene expression. The transcription levels of ALF*Pm*3 in MyD88- and Relish-silenced shrimps were down-regulated at 6 h post *V. harveyi* infection. While the transcription level of ALF*Pm*3 in MyD88-silenced shrimps down-regulated at 6 h post- *V. harveyi* infection, but up-regulated in Relish-silenced shrimp. Therefore, ALF*Pm*3 gene expression might be regulated by both Toll and IMD pathways, while ALF*Pm*6 gene expression might be regulated by Toll pathway.

According to the previous report, some antimicrobial peptides can be activated by both Toll and IMD pathways. In *Drosophilla*, Defensin and Metchnikowin were controlled by both IMD and Toll pathways (Hoffmann and Reichhart 2002, Lemaitre et al. 1995). These suggested that Toll and IMD pathways could interact synergistically that might cause the independent activation of overlapping target genes. For instance, some target promoters might contain TF-binding sites for both Dif and Relish.

Therefore, they could be activated independently by both pathways and the response depends on the affinity and number of NF-κB sites (Tanji et al. 2007). The cooperation regulation is sometime mediated through an interaction of the NF-κB-related transcription factors in the two pathways. In *Drosophila*, constitutive activation of Toll and PGRP-LC/IMD could mimic the synergistic stimulation (Tanji et al. 2007). The Rel/NF-κB TF-binding sites on the promoter active region of ALF*Pm*3 might be bound by both Dif/Dorsal and Relish. Therefore, the ALF*Pm*3 gene expression could be regulated by both NF-κB signaling pathways. Toll pathway could regulate both ALF*Pm*3 and ALF*Pm*6 gene expression, thus we predicted that Toll rather than IMD pathway might be more responsible for controlling transcription of ALF genes. It is noteworthy that the up-regulated of ALF*Pm*6 gene expression was detected at 6 and 24 hpi in Relish knockdown shrimp. These suggested that IMD pathway was not involve in the regulation of ALF*Pm*6 gene expression. However, the effect of Relish knockdown in shrimp to the up-regulated of ALF*Pm*6 gene is remain unclear and need further investigation.

CHAPTER V
CONCLUSIONS

1. The recombinant ALF*Pm*6 protein (rALF*Pm*6) with the expected size and pI of 12 kDa and 9.69, respectively, was successfully produced in *Pichia pastoris* KM71. The crude rALF*Pm*6 protein showed antibacterial activities against both Gram-positive and Gram-negative bacteria, such as *Bacillus megaterium* and *Escherichia coli* 363, respectively. However, purification of rALF*Pm*6 could not be accomplished.

2. The synthetic cyclic ALF*Pm*6#29-52 peptide corresponding to ALF*Pm*6 LPS-binding site showed antibacterial activity against some tested bacteria including *E. coli* 363, *B. megaterium*, *A. viridans,* and *M. luteus* with MBC value of 25-50 μM. Bacterial agglutination was found to be involved in ALF*Pm*6 antibacterial activity.

3. The promoter regions of ALF*Pm*3 and ALF*Pm*6 were successfully acquired by genome walking technique whose size of about 1780 bp and 504 bp, respectively.

4. The promoter active region of ALF*Pm*3 gene was mapped to a region from nucleotide -814 to +302. The activator-binding site from -814 to -274 was also found and it contained the predicted transcriptional factor binding sites of Rel/NF-**κ**B, SP-1, ICSBP and 21 units of GAAAGAGAGTAAGAG[T/C] tandem repeat.

5. The promoter active region of ALF*Pm*6 gene was mapped to a region from nucleotide -282 to +85. The activator-binding site from -282 to -80 was also found and containing transcriptional factor binding sites of OCT-1, SP-1, ICSBP, and C/EBPβ.

6. Site directed mutagenesis revealed that the Rel/NF-**κ**B binding site (-280/-270) in the ALF*Pm*3 promoter and the C/EBPβ binding site (-78/-88) in the ALF*Pm*6 promoter are the activator-binding site.

7. RNAi knockdown of MyD88 and Relish in *V. harveyi*-infected *P. monodon* suggested that ALF*Pm*3 gene expression might be regulated by both Toll and IMD pathways, while ALF*Pm*6 gene expression might be regulated by Toll pathway.

REFERENCES

Abdolhosseini, M., S. R. Nandula, J. Song, H. Hirt & S.-U. Gorr (2012) Lysine substitutions convert a bacterial-agglutinating peptide into a bactericidal peptide that retains anti-lipopolysaccharide activity and low hemolytic activity. *Peptides,* 35**,** 231-238.

Ahantarig, A., N. Chantawat, N. R. Waterfield & P. Kittayapong (2009) PirAB toxin from *Photorhabdus asymbiotica* as a larvicide against dengue vectors. *Applied and environmental microbiology,* 75**,** 4627-4629.

Akira, S., S. Uematsu & O. Takeuchi (2006) Pathogen recognition and innate immunity. *Cell,* 124**,** 783-801.

Amparyup, P., S. Donpudsa & A. Tassanakajon (2008a) Shrimp single WAP domain (SWD)-containing protein exhibits proteinase inhibitory and antimicrobial activities. *Dev Comp Immunol,* 32**,** 1497-509.

Amparyup, P., H. Kondo, I. Hirono, T. Aoki & A. Tassanakajon (2008b) Molecular cloning, genomic organization and recombinant expression of a crustin-like antimicrobial peptide from black tiger shrimp *Penaeus monodon*. *Mol Immunol,* 45**,** 1085-93.

Arts, J. A., F. H. Cornelissen, T. Cijsouw, T. Hermsen, H. F. Savelkoul & R. J. Stet (2007) Molecular cloning and expression of a Toll receptor in the giant tiger shrimp, *Penaeus monodon*. *Fish Shellfish Immunol,* 23**,** 504-13.

Bartlett, T. C., B. J. Cuthbertson, E. F. Shepard, R. W. Chapman, P. S. Gross & G. W. Warr (2002) Crustins, homologues of an 11.5-kDa antibacterial peptide, from two species of penaeid shrimp, *Litopenaeus vannamei* and *Litopenaeus setiferus*. *Mar Biotechnol (NY),* 4**,** 278-93.

Belvin, M. P. & K. V. Anderson (1996) A conserved signaling pathway: the *Drosophila* toll-dorsal pathway. *Annu Rev Cell Dev Biol,* 12**,** 393-416.

Blackburn, M. B., R. R. Farrar, N. G. Novak & S. D. Lawrence (2006) Remarkable susceptibility of the diamondback moth (*Plutella xylostella*) to ingestion of *Pir*

toxins from *Photorhabdus luminescens*. *Entomologia experimentalis et applicata,* 121**,** 31-37.

Brogden, K. A. (2005) Antimicrobial peptides: pore formers or metabolic inhibitors in bacteria? *Nat Rev Microbiol,* 3**,** 238-50.

Brown, K. L. & R. E. Hancock (2006) Cationic host defense (antimicrobial) peptides. *Current opinion in immunology,* 18**,** 24-30.

Choe, K. M., T. Werner, S. Stoven, D. Hultmark & K. V. Anderson (2002) Requirement for a peptidoglycan recognition protein (PGRP) in Relish activation and antibacterial immune responses in *Drosophila*. *Science,* 296**,** 359-62.

Cruciani, R. A., J. L. Barker, M. Zasloff, H. C. Chen & O. Colamonici (1991) Antibiotic magainins exert cytolytic activity against transformed cell lines through channel formation. *Proc Natl Acad Sci U S A,* 88**,** 3792-6.

Destoumieux, D., P. Bulet, D. Loew, A. Van Dorsselaer, J. Rodriguez & E. Bachere (1997) Penaeidins, a new family of antimicrobial peptides isolated from the shrimp *Penaeus vannamei* (Decapoda). *J Biol Chem,* 272**,** 28398-406.

Dupuy, J. W., J. R. Bonami & P. Roch (2004) A synthetic antibacterial peptide from *Mytilus galloprovincialis* reduces mortality due to white spot syndrome virus in palaemonid shrimp. *J Fish Dis,* 27**,** 57-64.

Flegel, T. W. (2007) Update on viral accommodation, a model for host-viral interaction in shrimp and other arthropods. *Dev Comp Immunol,* 31**,** 217-31.

Georgel, P., S. Naitza, C. Kappler, D. Ferrandon, D. Zachary, C. Swimmer, C. Kopczynski, G. Duyk, J. M. Reichhart & J. A. Hoffmann (2001) *Drosophila* immune deficiency (IMD) is a death domain protein that activates antibacterial defense and can promote apoptosis. *Dev Cell,* 1**,** 503-14.

Gottar, M., V. Gobert, T. Michel, M. Belvin, G. Duyk, J. A. Hoffmann, D. Ferrandon & J. Royet (2002) The *Drosophila* immune response against Gram-negative bacteria is mediated by a peptidoglycan recognition protein. *Nature,* 416**,** 640-644.

Hancock, R. E. & G. Diamond (2000) The role of cationic antimicrobial peptides in innate host defences. *Trends Microbiol,* 8**,** 402-10.

Hannan, A. J. (2010) Tandem repeat polymorphisms: modulators of disease susceptibility and candidates for 'missing heritability'. *Trends in Genetics,* 26**,** 59-65.

Hedengren, M., B. Asling, M. S. Dushay, I. Ando, S. Ekengren, M. Wihlborg & D. Hultmark (1999) Relish, a central factor in the control of humoral but not cellular immunity in *Drosophila*. *Mol Cell,* 4**,** 827-37.

Hikima, S., J. Hikima, J. Rojtinnakorn, I. Hirono & T. Aoki (2003) Characterization and function of kuruma shrimp lysozyme possessing lytic activity against *Vibrio* species. *Gene,* 316**,** 187-95.

Hoess, A., S. Watson, G. R. Siber & R. Liddington (1993) Crystal structure of an endotoxin-neutralizing protein from the horseshoe crab, Limulus anti-LPS factor, at 1.5 A resolution. *EMBO J,* 12**,** 3351-6.

Hoffmann, A., A. Levchenko, M. L. Scott & D. Baltimore (2002) The IkappaB-NF-kappaB signaling module: temporal control and selective gene activation. *Science,* 298**,** 1241-5.

Hoffmann, J. A. & J.-M. Reichhart (2002) *Drosophila* innate immunity: an evolutionary perspective. *Nature immunology,* 3**,** 121-126.

Hou, F., S. He, Y. Liu, X. Zhu, C. Sun & X. Liu (2014) RNAi knock-down of shrimp *Litopenaeus vannamei* Toll gene and immune deficiency gene reveals their difference in regulating antimicrobial peptides transcription. *Dev Comp Immunol,* 44**,** 255-60.

Huang, X.-D., Z.-X. Yin, X.-t. Jia, J.-p. Liang, H.-S. Ai, L.-S. Yang, X. Liu, P.-H. Wang, S.-d. Li & S.-P. Weng (2010) Identification and functional study of a shrimp Dorsal homologue. *Developmental & Comparative Immunology,* 34**,** 107-113.

Huang, X.-D., Z.-X. Yin, J.-X. Liao, P.-H. Wang, L.-S. Yang, H.-S. Ai, Z.-H. Gu, X.-T. Jia, S.-P. Weng & X.-Q. Yu (2009) Identification and functional study of a shrimp Relish homologue. *Fish & shellfish immunology,* 27**,** 230-238.

Imjongjirak, C., P. Amparyup, A. Tassanakajon & S. Sittipraneed (2007) Antilipopolysaccharide factor (ALF) of mud crab *Scylla paramamosain*: molecular cloning, genomic organization and the antimicrobial activity of its synthetic LPS binding domain. *Mol Immunol,* 44**,** 3195-203.

Inouye, K., S. Miwa, N. Oseko, H. Nakano, T. Kimura, K. Momoyama & M. Hiraoka (1994) Mass mortalities of cultured kuruma shrimp *Penaeus japonicus* in Japan in 1993: electron microscopic evidence of the causative virus. *Gyobyo Kenkyu= Fish Pathology,* 29**,** 149-158.

Jaree, P., A. Tassanakajon & K. Somboonwiwat (2012) Effect of the anti-lipopolysaccharide factor isoform 3 (ALF*Pm*3) from *Penaeus monodon* on *Vibrio harveyi* cells. *Dev Comp Immunol,* 38**,** 554-60.

Jenssen, H., P. Hamill & R. E. Hancock (2006) Peptide antimicrobial agents. *Clin Microbiol Rev,* 19**,** 491-511.

Jiravanichpaisal, P., B. L. Lee & K. Soderhall (2006) Cell-mediated immunity in arthropods: hematopoiesis, coagulation, melanization and opsonization. *Immunobiology,* 211**,** 213-36.

Khimmakthong, U., P. Kongmee, P. Deachamag, U. Leggat & W. Chotigeat (2013) Activation of an immune response in *Litopenaeus vannamei* by oral immunization with phagocytosis activating protein (PAP) DNA. *Fish Shellfish Immunol,* 34**,** 929-38.

Krepstakies, M., J. Lucifora, C. H. Nagel, M. B. Zeisel, B. Holstermann, H. Hohenberg, I. Kowalski, T. Gutsmann, T. F. Baumert, K. Brandenburg, J. Hauber & U. Protzer (2012) A new class of synthetic peptide inhibitors blocks attachment and entry of human pathogenic viruses. *J Infect Dis,* 205**,** 1654-64.

Krusong, K., P. Poolpipat, P. Supungul & A. Tassanakajon (2012) A comparative study of antimicrobial properties of crustin*Pm*1 and crustin*Pm*7 from the black tiger shrimp *Penaeus monodon*. *Dev Comp Immunol,* 36**,** 208-15.

Lan, J. F., J. Zhou, X. W. Zhang, Z. H. Wang, X. F. Zhao, Q. Ren & J. X. Wang (2013) Characterization of an immune deficiency homolog (IMD) in shrimp (*Fenneropenaeus chinensis*) and crayfish (*Procambarus clarkii*). *Dev Comp Immunol,* 41**,** 608-17.

Leaño, E. M. & C. Mohan (2012) Early mortality syndrome threatens Asia's shrimp farms. *Global Aquaculture Advocate***,** 38-39.

Leclerc, V. & J. M. Reichhart (2004) The immune response of *Drosophila melanogaster*. *Immunol Rev,* 198**,** 59-71.

Lemaitre, B. & J. Hoffmann (2007) The host defense of *Drosophila melanogaster*. *Annu Rev Immunol,* 25**,** 697-743.

Lemaitre, B., E. Kromer-Metzger, L. Michaut, E. Nicolas, M. Meister, P. Georgel, J. M. Reichhart & J. A. Hoffmann (1995) A recessive mutation, immune deficiency (IMD), defines two distinct control pathways in the *Drosophila* host defense. *Proc Natl Acad Sci U S A,* 92**,** 9465-9.

Lemaitre, B., E. Nicolas, L. Michaut, J. M. Reichhart & J. A. Hoffmann (1996) The dorsoventral regulatory gene cassette spatzle/Toll/cactus controls the potent antifungal response in *Drosophila* adults. *Cell,* 86**,** 973-83.

Lemaitre, B., J. M. Reichhart & J. A. Hoffmann (1997) *Drosophila* host defense: differential induction of antimicrobial peptide genes after infection by various classes of microorganisms. *Proc Natl Acad Sci U S A,* 94**,** 14614-9.

Li, F. & J. Xiang (2013a) Signaling pathways regulating innate immune responses in shrimp. *Fish Shellfish Immunol,* 34**,** 973-80.

Li, F., H. Yan, D. Wang, T. A. Priya, S. Li, B. Wang, J. Zhang & J. Xiang (2009) Identification of a novel relish homolog in Chinese shrimp *Fenneropenaeus chinensis* and its function in regulating the transcription of antimicrobial peptides. *Dev Comp Immunol,* 33**,** 1093-101.

Li, S., S. M. Langenegger & R. Haner (2013) Control of aggregation-induced emission by DNA hybridization. *Chem Commun (Camb),* 49**,** 5835-7.

Li, X. C., L. Zhu, L. G. Li, Q. Ren, Y. Q. Huang, J. X. Lu, W. H. Fang & W. Kang (2013) A novel myeloid differentiation factor 88 homolog, SpMyD88, exhibiting SpToll-binding activity in the mud crab *Scylla paramamosain*. *Dev Comp Immunol,* 39**,** 313-22.

Lightner, D. V., R. M. Redman, C. R. Pantoja, K. F. Tang, B. L. Noble, P. Schofield, L. L. Mohney, L. M. Nunan & S. A. Navarro (2012) Historic emergence, impact and current status of shrimp pathogens in the Americas. *J Invertebr Pathol,* 110**,** 174-83.

Lo, C., J.-H. Leu, C. Ho, C. Chen, S. Peng, Y. Chen, C. Chou, P. Yeh, C. Huang & H. Chou (1996) Detection of baculovirus associated with white spot syndrome (WSBV) in

penaeid shrimps using polymerase chain reaction. *Diseases of aquatic organisms,* 25**,** 133-141.

Lynch, M., W. Sung, K. Morris, N. Coffey, C. R. Landry, E. B. Dopman, W. J. Dickinson, K. Okamoto, S. Kulkarni & D. L. Hartl (2008) A genome-wide view of the spectrum of spontaneous mutations in yeast. *Proceedings of the National Academy of Sciences,* 105**,** 9272-9277.

Maeda, M., T. Itami, E. Mizuki, R. Tanaka, Y. Yoshizu, K. Doi, C. Yasunaga-Aoki, Y. Takahashi & T. Kawarabata (2000) Red swamp crawfish (*Procambarus clarkii*): an alternative experimental host in the study of white spot syndrome virus. *Acta Virol,* 44**,** 371-4.

Mekata, T., T. Kono, T. Yoshida, M. Sakai & T. Itami (2008) Identification of cDNA encoding Toll receptor, MjToll gene from kuruma shrimp, *Marsupenaeus japonicus*. *Fish Shellfish Immunol,* 24**,** 122-33.

Mooney, A. (2012) An emerging shrimp disease in Vietnam, microsporidiosis or liver disease? . *Available at: http://aquatichealth.net/issue/38607*.

Mora, P., D. La Paz, M. López & E. Pérez‐Payá (2008) Bioactive peptides derived from the Limulus anti‐lipopolysaccharide factor: structure‐activity relationships and formation of mixed peptide/lipid complexes. *Journal of Peptide Science,* 14**,** 963-971.

Muta, T., T. Miyata, F. Tokunaga, T. Nakamura & S. Iwanaga (1987) Primary structure of anti-lipopolysaccharide factor from American horseshoe crab, *Limulus polyphemus*. *J Biochem,* 101**,** 1321-30.

Nagoshi, H., H. Inagawa, K. Morii, H. Harada, C. Kohchi, T. Nishizawa, Y. Taniguchi, M. Uenobe, T. Honda, M. Kondoh, Y. Takahashi & G. Soma (2006) Cloning and characterization of a LPS-regulatory gene having an LPS binding domain in kuruma prawn *Marsupenaeus japonicus*. *Mol Immunol,* 43**,** 2061-9.

O'Leary, N. A. & P. S. Gross (2006) Genomic structure and transcriptional regulation of the penaeidin gene family from *Litopenaeus vannamei*. *Gene,* 371**,** 75-83.

Ongvarrasopone, C., M. Chanasakulniyom, K. Sritunyalucksana & S. Panyim (2008) Suppression of *Pm*Rab7 by dsRNA inhibits WSSV or YHV infection in shrimp. *Mar Biotechnol (NY),* 10**,** 374-81.

Pan, C. Y., T. T. Chao, J. C. Chen, J. Y. Chen, W. C. Liu, C. H. Lin & C. M. Kuo (2007) Shrimp (*Penaeus monodon*) anti-lipopolysaccharide factor reduces the lethality of *Pseudomonas aeruginosa* sepsis in mice. *Int Immunopharmacol,* 7**,** 687-700.

Ponprateep, S., S. Tharntada, K. Somboonwiwat & A. Tassanakajon (2012) Gene silencing reveals a crucial role for anti-lipopolysaccharide factors from *Penaeus monodon* in the protection against microbial infections. *Fish Shellfish Immunol,* 32**,** 26-34.

Prapavorarat, A., S. Pongsomboon & A. Tassanakajon (2010) Identification of genes expressed in response to yellow head virus infection in the black tiger shrimp, *Penaeus monodon*, by suppression subtractive hybridization. *Dev Comp Immunol,* 34**,** 611-7.

Rosa, R. D., A. Vergnes, J. De Lorgeril, P. Goncalves, L. M. Perazzolo, L. Sauné, B. Romestand, J. Fievet, Y. Gueguen & E. Bachère (2013a) Functional divergence in shrimp anti-lipopolysaccharide factors (ALFs): from recognition of cell wall components to antimicrobial activity. *PloS one,* 8.

Rosa, R. D., A. Vergnes, J. de Lorgeril, P. Goncalves, L. M. Perazzolo, L. Saune, B. Romestand, J. Fievet, Y. Gueguen, E. Bachere & D. Destoumieux-Garzon (2013b) Functional divergence in shrimp anti-lipopolysaccharide factors (ALFs): from recognition of cell wall components to antimicrobial activity. *PLoS One,* 8**,** e67937.

Rout, N., S. Kumar, S. Jaganmohan & V. Murugan (2007) DNA vaccines encoding viral envelope proteins confer protective immunity against WSSV in black tiger shrimp. *Vaccine,* 25**,** 2778-86.

Rutschmann, S., A. C. Jung, R. Zhou, N. Silverman, J. A. Hoffmann & D. Ferrandon (2000) Role of *Drosophila* IKK gamma in a Toll-independent antibacterial immune response. *Nat Immunol,* 1**,** 342-7.

Sambrook, J., and W. Russell David. 1989. *Molecular cloning: a laboratory manual. Vol. 3.* . Molecular cloning: a laboratory manual. Vol. 3. .

Samson, S. & N. Wong (2002) Role of Sp1 in insulin regulation of gene expression. *Journal of molecular endocrinology,* 29**,** 265-279.

Satoh, J., T. Nishizawa & M. Yoshimizu (2008) Protection against white spot syndrome virus (WSSV) infection in kuruma shrimp orally vaccinated with WSSV rVP26 and rVP28. *Dis Aquat Organ,* 82**,** 89-96.

Saulnier, D., J. C. Avarre, G. Le Moullac, D. Ansquer, P. Levy & V. Vonau (2000) Rapid and sensitive PCR detection of *Vibrio penaeicida*, the putative etiological agent of syndrome 93 in New Caledonia. *Dis Aquat Organ,* 40**,** 109-15.

Sharma, S., R. D. Yedery, M. S. Patgaonkar, C. Selvaakumar & K. V. Reddy (2011) Antibacterial activity of a synthetic peptide that mimics the LPS binding domain of Indian mud crab, *Scylla serrata* anti-lipopolysaccharide factor (*Ss*ALF) also involved in the modulation of vaginal immune functions through NF-kB signaling. *Microb Pathog,* 50**,** 179-91.

Shi, X. Z., R. R. Zhang, Y. P. Jia, X. F. Zhao, X. Q. Yu & J. X. Wang (2009) Identification and molecular characterization of a Spatzle-like protein from Chinese shrimp (*Fenneropenaeus chinensis*). *Fish Shellfish Immunol,* 27**,** 610-7.

Söderhäll, K. (1999) Invertebrate immunity. *Dev Comp Immunol,* 23**,** 263-6.

Somboonwiwat, K., M. Marcos, A. Tassanakajon, S. Klinbunga, A. Aumelas, B. Romestand, Y. Gueguen, H. Boze, G. Moulin & E. Bachere (2005) Recombinant expression and anti-microbial activity of anti-lipopolysaccharide factor (ALF) from the black tiger shrimp *Penaeus monodon*. *Dev Comp Immunol,* 29**,** 841-51.

Sotelo-Mundo, R. R., M. A. Islas-Osuna, E. de-la-Re-Vega, J. Hernandez-Lopez, F. Vargas-Albores & G. Yepiz-Plascencia (2003) cDNA cloning of the lysozyme of the white shrimp *Penaeus vannamei*. *Fish Shellfish Immunol,* 15**,** 325-31.

Stein, D. S. & L. M. Stevens (1991) Establishment of dorsal-ventral and terminal pattern in the *Drosophila* embryo. *Curr Opin Genet Dev,* 1**,** 247-54.

Supungul, P., S. Klinbunga, R. Pichyangkura, I. Hirono, T. Aoki & A. Tassanakajon (2004) Antimicrobial peptides discovered in the black tiger shrimp *Penaeus monodon* using the EST approach. *Dis Aquat Organ,* 61**,** 123-35.

Suraprasit, S., T. Methatham, P. Jaree, K. Phiwsaiya, S. Senapin, I. Hirono, C. F. Lo, A. Tassanakajon & K. Somboonwiwat (2014) Anti-lipopolysaccharide factor isoform 3 from *Penaeus monodon* (ALF*Pm*3) exhibits antiviral activity by interacting with WSSV structural proteins. *Antiviral Res,* 110**,** 142-50.

Tanaka, S., T. Nakamura, T. Morita & S. Iwanaga (1982) Limulus anti-LPS factor: An anticoagulant which inhibits the endotoxin-mediated activation of Limulus coagulation system. *Biochemical and biophysical research communications,* 105**,** 717-723.

Tanji, T., X. Hu, A. N. Weber & Y. T. Ip (2007) Toll and IMD pathways synergistically activate an innate immune response in *Drosophila melanogaster*. *Mol Cell Biol,* 27**,** 4578-88.

Tanji, T. & Y. T. Ip (2005) Regulators of the Toll and IMD pathways in the *Drosophila* innate immune response. *Trends Immunol,* 26**,** 193-8.

Tassanakajon, A., P. Amparyup, K. Somboonwiwat & P. Supungul (2010) Cationic antimicrobial peptides in penaeid shrimp. *Mar Biotechnol (NY),* 12**,** 487-505.

Tassanakajon, A., S. Klinbunga, N. Paunglarp, V. Rimphanitchayakit, A. Udomkit, S. Jitrapakdee, K. Sritunyalucksana, A. Phongdara, S. Pongsomboon, P. Supungul, S. Tang, K. Kuphanumart, R. Pichyangkura & C. Lursinsap (2006) *Penaeus monodon* gene discovery project: the generation of an EST collection and establishment of a database. *Gene,* 384**,** 104-12.

Tassanakajon, A., K. Somboonwiwat & P. Amparyup (2014) Sequence diversity and evolution of antimicrobial peptides in invertebrates. *Developmental & Comparative Immunology*.

Tassanakajon, A., K. Somboonwiwat, P. Supungul & S. Tang (2013) Discovery of immune molecules and their crucial functions in shrimp immunity. *Fish & shellfish immunology,* 34**,** 954-967.

Tharntada, S., S. Ponprateep, K. Somboonwiwat, H. Liu, I. Soderhall, K. Soderhall & A. Tassanakajon (2009) Role of anti-lipopolysaccharide factor from the black tiger

shrimp, *Penaeus monodon*, in protection from white spot syndrome virus infection. *J Gen Virol,* 90**,** 1491-8.

Tharntada, S., K. Somboonwiwat, V. Rimphanitchayakit & A. Tassanakajon (2008) Anti-lipopolysaccharide factors from the black tiger shrimp, *Penaeus monodon*, are encoded by two genomic loci. *Fish & shellfish immunology,* 24**,** 46-54.

Tone, M., Y. Tone, J. M. Babik, C.-Y. Lin & H. Waldmann (2002) The role of Sp1 and NF-**K**B in regulating CD40 gene expression. *Journal of Biological Chemistry,* 277**,** 8890-8897.

Tran, L., L. Nunan, R. M. Redman, L. L. Mohney, C. R. Pantoja, K. Fitzsimmons & D. V. Lightner (2013) Determination of the infectious nature of the agent of acute hepatopancreatic necrosis syndrome affecting penaeid shrimp. *Dis Aquat Organ,* 105**,** 45-55.

Tsukada, J., Y. Yoshida, Y. Kominato & P. E. Auron (2011) The CCAAT/enhancer (C/EBP) family of basic-leucine zipper (bZIP) transcription factors is a multifaceted highly-regulated system for gene regulation. *Cytokine,* 54**,** 6-19.

Verstrepen, K. J., A. Jansen, F. Lewitter & G. R. Fink (2005) Intragenic tandem repeats generate functional variability. *Nature genetics,* 37**,** 986-990.

Vinces, M. D., M. Legendre, M. Caldara, M. Hagihara & K. J. Verstrepen (2009) Unstable tandem repeats in promoters confer transcriptional evolvability. *Science,* 324**,** 1213-1216.

Wang, D., F. Li, S. Li, R. Wen & J. Xiang (2012) Expression profiles of antimicrobial peptides (AMPs) and their regulation by Relish. *Chinese Journal of Oceanology and Limnology,* 30**,** 611-619.

Wang, P. H., Z. H. Gu, X. D. Huang, B. D. Liu, X. X. Deng, H. S. Ai, J. Wang, Z. X. Yin, S. P. Weng, X. Q. Yu & J. G. He (2009) An immune deficiency homolog from the white shrimp, *Litopenaeus vannamei*, activates antimicrobial peptide genes. *Mol Immunol,* 46**,** 1897-904.

Wang, P. H., J. P. Liang, Z. H. Gu, D. H. Wan, S. P. Weng, X. Q. Yu & J. G. He (2012b) Molecular cloning, characterization and expression analysis of two novel Tolls (LvToll2 and LvToll3) and three putative Spatzle-like Toll ligands (LvSpz1-3) from *Litopenaeus vannamei*. *Dev Comp Immunol,* 36**,** 359-71.

Wonteerasupaya, C., J. E. Vickers, S. Sriurairatana, G. L. Nash, A. Akarajamorn, V. Boonsaeng, S. Panyim, A. Tassanakajon, B. Withyachumnarnkul & T. Flegel (1995) A non-occluded, systemic baculovirus that occurs in cells of ectodermal and mesodermal origin and causes high mortality in the black tiger prawn *Penaeus monodon*. *Diseases of aquatic organisms,* 21**,** 69-77.

Xi, Z., J. L. Ramirez & G. Dimopoulos (2008) The Aedes aegypti toll pathway controls dengue virus infection. *PLoS Pathog,* 4**,** e1000098.

Yan, F., Y. Zhang, R. Jiang, M. Zhong, Z. Hu, H. Du, J. Lun, J. Chen & Y. Li (2011) Identification and agglutination properties of hemocyanin from the mud crab (*Scylla serrata*). *Fish Shellfish Immunol,* 30**,** 354-60.

Yang, C., J. Zhang, F. Li, H. Ma, Q. Zhang, T. A. Jose Priya, X. Zhang & J. Xiang (2008) A Toll receptor from Chinese shrimp *Fenneropenaeus chinensis* is responsive to *Vibrio anguillarum* infection. *Fish Shellfish Immunol,* 24**,** 564-74.

Yang, L. S., Z. X. Yin, J. X. Liao, X. D. Huang, C. J. Guo, S. P. Weng, S. M. Chan, X. Q. Yu & J. G. He (2007) A Toll receptor in shrimp. *Mol Immunol,* 44**,** 1999-2008.

Yang, Y., H. Boze, P. Chemardin, A. Padilla, G. Moulin, A. Tassanakajon, M. Pugnière, F. Roquet, D. Destoumieux-Garzón & Y. Gueguen (2009) NMR structure of rALF-*Pm*3, an anti-lipopolysaccharide factor from shrimp: Model of the possible lipid A-binding site. *Biopolymers,* 91**,** 207-220.

APPENDIX

VITA

Miss Pitchayanan Kamsaeng was born in August 25, 1989 in Rayong. She graduated with the degree of Bachelor of Science from the Department of Biochemistry, Faculty of Science, Chulalongkorn University in 2011. She has studied for the degree of Master of Science, Program in Biochemistry and Molecular Biology, Department of Biochemistry, Faculty of Science, Chulalongkorn University since 2011.

1. Kamsaeng, P., Somboonwiwat, K., Tassanakajon, A., Antibacterial activity of antilipopolysaccharide factor from black tiger shrimp, Penaeus monodon. The 22nd Science Forum. 20-21 March 2014, Chulalongkorn University, Bangkok, Thailand. (Oral presentation)

2. Kamsaeng, P., Somboonwiwat, K., Tassanakajon, A., Antibacterial activity and gene regulation of antilipopolysaccharide factor from black tiger shrimp, Penaeus monodon. The 4th International Biochemistry and Molecular Biology Conference 2014 “Bridging ASEAN Biochemistry Reserch Communities”. 2-3 April 2014, Kasetsart University, Bangkok, Thailand. (Poster presentation)

3. Kamsaeng, P., Somboonwiwat, K., Tassanakajon, A., Antibacterial activity and gene regulation of antilipopolysaccharide factor from black tiger shrimp, Penaeus monodon. The 19th Biological Science Graduate Congress. 12-14 December 2014, National University of Singapore, Singapore. (Oral presentation)

4. Kamsaeng, P., Somboonwiwat, K., Tassanakajon, A., Cloning and expression of antilipopolysaccharide factor isoform 6 (ALFPm6) from black tiger shrimp, Penaeus monodon. ASEAN Graduate Studies International Conference (AGSIC) 2015, International School of Tourism, Suratthani Rajabhat University, Samui Island, Surat Thani, Thailand. (Publication proceeding)